Mirjam Doris Gabler, BSc.

Metabolic Short- and Longtime Response of *Saccharomyces cerevisiae* to High Carbon Dioxide Stimuli

MASTER'S THESIS

to achieve the university degree of

Diplom-Ingenieurin

Master's degree programme: Biotechnology

submitted to

Graz University of Technology

Supervisor

Dipl.-Ing Dr.nat.techn. Univ.-Doz. Mario Klimacek

Institute of Biotechnology and Biochemical Engineering

Supervisors from the University of Stuttgart
Prof. Dr.-Ing. Ralf Takors and for practical work Dipl. Biol. (t.o.) Gerhard Eigenstetter

Graz, December 2015

1 AFFIDAVIT

I declare that I have authored this thesis independently, that I have not used other than the declared sources/resources, and that I have explicitly indicated all material which has been quoted either literally or by content from the sources used. The text document uploaded to TUGRAZonline is identical to the present master‘s thesis.

_____ _____

Date Signature

Der Schatz des Wissens ist solch ein großes Vermögen, aus welchem die Blutverwandten nichts wegnehmen können, der Dieb nichts rauben kann,
und wenn du aus ihm noch soviel verteilst, wird es nie weniger.

Indisches Sprichwort

~  ~

2 CONTENT

1 Affidavit 2
2 Content 4
3 Abbreviations 7
4 List of Figures and Tables 9
5 Summary 11
6 Introduction 13
6.1 Saccharomyces Cerevisiae 13
6.1.1 Reproduction 13
6.1.2 Sugar Metabolism 13
6.1.3 Sugar Storage 14
6.1.4 Nitrogen Metabolism 17
6.2 Carbon Dioxide 18
6.2.1 Physicochemical Properties of Carbon Dioxide 19
6.2.2 State of the Art: Effects of CO_2 on *Saccharomyces cerevisiae* 20
7 Objective 22
8 Material and Methods 23
8.1 Material 23
8.1.1 Chemicals 23
8.1.2 Instruments 24
8.1.3 Equipment 26
8.1.4 Organism 27
8.2 Assembling of the Bioreactor 27
8.2.1 Composition of Media and Eluents 30
8.3 Methods 32
8.3.1 Process Overview 32
8.3.2 Preparation of Media 34
8.3.3 Preparation of the Bioreactor 35
8.4 Conduction of a Fermentation Process 36
8.4.1 Cryo-Culture 36
8.4.2 Pre-Culture 36
8.4.3 Batch Fermentation 36
8.4.4 Continuous Fermentation using Compressed Air and Gas-Mixture 36
8.5 Offline Measurements 37
8.5.1 Dilution Rate and Density 37

8.5.2 Optical Density (OD_{600}) ... 37
8.6 Sampling and Sample Preparation during Continuous Fermentation conducted with Compressed Air and Gas-Mixture ... 38
8.6.1 Methanol Quenching Samples ... 39
8.6.2 Biomass Dry Weight ... 39
8.6.3 Filtrate of the Fermentation Broth ... 39
8.6.4 Biomass Pellets for Glycogen and Trehalose assay and the Determination of Nitrogen to Carbon Ratio ... 39
8.6.5 Samples for Total Inorganic Carbon (TIC) Measurement ... 40
8.6.6 Transcript ... 40
8.7 Analysis of the Filtrate, the Quenching samples and the Biomass Pellets from Continuous Fermentation conducted with Compressed Air and Gas-Mixture ... 40
8.7.1 Quantification of the Intracellular Amino Acids ... 40
8.7.2 Quantification of Glycogen and Trehalose in Cell Pellets ... 42
8.7.3 Quantification of Sugars, Organic Acids and Ethanol present in the Filtrate (and the Feed) ... 44
8.7.4 Quantification of Carbon Species and Nitrogen by C/N- analyzer ... 45
8.8 Data Analysis ... 46
8.8.1 Biomass Dry Weight ... 46
8.8.2 Determination of the Intracellular Amino Acid Pools ... 46
8.8.3 Determination of Nitrogen to Carbon Ratio (N/C) in the Biomass Pellets and the Total Inorganic Carbon (TIC) in the TIC Samples ... 48
8.8.4 Determination of the Henry Coefficient ... 48
8.8.5 Determination of Sugars Organic Acids and Ethanol in the Filtrate ... 48
8.8.6 Glycogen und Trehalose Assay ... 49
8.8.7 Mass-balance of a Continuous Process ... 50
8.8.8 Specific Growth Rates ... 51
8.8.9 Substrate Uptake Rate ... 52
8.8.10 Product Formation Rate ... 53
8.8.11 Biomass to Substrate Yield and Maintenance ... 54
8.8.12 Oxygen Utilization Rate (OUR) ... 55
8.8.13 Carbon Dioxide Evolution Rate (CER) ... 56
8.8.14 Respiratory Quotient (RQ) ... 57
8.8.15 Elemental Carbon-Balance (C-balance) ... 57
8.8.16 Statistical Data Analysis ... 58
9 Results ... 59
9.1 Process Overview: Batch and Continuous Fermentation before and after CO_2 Shift ... 59
9.2 Carbon-balance and General Physiological Parameters During Steady State Conditions Before and After CO_2 Shift ... 60
9.2.1 General Physiological Parameters Before and After CO_2 Shift ... 60

9.2.2 Carbon-balance Before and After CO_2 Shift 61
9.2.3 Determination of the Henry Coefficient 63
9.3 By-product excretion into the Filtrate of the Fermentation Broth during CO_2 shift 64
9.4 Glycogen and Trehalose Content During CO_2 Shift 65
9.5 N/C-ratio in Biomass after CO_2 shift 66
9.6 Estimation of Respirational and Fermentational qCO_2 67
9.7 Intracellular Amino Acid Content Before and After CO_2 Shift 71
10 Discussion 76
10.1 Oscillating behavior during CO_2 Treatment 76
10.2 Changes in Physiological Parameters 76
10.3 By-product Formation 77
10.4 Degradation of Glycogen and Trehalose 77
10.5 Increase of N/C-ratio of the Biomass 77
10.6 Changes in Intracellular Amino Acid Pools 78
11 Acknowledgments 79
12 References 80

3 ABBREVIATIONS

Abbreviation	Meaning
μ	specific growth rate or micro
μ	micrometer
ace	acetate
AA	amino acids
ATP	adenosine triphosphate
bio	biomass
c	concentration
calib.	calibration
cAMP	cyclic adenosine monophosphate
Ca-pantothenate	calcium pantothenate
CDW	cell dry weight
CEN.PK 113-7D	name of used yeast strain
CER	carbon dioxide evolution rate
Cmol	moles of carbon
CO_2	carbon dioxide
$CO_{2(g)}$	carbon dioxide in-gas phase
$CO_{2(l)}$	carbon dioxide in liquid phase
cx	biomass dry weight concentration
D	dilution rate
ddH_2O	double destilled water
DNA	deoxyribonucleic acid
eth	ethanol
F	factor
ferm	fermentational
FMOC-Cl	fluorenylmethyloxycarbonyl chloride
g	gram
G0-phase	resting phase of the cell cycle
G1 -Phase	growth 1/Gap 1 phase
glc	glucose
gly	glycogen
GRAS	generally recognized as save
h	hours
TIC	total inorganic carbon
inorg.	inorganic
$k_La\ O_2$	volumetric oxygen mass transfer coefficient
L	liter
M	molecular weight
MF	multiplication factor
Mig1p	transcription factor
min	minutes
mL	milliliter
mM	mmol/L
ms	maintenance
Msn2p	transcriptional activator
Msn4p	transcriptional activator
n	moles
N	nitrogen
n.a	not available
N/C-ratio	nitrogen to carbon ratio
Nmol	moles of nitrogen
Nor	norvallin
OD_{600}	optical density at 600 nm
OPA	ortho-phthaldialdehyde
org.	organic
OUR	oxygen utilisation rate
PAS	serine/threonine-protein kinase
Pcl10p	cyclin partner of Pho85
Pcl19p	cyclin partner of Pho85
pCO_2	partial pressure of carbon dioxide
PDC	pyruvate decarboxylase
PDH	pyruvate dehydrogenase complex
PEPCK	phosphoenol pyruvate carboxykinase
pH	the negative logarithm to base 10 of the activity of the hydrogen ion
Pho85	cyclin dependent kinase
PKA	cAMP dependent protein kinase A
pO_2	partial pressure of oxygen
PP2A	serine/threonine protein phosphatase 2A
PTFE	polytetrafluorethylen

PYC	pyruvate carboxylase
q	biomass specific uptake/ consumption rate
Q	volumetric uptake/ consumption rate
resp	respirational
Rim15	protein kinase involved in cell proliferation in response to nutrients
rmp	rounds per minute
RNA	ribonucleic acid
RP- HPLC	reversed phase high presser liquid chromatography
RQ	respiratory quotient
s	substrate
SDH	succinate dehydrogenase
SEL	trace element solution
SNF1	serine/threonine protein kinase
SOK2	nuclear protein, kinase suppressor
S-phase	synthesis phase of the cell cycle
stdev	standard deviation
STRE	stress sensitive elements on the DNA
succ	succinate
T	temperature
Tap42p	essential protein involved in the TOR signaling pathway
TC	total carbon
TCA cycle	tricarboxylic acid cycle, citric acid cycle
TN	total nitrogen
TOC	total organic carbon
TOR	protein named target of rapamycin
TORC1	protein complex that contains at least TOR (target of rapamycin) and Raptor (regulatory-associated protein of TOR)
TPP	trehalose-6-phosphate phosphatase
TPS	trehalose-6-phosphate synthase
tre	trehalose
u.d.l	under detection limit
UAS_{PDS}	part of the promoter region of most of the glycogen and trehalose related genes
UDP	uridine diphosphate
UTP	uridine triphosphate
V	volume
x	biomass
y	volume fraction of a gas
YPG	yeast extract-peptone-glycerol
Yxs	biomass to substrate yield

4 LIST OF FIGURES AND TABLES

Figure 1 : Bioreactor setup: including bioreactor, exhaust-gas-module (yO_2 yCO_2), the process control system, the in-gas-module and the harvesting-module. Peristaltic pumps: 1 for the feed, 2 for the waste, 3 for the base, 4 for the acid and 5 for the antifoam (AF). Gas-mixture (nitrogen, oxygen and carbon dioxide) or compressed air as inflow gas were controlled by a mass flow controller (MFC) and entered the bioreactor through a sterile filter. The system was furnished with a pH probe and control, a pO_2 probe, a temperature (T) sensor and control and pressure (P) sensor and control. (inspired by [132]).....29

Figure 2: Process overview: the purchased dried *S. cerevisiae* strain CEN.PK 113-7D strain was used to produce the cryo-culture, which was applied for inoculation of the pre-culture. After reaching the exponential phase the pre-culture was transferred together with the batch medium to the fermenter, to start the batch process. Then the process is moved to a continuous fermentation with compressed air. After six residence times the gas inflow was shifted from compressed air to the gas-mixture (50 % CO_2, 29 % N_2 and 21 % O_2) and after six additional residence times the process was finished. (x = biomass and s = substrate).....33

Figure 3: Sampling overview: at the continuous fermentation using compressed air, samples were withdrawn at residence time (RT) 5 and 6. At the continuous fermentation with gas-mixture (50 % CO_2, 29 % N_2 and 21 % O_2) samples were withdrawn during the shift from compressed air and gas-mixture (0-180 min) and at RT 5 and 6. 38

Figure 4 : Process overview of process 2: in A the pO_2 [%] and the rotation number N [1/min], in B the temperature T [°C], pH [ ] and overpressure p [bar] and in C the yCO_2 and yO_2 [%] values are blotted against the process time [h]. 0: start of batch fermentation, 1: batch fermentation, 2: starvation phase, 3: continuous fermentation with compressed air, 4: interpose of gas mixer, 5: continuous fermentation with gas-mixture containing 50 % CO_2, 6: end of process.....60

Figure 5: Biomass specific glucose uptake rate (*qs*, A), biomass-substrate yield (*Yxs*, B), cell dry weight concentration (*cx*, C) and maintenance (*ms*, D) during CO_2 shift of process 1 and 2. *qs* and ms were increasing, while *cx* and *Yxs* were decreasing during the shift. 61

Figure 6: Carbon-balance before and after CO_2 shift at steady state conditions of process 1 and 2. Biomass fraction was decreasing, while by-products were increasing. Because of high standard deviation during off-gas measurement, limited accuracy about the CO_2 production can be made.....62

Figure 7: Oscillation behavior of yCO_2 [%], yO_2 [%] and pO_2 [%] during CO_2 treatment of process 2. 63

Figure 8: Determination of Henry coefficient during continuous fermentation with compressed air and gas-mixture (this work) in comparison to calculated concentrations of CO_2 by using the Henry coefficient for 30°C an 1.5 bar, which is 0.029 mol/L/bar (0.044 for the pressure of 1.5 bar) and the published data by Aguliera et al. (2005) [1]. The slope of the line is the Henry coefficient (44.06 mmol/L/bar).....63

Figure 9: By-product content in filtrate during CO_2 shift of process 1 and 2. Succinate, acetate and ethanol were detected extracellular, where acetate and ethanol were produced short-term and succinate short- and long-term. In process 1 sampling was only conducted between 0-60 minutes and long-term, while in process 2 sampling was extended from 60 -180 min every 20 minutes, due to the results obtained from process 1.....64

Figure 10: Biomass specific rates of succinate (*qsuccinate*), ethanol (*qetahnol*) and acetate (*qacetate*) [µmolGlc/gCDW/h] during CO_2 shift of process 1 and 2. Succinate was produced during the whole CO_2 treatment, while ethanol and acetate were produced in the first hour and consumed afterwards. (negative rate = production and positive rate = consumption).....65

Figure 11: Intracellular glycogen and trehalose content during CO_2 shift of process 1 and 2. During CO_2 shift carbon storage was degraded and stayed at a low level even when exposed long-term (6000 and 7000 min) to elevated CO_2 concentrations. Breakdown was highest at the first 30 minutes and happened more intensely for trehalose than for glycogen.....66

Figure 12: Nitrogen to carbon ratio (N/C) from biomass during CO_2 shift of process 1 and 2. N/C-ratio increased during CO_2 shift in process 1 and 2 66

Figure 13: Carbon-balance of biomass specific yields during CO_2 shift of process 1 and 2. Biomass specific rates of the substrate added by biomass specific rates of glycogen and trehalose and subtracted by biomass specific rates of the by-products in glucose equivalents ($\boldsymbol{qs + qglytre - (qsucc + qace + qeth)/2}$). The balance is negative at 30 minutes, which indicates that the released glucose molecules are stored in the cell before being converted into by-products.....68

Figure 14: Estimation of biomass specific respirational CO_2 production rate in comparison to the biomass specific rates of by-product, substrate and glycogen and trehalose during CO_2 shift of process 1 and 2. qCO_2 respirational decreased at 30 minutes and increased at 60 minutes after CO_2 shift.....70

Figure 15: Comparison of biomass specific rates of respirational CO_2 and fermentational CO_2. The fermentational CO_2 rate is highest at 30 and 60 minutes and increases afterwards, while the respirational CO_2 rate is increasing at 30 minutes and decreasing at 60 minutes of CO_2 shift.....71

Figure 16: Intracellular amino acid content during CO_2 shift of process 1 and 2 (part 1/4): no significant change was measured for asparagine, methionine and isoleucine and slight changes were measured for phenylalanine and histidine.....72

Figure 17: Intracellular amino acid content during CO_2 shift of process 1 and 2 (part 2/4). Descriptions see text. 73
Figure 18: Intracellular amino acid content during CO_2 shift of process 1 and 2 (part 3/ 4). Descriptions see text. 74
Figure 19: Intracellular amino acid content during CO_2 shift of process 1 and 2 (part 4/ 4). Descriptions see text. 75
Figure 20: Correlation between N/C-ratio and dilution rate according to Lange and Heijnen, 2001 [149]. 78

Table 1: List of applied chemicals....23
Table 2: List of applied instruments....24
Table 3: List of applied equipment....26
Table 4: List of applied software....26
Table 5: Description of the genotype of the *S. cerevisiae* strain CEN.PK 113-7D [131]. 27
Table 6: Composition of trace element solution (SEL) for every medium according to [133]. 30
Table 7: Composition of the vitamin solution for every medium [modified after [133]. 30
Table 8: Composition of YPG-medium for the initial cultivation of strain CEN.PK 113-7D. Prepared in demineralized water. 30
Table 9: Composition of pre-cryo medium, prepared in demineralized water. 30
Table 10: Composition of cryo-medium prepared in demineralized water. 31
Table 11: Composition of pre-culture medium prepared in demineralized water. 31
Table 12: Composition of the batch medium, prepared in demineralized water. 31
Table 13: Composition of the feed medium. Compounds of section A are dissolved, adjusted to pH 5 and sterilized. Solutions of section B are separately sterilized in demineralized water and added to the cooled down mixture of section A. 31
Table 14: Composition of eluent A for amino acid quantification by RP- HPLC....32
Table 15: Composition of eluent B for amino acids quantification by RP-HPLC....32
Table 16: Composition of the eluent for the quantification of sugars, organic acids and ethanol. 32
Table 17: Operation conditions for batch and continuous fermentation. 33
Table 18: Composition of the concentration levels for quantification of amino acids by RP-HPLC. 42
Table 19: Composition of concentration levels for glucose and trehalose quantification by RP- HPLC. 44
Table 20: Composition of stock solution A and B for quantification of organic acids, sugars and ethanol out of the filtrate....45
Table 21: Composition of concentration levels to quantify TIC, TC, TOC and TN by N/C-analyzer. 45
Table 22: Retention times of the amino acids analyzed by RP-HPLC....47
Table 23: Retention times of sugars , organic acids and ethanol 49
Table 24: Carbon-balances of process 1 and 2 in % regarding to the carbon inflow of the feed. 62
Table 25: Biomass specific glucose production rate ($q_{excess\ glucose}$) of process 1 and 2 68

5 SUMMARY

CO_2 is an important metabolic compound as product and substrate in *Saccharomyces cerevisiae.* High CO_2 concentrations are well known to have negative impact on yeast physiology, which is important in the industry, because product formation and growth inhibition by CO_2-stress may lower the productivity of industrial fermentations [1]. This is especially the case in large bioreactors, high hydrostatic pressure and poor mixing lead to high dissolved carbon dioxide concentrations [2,3]. The molecular mechanism behind the negative effect of CO_2 on yeast is still not fully understood, but would be essential to develop CO_2 tolerance by metabolic engineering. Therefore the aim of this work was to further investigate the negative effect of CO_2 on *S. cerevisiae* for short and long-term response in order to achieve more knowledge about the adaption process of yeast to high CO_2 concentration.

For this purpose stimulus response experiments were conducted in aerobic and carbon-limited continuous processes with a dilution rate of 0.05 1/h, where the dissolved CO_2 concentration was shifted from 1.18 mM to 23.29 mM.

In the short-term, a fast degradation of the storage carbohydrate pools could be observed. This depletion was followed by the formation of fermentative by-products where where acetate was the predominant by-product followed by ethanol. Additionally, decreased (aspartate and glutamate) and increased (serine, alanine, threonine, valine, proline, glycine and lysine) intracellular amino acid levels were measured during CO_2 treatment. Only the amino acid, which are delivered from the central carbon metabolism were affected. This behavior indicates a sudden energy drain caused by the increase in CO_2 concentration.

On the long-term, the increased energy requirement of the organism appears in a decreased biomass substrate yield and increased respiration. The adaptation to the CO_2 enriched environment leads to an ongoing production of succinate, permanent low storage carbohydrate pools and a nitrogen-carbon ratio, that is typical of growth rates five times higher than 0.05 1/h. Some intracellular amino acid levels increased (glutamine) and decreased (lysine and glycine) as well and again only the ones delivered from the central carbon metabolism were affected. These changes indicate the permanent participation of global regulatory mechanisms to compensate the impact of environments of high in CO_2 concentrations.

This work illustrates how complex the impact of CO_2-stress on *Saccharomyces cerevisiae* is and helps gaining a better understanding about the processes taking place during CO_2-stress.

Zusammenfassung:

CO_2 stellt eine wichtige Komponente im Stoffwechsel als Produkt sowie auch als Substrat von *Saccharomyces cerevisiae* dar. Hohe CO_2-Konzentrationen sind bekannt einen negativen Einfluss auf die Physiologie von Hefe zu haben, was in der Industrie relevant ist, da die Produktbildung und die Wachstumsinhibierung durch CO_2 und die Produktivität in industriellen Fermentationen erniedrigen werden können [1]. Besonders in großen Bioreaktoren kommt es zu hohen hydrostatischen Drücken und schlechter Durchmischung, was eine hohe gelöst CO_2-Konzentrationen zur Folge hat [2,3]. Der molekulare Mechanismus der für den negativen Effekt von CO_2 auf Hefe verantwortlich ist, ist immer noch nicht komplett verstanden, würde aber essentiell für die Entwicklung von CO_2-toleranten Stämmen durch Metabolic Engineering sein. Daher war das Ziel dieser Arbeit, den negativen Effekt von CO_2 auf *S. cerevisiae* in der kurz und langzeitantwort näher zu untersuchen um mehr Erkenntnis über den Anpassungsprozess von Hefe auf hohe CO_2-Konzentrationen zu erlangen.
Hierzu wurden Stimulus-Response-Experimente in aeroben, Kohlenstoff-limitierten kontinuierlichen Prozessen mit einer Durchflussrate von 0.05 1/h und mit einem Übergang von 1.18 mM auf 23.29 mM gelöst-CO_2 durchgeführt. Als Kurzzeitantwort konnte ein schneller Abbau der Speicherzucker beobachtet werden, gefolgt von der Produktion fermentativer Nebenprodukte, bei der Ethanol in einer geringeren Menge als Acetat vorkam. Zusätzlich konnte eine Verringerung (Aspartat und Glutamat) und eine Erhöhung (Serin, Alanin, Threonin, Valin, Prolin, Glycin und Lysin) mancher intrazellulären Aminosäurepools während der Behandlung mit CO_2 festgestellt werden. Nur die Aminosäuren, welche aus Komponenten des zentralen Kohlenstoff Metabolismus synthetisiert werden, waren betroffen. Das Verhalten weißt auf einen erhöhten Energieabfluss hin, welcher durch die erhöhte CO_2-Konzentration verursacht wurde.
Als Langzeitantwort konnte ein erhöhter Energiebedarf des Organismus veranschaulicht durch die Erniedrigung der Biomassen Substrat Ausbeute und erhöhter Respiration, festgestellt werden. The Anpassung an die mit CO_2 angereicherte Umgebung führte zu einer fortwährenden Produktion von Succinat, permanent geringe Mengen an Speicherzucker und zu einem Stickstoff zu Kohlenstoff Verhältnis, welches eigentlich typisch für Wachstumsraten größer als 0.05 1/h ist. Einige intrazelluläre Aminosäurepools erhöhten (Glutamin) und erniedrigten (Glycin und Lysin) sich auch in der Langzeitantwort, wobei wieder nur solche betroffen waren, die aus Komponenten des zentralen Kohlenstoff Metabolismus synthetisiert werden. Diese Änderungen deuten auf eine permanente Teilnahme des globalen regulatorischen Mechanismus hin um den Einfluss von hohen CO_2-Konzentrationen zu kompensieren.
Diese Arbeit zeigt auf, wie komplex die Auswirkungen von CO_2-Stress auf *S. cerevisiae* ist und konnte zu einem besseren Verständnis über die Prozesse, welche während der Behandlung mit erhöhten CO_2 Konzentrationen ablaufen führen.

6 INTRODUCTION

6.1 SACCHAROMYCES CEREVISIAE

The heterotrophic, facultative anaerobe *S. cerevisiae* [4] was the first eukaryote organism whose genome was completely sequenced [5] and is used in research as an eukaryotic model organism [6]. The organism has several advantages in being used as a cell factory: it is generally recognized as a safe organism (GRAS) [6], it shows good tolerance to low pH, which leads to low risk of bacterial contamination [7], It has a broad substrate spectrum [4], it is inexpensive to maintain and grow [8] and it is stable in diploid and haploid states [6].
The single cell fungus [6] is traditionally used for the production of ethanol in beer, spirits, wine (brewer's yeast) and pastries (baker`s yeast). Furthermore yeast is industrially used for the production of biofuels [8], enzymes [7], pharmaceuticals (insulin, vaccines [8] etc.), nutritional ingredients [7], cosmetic ingredients [7] and chemicals (pyruvate [9], glycerol [10], isoprenoides [11], poliketides [12] and organic acids for example lactic acid [13], malic acid [14] or succinic acid [15]).
All of these examples show that *S. cerevisiae* is an important cell factory in industrial production. This fact is also manifested by several reports that argue that the worldwide yeast market has been growing by 8.6 % annually until 2016 [16,17].

6.1.1 REPRODUCTION

S. cerevisiae exist either in haploid or in diploid state [18]. There are two types of haploid cells: the ones harboring mating type a and the others harboring mating type α [18]. Only cells with opposite mating type are able to mate, while diploid cells with mating type a/α are not [18]. Haploid and diploid cells can propagate asexually by budding, when exposed to nutrient rich conditions [18]. In nutrient poor conditions a diploidic cell is able to form four (or more) haploidic spores by sporulation [18]. When conditions improve the four haploidic spores can germinate into haploid cells [18]. Wildtype yeast strains are capable to switch their mating type after every deviation (except the first one), by the action of an endonuclease encoded by *HO* (homothallic strains) [19]. Most strains used in laboratories cannot switch mating type, because of deletion in *HO* gene (heterothallic strains), which is conducted to enable a stable haploid yeast cells for scientific research [19].

6.1.2 SUGAR METABOLISM

S. cerevisiae is able to utilize a large variety of carbon sources. Depending on the type of source different enzymes and metabolic pathways are used. Yeast is able to change gene expression patterns to adapt to the new environmental situation, when nutrient availability is changing [4].
Different types of sugar metabolism are known in *S. cerevisiae*: oxidative (respiration, aerobic), fermentative (anaerobic) and oxido-reductive (aerobic) metabolism. During oxidative growth carbohydrates are completely oxidized to CO_2 by TCA and no fermentational by-products are formed, while in oxido-reductive metabolism the carbohydrates are mostly converted to CO_2 by TCA, but fermentatio products are also formed.
Under anaerobic conditions *S. cerevisiae* only performs fermentation metabolism to regenerate the NADH, which was build during glycolysis [4]. At aerobic conditions with low glycolytic fluxes most of the carbon reacts to acetyl-CoA, because of the high affinity of mitochondrial pyruvat dehydrogenase complex [21]. This is energetically favorable, because the cytosolic acetyl-CoA synthase needs ATP to

produce acetyl-CoA [22]. When the glycolytic flux increases, the pyruvate dehydrogenase by-pass becomes saturated and therefore ethanol production starts ("Crabtree effect") [23]. High extracellular glucose concentrations lead to increased pyruvate decarboxylase activity as well as decreased acetaldehyde dehydrogenase activity and therefore support the fermentative metabolism [21].
The TCA is slightly active in anaerobic conditions, when only used for precursor synthesis in biomass formation. However, the cycle is not conducted completely: it is separated into an oxidative and an reductive part, where both parts are able to undergo the cycle until succinate [24]. Succinate dehydrogenase is not active in anaerobic conditions, the reaction from fumarate to succinate is therefore catalyzed by two fumarate reductases [4,25,26].

6.1.3 SUGAR STORAGE

Glycogen and trehalose are the main sources of carbon storage in *Saccharomyces cerevisiae* [27] and can reach 25 % of its dry weight [28]. In the following chapter, the metabolic pathways of those two molecules are described in detail, because elevated CO_2 levels are known to have an influence on the sugar storage [29] and therefore this effect was also investigated in this work.

6.1.3.1 UDP-glucose as Precursor of Glycogen and Trehalose Biosynthesis

UDP-glucose (uridine diphosphate glucose) is needed for the synthesis of glycogen and trehalose [27]. UDP-glucose phosphorylase [30] catalyzes the reaction of UTP (uridine tripohsphate) and glucose to UDP-glucose [30]. Besides its application in glycogen and trehalose synthesis, UDP-glucose has a central function in yeast metabolism: N-glycosylation of proteins, the use of galactose as carbon source and the synthesis of β-glycan for the cell wall [31]. UDP-glucose is transported either to the plasma membrane for cell wall synthesis or to the cytoplasm for glycogen and trehalose synthesis, depending on its phosphorylation status [32-35]. Furthermore, the nutrient and cell integrity statuses rely on whether UDP glucose is phosphorylated or not [32,36].

6.1.3.2 Metabolic Pathways of Glycogen

Glycogen is a spherical shaped macro molecule, based on α(1,4)-glycosyl chains, which are branched by α(1,6)-linked glucose molecules [27,37]. There are two pools of glycogen in *Saccharomyces cerevisiae*: the cell wall bound pool, also reported as acid soluble [38], and the intracellular pool [39]. In the following, glycogen biosynthesis and degradation are described in detail.

6.1.3.2.1 Glycogen Biosynthesis

The glycogen biosynthesis consists of three steps: initiation, elongation and branching [40]. The initiation is performed by the enzyme glycogenin [40], which reacts with UDP-glucose, to release UDP and transfer glucose to one of its tyrosine residues (glucosyl-glycogenin) [40,41]. Glycogenin has a self-glycosylation activity, which leads to the formation of a small α(1,4)-glycosyl chain [40], that is then extended to the non reducing end by the enzyme glycogen synthase. Finally the glycogen branching enzyme (amylo(1,4)→(1,6)-transglucosidase), forms α(1,6)-linkages by transferring 6-8 residues of an α(1,4)-glycosyl chain end to an internal glycosyl unit [40].

The glycogen synthase is regulated post transcriptional by glucose-6-phophate and by reversible covalent phosphorylation [27]. A three state model can be used to describe the control of glycogen synthase activity by glucose-6-phosphate: the phosphorylated enzyme in absence of glucose-6-

phosphate has the lowest activity, the dephosphorylated enzyme in absence of glucose-6-phophate has intermediate activity and dephosphorylated enzyme with bound glucose-6-phosphate has the highest activity [30]. The cyclin-dependent Pho85 kinase with its cyclin partners Pcl19p and Pcl10p and the PAS kinase act as glycogen synthase kinase and therefore inactivate the enzyme [30,42,43]. Additionally to its function as allosteric activator, glucose-6-phophate stimulates dephosphorylation and inhibits phosphorylation [44-46], which leads to the hypothesis, that any drastic change in glucose-6-phosphate levels in the cell should effect glycogen synthesis [27] .

6.1.3.2.2 Glycogen Degradation

There are two possible mechanisms of glycogen degradation: sequential degradation by glycogen phophorylase and glycogen debranching enzyme [27] or amylolysis by amylo(1,4), (1,6)glycosidase [27,40]. The sequential degradation takes place in the cytosol, where glycogen phosphorylase, releases piecewise glucose-1-phophate from the α(1,4)-glycosyl chain until it is near by a α(1,6)-linkage, where it cannot operate anymore [40]. Therefore the action of glycogen debranching enzyme is needed: it transfers maltosyl (or maltotrisyl) residue to a neighbouring α(1,4)-glycosyl chain and cleaves the α(1,6)-linkage [40]. After the branch is removed, glycogen phosphorylase is able to proceed again [40]. The second option for glycogen degradation is the breakdown by amyloglycosidase, which is located in the vacuole, where the glycogen is inserted by autophagy during growth on glucose [27,47]. In the vacuoles glycogen is protected from cytosolic utilization [48]. Amylo(1,4),(1,6) glycosidase, degrades glycogen and releases glucose as the final product [49,50].

Glycogen phosphorylase is expressed at the end of logarithmic growth [51], where PKA is required [52] for the activation by phosphorylation [45,53,54]. Glucose-6-phophate acts as a central part in the transcriptional control: it allows the dephosphorylation and inactivation of glycogen phosphorylase [55]. Glycogen phosphorylase may also be controlled by Pho85-Pc16/Pc17 complex [30]. However a glycogen phosphorylase kinase has not been identified, but a PKA was found to phosphorylate the enzyme in vitro [30,57,58].

6.1.3.3 Metabolic Pathways of Trehalose

Trehalose is a disaccharide, composed by two glucose molecules connected by an α(1,1) linkage [27]. It can be synthesized and degraded by the cell or it can be captured from the environment [27].

6.1.3.3.1 Trehalose Biosynthesis

Trehalose is synthesized from UDP-glucose and glucose-6-phosphate, by the action of trehalose-6-phosphate synthase (TPS) and trehalose-6-phosphate phosphatase (TPP) [40]. TPS catalyzes the formation of trehalose-6-phosphate from UDP-glucose and glucose-6- phosphate, which reacts afterwards with water to trehalose catalyzed by TPP [27]. These two enzyme activities originate from one enzyme complex [27], that consists of four protein subunits.

The main allosteric effectors acting on TPS and TPP are Pi and fructose-6-phophate [59,60]. Pi inhibits binding of glucose-6-phospate and UDP-glucose to TPS and activates TPP, where fructose-6-phosphate acts as an allosteric effector on glucose-6-phosphate, binding to TPS [27,59,60]. Additionally TPS is suppressed by glucose [61,62].
Trehalose-6-phosphate or TPS may have regulatory function in coordinating cell growth, budding and cell wall synthesis according to carbon availability (the exact mechanism is still unclear) [27].

6.1.3.3.2 Trehalose Degradation

There are two types of trehalase available, both performing hydrolyzation of trehalose into two units of glucose: the acid trehalase and the neutral trehalase [27]. The neutral trehalase, which is most active at neutral pH (6.8-7) [40], is located in the cytoplasm [63], where it is activated by phosphorylation through PKA [27]. Additionally complete activation of the neutral trehalase requires the binding of a protein called 14-3-3 [64]. The acid trehalase, which is most active at pH 4.5-5 [65], is located in the vacuole and on the cell surface [63,66]. Only the trehalase on the cell surface, is able to hydrolyze extracellular trehalose for utilization as carbon source [63,66]. Another option to assimilate exogenous trehalose is to import trehalose into the cytoplasm by using the trehalose-H^+-symporter and hydrolysis by neutral trehalose [63].

6.1.3.3.3 Growth Control by Trehalose and Glycogen

The accumulation of glycogen and trehalose is favored, at low growth rate under carbon or nitrogen-limited conditions [27]. Moreover glycogen and trehalose play a role in the progression of cell deviation [67], which can be seen by cell cycle related oscillating behavior, monitored as periodical change in budding index, ethanol production, dissolved O_2, biomass concentration and content of carbon storage [68-72] in continuous cell cultures at a low dilution rate [67]. Other experiments in the same conditions showed that trehalose and glycogen concentrations increased proportionally to the G1-phase of the cell cycle [73-75]. The carbon stores were therefore mobilized before the cell passes over the S-phase, to temporarily increase the glycolytic flux, which provides enough energy for the next cell deviation [74]. Interestingly mutants, which cannot synthesize neither glycogen nor trehalose, are able to perform cell deviation, but the transition to the next deviation round was way slower in comparison to the wildtype [74]. These mutants generate higher ATP fluxes to pass the deviation cycle, instead of using the energy from glycogen and trehalose degradation (wildtype) [74]. The advantage in producing glycogen and trehalose, besides that the next cell deviation occurs faster, is that the wildtype survives much better under carbon starvation than the mutant [74]. They can survive a long period using the carbon storage, when extracellular carbon source is exhausted or they can go quickly to a cell deviation round when conditions improve [74].

6.1.3.4 Stress Protection by Trehalose

Trehalose is found to function as stress protector, because it protects membrane from dehydration and it is able to exclude water from protein surfaces, which leads to a protection against denaturation [76-78]. Its function is additionally supported by the fact that its level increases under harmful conditions [79,80]. Trehalose was reported as protector at desiccation, temperature (high and low), saline, hydrogen peroxide, copper sulfate, high ethanol (> 7 %) or weak acid stresses [40,81-91].

6.1.3.5 Nutrient Control of Glycogen and Trehalose Levels

Glycogen and trehalose levels in yeast depend on the availability of nutrition and on stress conditions [40]. These sugar stores are transcriptionally and posttranscriptionally controlled by several pathways [27]. The major transcriptional control is conducted by the PKA pathway and the major metabolic effector is glucose-6-phosphate [27], because it is substrate for trehalose synthesis, activator of glycogen synthase and inhibitor of glycogen phosphorylase [27].

The main nutrition sensing pathways in yeast are PKA, TOR and SNF1 [27]. Under glucose-rich conditions, the accumulation of trehalose and glycogen is inhibited because PKA and TORC1 (part of TOR pathway) are active, when under glucose-limitations the accumulation is favored [27]. It should

be pointed out that the production of glycogen and trehalose depends on the type of nutrition limitation [27], meaning that not every limitation leads to accumulation of the storage sugars [27].

6.1.3.5.1 PKA Pathway

The transcription factors Msn2p/4p are key regulators for stress [92]. Under normal conditions, they are located in the cytoplasm, because they are phosphorylated by PKA [93,94]. Under stress conditions, the phosphorylation of the transcription factors are reduced, because of down regulation of PKA or activation of protein phophatase [94,95] and so they are translocated into the nucleus [94]. Msn2p/4p are then able to bind to stress sensitive elements (STRE) on the DNA, located in the promoter of stress sensitive genes [96,97], where glycogen and glucose related genes belong to [27] .

The transcriptional repressor SOK2 is also controlled by PKA [98], which is also present in the promoter region of all trehalose and glycogen-related genes [27]. Additionally PKA blocks the Rim15-Gis1p cascade [27], which binds to the UAS_{PDS} element, that is also present in the promoter region of most of the glycogen and trehalose related genes [27]. The Rim15-Gis1p cascade is only active in stationary phase or when passing over to the G0-phase [99,100].

6.1.3.5.2 TOR Pathway

The TOR pathway also controls glycogen and trehalose-related genes in a negative way: Tap42p is phosphorylated and binds to serine/threonine protein phosphatase 2A (PP2A). Therefore PP2A is not able to dephosphorylate Msn2/4p anymore [101]. Further, TOR controls Rim15-Gis1p cascade negatively, by the protein kinase Sch9 [102].

6.1.3.5.3 Snf1 and Pho85

There are two more nutrient senor kinases, which are known to control glycogen and trehalose storage: the Pho85 kinase and the Snf1 kinase [27]. These kinases perform their controlling function at transcriptional and post transcriptional levels [27]. Snf1 interacts with the transcription factors Adr1p and Mig1p, which activates the transcription of glycogen and trehalose-related genes [103]. Furthermore Snf1 can indirectly affects glycogen storage, due to its positive control on the glycogen autophagy process, which causes the storage of glycogen in the vacuole [48,27]. The Pho85 kinase acts as an antagonist on Snf1, according to the autophagy process, where Snf1 act as an antagonist on Pho85 dependent phosphorylation of glycogen synthase [48,104,105].

6.1.4 NITROGEN METABOLISM

In this work, the intracellular amino acid concentrations were analyzed, even though no effect of CO_2 on yeast has been published yet. The synthesis and degradation are therefore described to give a better overview.

6.1.4.1 Amino Acids: Biosynthesis and Degradation

S. cerevisiae is able to synthesize all proteinogenic L-amino acids, when growing on adequate source of carbon and ammonium [106]. Depending on the derived molecule the amino acids are divided into the glutamate family (glutamate, glutamine, arginine, proline, and lysine), the aromatic family (phenylalanine, tyrosine and tryptophane), the serine family (serine, glycine, cysteine and methionine), the aspartate family (aspartate, asparagine, threonine and also cysteine and methionine), the pyruvate

family (alanine, valine, leucine and isoleucine) and histidine, whose biosynthesis is connected to the nucleotides [107].

The glutamate and the aspartate family derive from TCA intermediates: glutamate from α-ketoglutarate and aspartate from oxalacetate [107]. The precursor of the aromatic family is chorismate, which is build up by the chorismate pathway, starting with phosphoenolpyruvate and erythrose-4-phosphate [106]. Histidine requires phosphoribosylpyrophosphate as precursor, which is build up from ribose-5-phosphate [108]. Two families derive from glycolytic metabolites: the pyruvate family, where pyruvate is logically the precursor and the serine family, where 3-phosphoglycerate is the precursor for the pathway [107].

Glutamate and glutamine function in addition in transamination reactions and are therefore required for the synthesis of every amino acid [107,109-111]. They thus play a central role in nitrogen metabolism [107].

S. cerevisiae is able to use a variety of nitrogen compounds as nitrogen source [109]. All proteinogenic amino acids can be used exclusively as a substrate - except for lysine, cysteine and histidine [107]. However, yeast has preferred and non-preferred nitrogen sources [109-111]. The amino acids, which are part of the preferred sources, are arginine, asparagine, serine, alanine, glutamate and glutamine [107]. The preferred nitrogen sources are incorporated into glutamate and the resulting carbon skeletons are integrated in the metabolism [107,112]: six of these seven preferred amino acids are substrates of transaminases or deaminases that results in pyruvate, TCA cycle intermediates, oxalacetate or α-ketoglutarate [107,109].

Non preferred nitrogen source, like the amino acids leucine, isoleucine, tyrosine, tryptophane and methionine (except for threonine) are transaminated and the resulting carbon skeletons are converted into fusel oils (Ehrlich pathway), which have an growth inhibiting effect and are no longer catabolized [113, 107].

6.2 CARBON DIOXIDE

The linear molecular shaped carbon dioxide (CO_2) is a colorless and odorless gas [2]. As part of the Earth atmosphere, CO_2 is found to increase its levels, due to burning fossil fuels and deforestation [114]. As the second most important greenhouse gas in the atmosphere [114], it was found to play a major role in global warming [115].
Besides the fact that CO_2 is produced during respiration, it functions in microbial metabolism as biosynthetic substrate in carboxylation reactions [116].
Elevated levels of carbon dioxide were found to have an inhibitory effect on the metabolism [117] and CO_2 is therefore used to inactivate microorganism in food products [5,117], because it is ultra pure, free from toxicity and can be removed easily [118].
In the following, the physicochemical properties of CO_2 and its effect on *S. cerevisiae* are discussed in detail.

6.2.1 PHYSICOCHEMICAL PROPERTIES OF CARBON DIOXIDE

Carbon dioxide dissociates in water: the gaseous carbon dioxide ($CO_{2(g)}$) enters liquid phase ($CO_{2(l)}$) and forms with water carbonic acid, which dissociates to bicarbonate and hydrogen. Biocarbonate further dissociates to a carbenium and hydrogen (see Eq. 1).

$$CO_{2(g)} \leftrightarrow CO_{2(l)} + H_2O \underset{[slow]}{\longleftrightarrow} H_2CO_3 \underset{[fast]}{\longleftrightarrow} HCO_3^- + H^+ \underset{[fast]}{\longleftrightarrow} CO_3^{2-} + 2\,H^+ \qquad \textbf{Eq. 1}$$

The reaction of carbon dioxide and water to form carbonic acid is the rate limiting step and is catalyzed in *S. cerevisiae* by the enzyme carbonic anhydrase, encoded by *NCE103* [119]. The other steps in CO_2 dissociation are fast and therefore action of an enzyme is not needed (Eq. 1). CO_2/ HCO_3^- function furthermore as buffer, where HCO_3^- is able to buffer protons and form H_2CO_3 and the other way around [120].
The carbonic anhydrase is transcriptional up-regulated under low CO_2 levels (0.035 %), because at high levels (5 % CO_2), enough bicarbonate is formed spontaneously to deliver the required amount of bicarbonate for the organism [119].

The ratio of CO_2 species depend on the pH of the liquid [117]. In this work experiments were conducted at pH 5, therefore and due to the fact that the intracellular pH of *S. cerevisiae* is between 5.2-7 [120], carbenium ions are negligible because they are not present in conditions were pH is lower than 8 [121].

The dissolved CO_2 concentration during a fermentation depends on the CO_2 production rate of the organism, on the equilibrium with the other CO_2 species and on the mass transfer rate of CO_2 between liquid and gas phase [29]. Considering mass transfer characteristics of CO_2 one can see that the highest concentration in CO_2 is to be found in the proximate microenvironment of the cell [2], because CO_2 is produced in the cells and then transported through the surrounding liquid film by diffusion [2]. After leaving the liquid film, CO_2 enters the well-mixed zone, where it can diffuse again to a cell or to an air bubble [2]. In contrast to CO_2, HCO_3^- is not able to pass the plasma membrane of the yeast cell by diffusion, because a transporter has not been found yet [119]. The concentration of dissolved CO_2 can be calculated by using the Henry´s law:

$$c_{CO_2} = H_{CO_2}\, p_{CO_2} \qquad \textbf{Eq. 2}$$

where c_{CO_2}[mmol/L] is the concentration of carbon dioxide in the liquid, H_{CO_2} is the Henry coefficient for CO_2 [mmol/L/bar] and p_{CO_2} [bar] is the partial pressure of dissolved carbon dioxide. A decreasing value of the Henry coefficient displays decreasing gas solubility [2]. Furthermore the Henry coefficient is compound, temperature- and liquid-dependent [2].
The Henry´s law indicates the relevance of carbon dioxide in large scale processes, where there is poor mixing, high hydrostatic pressure and therefore high partial CO_2 concentrations [2,3]. Additionally high CO_2/ HCO_3^- concentrations affect the pH buffer capacity in large-scale bioreactors [2].

6.2.2 *STATE OF THE ART: EFFECTS OF CO_2 ON SACCHAROMYCES CEREVISIAE*

CO_2 plays a major role in the metabolism of living cells as a substrate (CO_2/HCO_3^-) for carboxylases and as a product (CO_2) of reactions catalyzed by decarboxylases [116]. These reactions are involved in ana- and catabolism as well as the energy metabolism [2]. In *S. cerevisiae* several enzymes catalyzing carboxylation reactions are known: pyruvate carboxylyase (PYC), phosphoenol pyruvate carboxykinase and acetyl-CoA carboxylase [20]. Carbon dioxide is therefore essential to the yeast metabolism, but it is also well known that elevated levels of CO_2 have a negative effect on yeast physiology [116] up to cell inactivation under high-pressure carbon dioxide conditions [122].

In 1877 Pasteur and Joubert [123] were among the first scientists to argue in their works, that CO_2 has a negative effect on bacteria. They reported that under influence of CO_2, *Bacillus anthracis* was killed. 100 years later, the inhibitory effect of carbon dioxide on yeast growth was demonstrated by Chen and Gutmanis (1976) [124]. They conducted experiments in aerobic carbon-limited fed-batch process, where inhibition of yeast growth was negligible below 20 % (v/v), slight inhibition at 40 % (v/v) and strong inhibition at 50 % (v/v) CO_2 in the in-gas [124]. In addition to this Norton and Krauss (1972) argued, that CO_2 inhibits cell deviation and bud formation and that the DNA content was doubled [125]. Akashi et al. (1979) pointed out that in aerobic batches of *Brevibacterium flavum* growing on glucose, histidine and arginine levels decrease with higher pCO_2 levels, which can be explained by the inhibition of decarboxylation reactions required for amino acid production. Unfortunately no articles dealing with the alteration of intracellular amino acid pool at elevated CO_2 levels of *S. cerevisiae* are available today [126]. A few years later Jones and Greenfield (1982) reviewed that the growth inhibition by CO_2 appears for all living cells and mentioned that the TCA is the side of inhibition in fungi [116]. Interestingly, it is not known whether CO_2 and/or HCO_3^- are responsible for the growth inhibition [116], but it is known that high bicarbonate levels added to the medium show less inhibitory effects than the same amount of dissolved CO_2 (reviewed by [116]). The intracellular concentration of HCO_3^- is known to activate and inactivate enzymes [116], which plays a central role in the regulation of the cellular metabolism [116]. Bicarbonate may act on enzymes at their anion-sensitive side, therefore this is the reason why CO_2 may not have such function [116]. Later in 1993, Kuriyama et al. investigated the effect of CO_2 on *S. cerevisiae* in glucose-limited chemostat experiments [127]. They also found a decrease in biomass concentration, increased ethanol and decreased glycerol concentration [127]. They also mentioned that in higher CO_2 concentrations more ATP was required for maintenance.
Stress responses of *S. cerevisiae* are broadly investigated and therefore it is known that stress causes transcriptional up- and down-regulation of genes in order to adapt the organism to the new conditions [1]. Paradoxically, the first data for transcriptional response to CO_2-stress for *S. cerevisiae* was published in 2005 [1]. The work investigated the transcriptional response in high CO_2 concentration (79 % (v/v)), analyzed in aerobic and anaerobic glucose-limited continuous cultures [1]. The resulting data confirmed the findings of the other mentioned authors [116,124,125,127], that elevated CO_2 concentrations lead to a decrease in biomass yield and could also show that anaerobic cultures are less sensitive than aerobic [1]. Contrary to Kuriyama et al. [127] there was no ethanol formation, but a succinate production was measured. That was confirmed by a publications released five years later, which showed, that CO_2 enrichment had a positive effect on the production of malate and succinate in *S. cerevisiae* [128]. Furthermore Aguilera et al. showed that 50 % of the affected genes of the aerobic and C-limited culture, which changed their transcript level, when treated with CO_2, were encoding mitochondrial proteins. Other authors conducted experiments in glucose/ethanol-limited chemostat, where the CO_2 concentration in the in-gas was increased from 0.04 to 1 % (v/v) and showed that the storage sugars of *S. cerevisiae* were transiently mobilized [20,129]. Also Aboka et al. (2012) measured a decrease in glycogen and trehalose content, during a 50 % shift-up in *qGlc* (biomass specific glucose uptake rate) in a continuous aerobic culture, that resulted in elevated dissolved CO_2 concentrations, because qCO_2 tripled [130]. Then in 2014, Richards et al. investigated the transient and long-term carbon dioxide-stress response of *S. cerevisiae* in aerobic chemostat cultures [29]. The

work also showed a mobilization of storage sugars and ethanol, acetate and succinate secretion during a CO_2 shift-up. Furthermore, they found an energy drain generated by increasing CO_2 levels and they pointed out that yeast may adapt to high CO_2 concentrations on the long- term.
Garcia-Gonzalez et al (2007) reviewed hypothetical explanations, on why pressurized CO_2 has a bacteriostatic effect, but also pointed out, that the exact mechanism is still unclear: firstly, CO_2 dissolves itself in the surrounding liquid; secondly, it diffuses itself into the plasma membrane, where it may accumulate and lead to modifications that increase its fluidity ("anastesia effect"); thirdly, CO_2 enters the intracellular space, where it dissociates and leads to pH decrease. Fourthly, the decrease of intracellular pH inactivates enzymes followed by the inhibition of cellular metabolism. Fifthly, CO_2/HCO_3^- directly inhibits the metabolism by activating and inactivating enzymes. Sixthly, the electrolyte balance is disordered, by elevated HCO_3^- levels and seventh, CO_2 may extract cell compounds out of the cell [122]. The same explanations were also used to explain the effect of CO_2 on *S. cerevisiae* (reviewed by [116]). Unfortunately, none of these mechanisms could be proven up to now, and therefore the inhibitory effect of CO_2 on *S. cerevisiae* remains unknown.

7 OBJECTIVE

Although lot of works have been published, dealing with carbon dioxide and its impact on *S. cerevisiae* , nowadays only little is known about the molecular mechanism involved in CO_2 sensitivity. Several hypotheses have been formulated to explain the negative effect of CO_2, but they remain to be proven. Therefore the overarching objective of this work is to further investigate the impact of CO_2 on *S. cerevisiae* for short and long-term response to achieve more knowledge about the adaption process of yeast to high CO_2 concentration published [29].

The following targets were set to achieve the objective:

- conduction of two stimulus response experiments, where the in-gas composition of an aerobic and carbon-limited continuous fermentation (D=0.05 1/h) is shifted from 0.06 to 50 % (v/v) CO_2,
- analysis of intracellular amino acid content before and after the CO_2 shift via reversed phase high presser liquid chromatography (RP-HPLC),
- analysis of the nitrogen to carbon ration of the biomass before and after the CO_2 shift via N/C-analyzer,
- analysis of the filtrate derived from the fermentation broth before and after the CO_2 shift via RP-HPLC,
- analysis of the biomass dry weight of the fermentation broth before and after the CO_2 shift and
- analysis of the intracellular glycogen and trehalose content before and after the CO_2 shift.

The subject of this master thesis is part of the dissertation of Gerhard Eigenstetter, where physicochemical and physiological effects of CO_2/HCO_3^- on *S. cerevisiae* are investigated.

8 MATERIAL AND METHODS

8.1 MATERIAL

8.1.1 CHEMICALS

Table 1: List of applied chemicals

Chemicals	Company
AIBA (2-aminoisobutyric acid), 98 %	Sigma Aldrich, Germany
L-asparagine, ≥ 99.0 % (NT)	Sigma Aldrich, Germany
18-amino acid mix	Sigma Aldrich, Germany
acetone, ≥ 99.8 %	Carl Roth GmbH & Co. KG, Germany
acetonitrile, ≥ 99.9 %	Carl Roth GmbH & Co. KG, Germany
acidic acid, ≥ 99.7 %	Sigma Aldrich, Germany
agar-agar, BioScience, granulated	Carl Roth GmbH & Co. KG, Germany
ammonium sulfate, ≥ 99 %	Carl Roth GmbH & Co. KG, Germany
amyloglycosidase, 6000U/ml	Böhringer, Germany
antifoam solution, struktol	Schill and Seilacher, Germany
biotin (vitamin B7), ≥ 98.5 %	Sigma Aldrich, Germany
calcium chloride dihydrate, ≥ 99 %	Sigma Aldrich, Germany
calcium penthotenate (vitamin B5), > 99 %	Sigma Aldrich, Germany
cobalt(II) chlorid hexahydrate, ≥ 98 %	Sigma Aldrich, Germany
copper sulfate pentahydrate, ≥ 99.5 %	Carl Roth GmbH & Co. KG, Germany
D-(+)-trehalose dihydrate, ≥ 99 %	Sigma Aldrich, Germany
ddH_2O, ROTISOLV® HPLC Gradient Grade	Carl Roth GmbH & Co. KG, Germany
dipotassium hydrogenphophate, ≥ 98 %	Carl Roth GmbH & Co. KG, Germany
disodium hydrogenphosphate dihydrate, ≥ 99.5 %	Sigma Aldrich, Germany
D-malic acid, analytical standard	Sigma Aldrich, Germany
EDTA, ≥ 99 %	Carl Roth GmbH & Co. KG, Germany
ethanol, ≥ 99.8 %	Carl Roth GmbH & Co. KG, Germany
gamma-aminobutyric acid, for HPLC, ≥ 97.0 %	Sigma Aldrich, Germany
glycerine, ≥ 99.5	Carl Roth GmbH & Co. KG, Germany
HCl, ACS reagent, 37 %	Sigma Aldrich, Germany
ironsulfate heptahydrate, ≥ 99.5 %	Merck KGaA, Germany
L-glutamine, ≥99.0% (NT)	Sigma Aldrich, Germany
L-ornithine monohydrate, ≥ 99.0 % (AT)	Sigma Aldrich, Germany
L-tryptophane, ≥ 99.0 % (NT)	Sigma Aldrich, Germany
L-norvalinee, ≥ 99 %	Sigma Aldrich, Germany
L-phenylalanine, 99 %	Sigma Aldrich, Germany
magnesium sulfate heptahydrate, > 99 %	Carl Roth GmbH & Co. KG, Germany
maltose monohydrate, ≥ 95 %	Merck KGaA, Germany
manganese(II)chlorid dihydrate, ≥ 99 %	Merck KGaA, Germany
methanol, CHROMASOLV®, for HPLC, ≥ 99.9 %	Sigma Aldrich, Germany

myo-inositol, ≥ 99 %	Sigma Aldrich, Germany
nicotinic acid (vitamine B3), ≥ 98 %	Sigma Aldrich, Germany
p-aminobenzoic acid, ≥ 99 %	Sigma Aldrich, Germany
peptone	Carl Roth GmbH & Co. KG, Germany
phosphoric acid, for HPLC, 85 %	Sigma Aldrich, Germany
potassium dihydrogenphosphate, ≥ 98%	Carl Roth GmbH & Co. KG, Germany
potassium hydroxyde, ≥ 85 %	Carl Roth GmbH & Co. KG, Germany
potassium iodide, ≥ 99 %	Merck KGaA, Germany
potassium sufate, , ≥ 99%	Carl Roth GmbH & Co. KG, Germany
pyridoxal HCl (Vitamin B6), ≥ 98 %	Sigma Aldrich, Germany
sodium acetate, ≥ 99 %	Merck KGaA, Germany
sodium azide , ≥ 99.5 %	Sigma Aldrich, Germany
sodium carbonate, ≥ 99.0 %	Sigma Aldrich, Germany
sodium chloride, ≥ 99.5 %	Merck KGaA, Germany
sodium hydroxyde, ≥ 99 %	Carl Roth GmbH & Co. KG, Germany
sodium L-lactate, ≥99.0% (NT)	Sigma Aldrich, Germany
sodium molybdate dihydrate, ≥ 99.5 %	Sigma Aldrich, Germany
sodium succinate dibasic hexahydrate, ≥ 99.0 % (NT)	Sigma Aldrich, Germany
sodium sulfate decahydrate, ≥ 99 %	Carl Roth GmbH & Co. KG, Germany
sodium tetraborate decahydrate, ≥ 99.5 %	Sigma Aldrich, Germany
sulphuric acid, 95-98% and for HPLC 49-51 %	Sigma Aldrich, Germany
thiamine HCl (Vitamin B1), ≥ 99 %	Sigma Aldrich, Germany
trehalase, 1.4 units/mg protein	Sigma Aldrich, Germany
yeast extract from *S.c.* type I	Sigma Aldrich, Germany
zinc sulfate heptahydrate, ≥ 99 %	Sigma Aldrich, Germany
α-D-glucose monohydrate, ≥ 99.5 %	Carl Roth GmbH & Co. KG, Germany

8.1.2 INSTRUMENTS

Table 2: List of applied instruments

Instrument	Name	Company
areometer	1.000-1.100 g/mL	Carl Roth, Germany
autoclave	PACS 2000	Getinge Group, Germany
	DX-23	Systec GmBH, Germany
balance	2151WC	Hardy Instruments, USA
	PM6100	Mettler-Toledo GmbH, Germany
	PG 8001-S	
	PM600	
bioreactor	KLF200	Bioengineering AG, Switzerland
C/N-analyzer	Multi N/C 2100s	Analytik Jena, Germany
centrifuge	5417 R	Eppendorf AG, Germany
	Avanti J-25	Beckman Coulter GmbH, Germany

cryostat	instrument	F33	Julabo GmbH, Germany
	cooling agent	TYFOXIT F50	Tyfo, Germany
drying chamber		UT 6200	Heraeus Holding GmbH, Germany
evaporator		RVC 2-33 IR	Christ, Germany
fotomerter		Dr. Lange DR 2800	Hach Lange GmbH, Germany
freezer		Comfort NoFrost	Liebherr GmbH, Germany
		Liebherr Premium	
fridge		ERN16510	Electrolux GmbH, Germany
		FSK3610	Liebherr GmbH, Germany
gasmixer		Digamix M300a	H. Wösthoff GmbH, Germany
HPLC for amino acids	Agilent 1200 series		Agilant Technologies, USA
	pre-column	Zorbax Eclipse Plus C18, Guard Columns, 4.6 x 12.5 mm, 5 µm	
	column	Zorbax Eclipse Plus C18, 4,6 x 250 mm, 5 µL	
	fluorescence detector	G1321A	
HPLC for sugars, organic acids and ethanol	Agilent 1200 series		
	diode array detector	G1315B DAD	
	colmn	Zorbax Eclipse XDB-C18 993967-907	
	pre-column	Zorbax Eclipse XDB-C18 820950-925	
magnetic stirer		R1000	Carl Roth GmbH & Co. KG, Germany
		big squid white	IKA Werke GmbH & Co. KG, Germany
mass flow controller		GFC171S	Analyt-MTC GmbH, Germany
		TG 3/5	Ritter, Germany
mixer		Vortexer M10	VWR international GmBH, Germany
offgas analyzer		BlueSens RS232	BlueSens GmbH, Germany
overhead shaker		CMV-ROM	Ltf-Labortechnik, Germany
peristaltic pumps		120U	Watson Marlow GmbH, Germany
		101 U/R	
		101 U	
pH probe		408-DPAS-SC-K8S/200	Mettler-Toledo GmbH, Germany
pipettes		Eppendorf Research 0.5 - 10 µL	Eppendorf AG, Germany
		Eppendorf Research 10 - 100 µL	
		Eppendorf Research 100 µL	
		Eppendorf Reference 100 µL	
		Eppendorf 200 µL	

	Eppendorf Research 100 - 1000 µL	
	Eppendorf Research 500 - 5000 µL	
pO_2 probe	InPro® 6800	Mettler-Toledo GmbH, Germany
pressure sensor	PR-35 X HAT	KELLER Druckmesstechnik, Germany
shaking table	G-53	New Brunswick Scientic Co.,Inc., USA
sonicator bath	Sonorex super RK 510	Bandeln, Germany
temperature sensor	Pt 100	Bioengineering, Switzerland
thermomixer	Eppendorf Thermomixer 5436	Eppendorf, Germany
water bath	MS / M6 Lauda	LAUDA GmbH & Co. KG, Germany

8.1.3 EQUIPMENT

Table 3: List of applied equipment

Equipment	Name	Company
air filter	Midisartr200	Sartorius AG, Germany
buffeled shake flasks	0.5 L, 1 L and 2 L	Schott AG, Germany
centrifuge tubes	15 mL centrifuge tubes with screw caps, REF N459.1	Carl Roth GmbH & Co. KG, Germany
	50 mL centrifuge tubes with screw caps, REF N463.1	Carl Roth GmbH & Co. KG, Germany
centrifuge vessels (glas)	LP41.1	Carl Roth GmbH & Co. KG, Germany
cryo vessels	LCR20-AG-SB-YS	National Lab BmBH, Germany
glass bottles	0.2 L, 0.5 L, 1 L and 2 L	Schott AG ,Germany
HPLC vessels	SCREW TOP VIAL KIT 2 mL	Brown Chromatography Supplies GmbH, Germany
	200 µL insert	
pipette tips	5 mL (epT.I.P.S. standard/bulk 100-5000)	Eppendorf AG, Germany
	1 mL (ITEM number 686290)	Greiner Bio-One GmbH, Germany
	100 µL (ITEM number 685290)	
	10 µL (MultirKRISTALL 2393.1)	Carl Roth GmbH & Co. KG, Germany
polystyrole cuvette	ArtNo. 2712120	Ratiolab GmbH, Germany
	REF 67.742	Sarstedt AG & Co., Germany
sterlile filter	PTFE 0.2 µm	Sartorius AG, Germany
vessels	Safe-Lock Tubes 1,5 mL	Eppendorf AG, Germany
	SafeSeal Reargiergef. 2 mL, PP	Sarstedt AG & Co., Germany

Table 4: List of applied software

Type	Name	Company
process control system	LabVIEW 8.2	National Instruments, USA
HPLC software	ChemStation for LC 3D Systems	Agilent Technologies, USA

8.1.4 ORGANISM

In this work, the *S. cerevisiae* strain CEN.PK 113-7D obtained from the Institute of Centraalbureau voor Schimmelcultures Fungal Biodiversity Centre of the Royal Netherlands Academy of Arts and Sciences was applied. The organism is wildly used in industry and science in the field of Metabolic Engineering and Systems Biology. The strain is haploid (mating type a) with the genotype described in Table 5.

Table 5: Description of the genotype of the *S. cerevisiae* strain CEN.PK 113-7D [131].

Gen	Description
MATa	mating type locus a
URA3	codes ortidine-5ʹphosphate decarboxylase, involved in de-novo biosynthesis of pyrimidine nucleobases
HIS3	codes imidazoleglycerol-phophate dehydratase, involved in histidine biosynthesis
LEU2	codes beta-isopropylmalate dehydrogenase, involved in leucin biosynthesis and the glyoxylate cycle
TRP1	codes phophoribosylanthranilate isomerase, involved in tryptophan biosynthesis
MAL2-8c	codes a multigene complex for maltose fermentation
SUC2	codes Invertase (sucrose hydrolyzing enzyme)

8.2 ASSEMBLING OF THE BIOREACTOR

The main elements of the fermentation facility consisted of the bioreactor, the exhaust-gas-module, the process control system, the in-gas-module and the harvesting-module (Figure 1).
The 3 L cylindrical shaped bench-top bioreactor (KLF 200, 1.5 L working volume) used for this work was made of stainless steel with a glass window. The agitator shaft was extended from the bottom plate through the mechanical seal into the bioreactor. A rushton-turbine with six stirring blades was fixed to the agitator shaft. The distance between every blade was 6 cm (measured from the top edge on). Inside the bioreactor baffles were installed, to increase the turbulence during fermentation.
The top and the base plates of the bioreactor had eight connection possibilities. Connectors, which were not used, were sealed with blind plugs. On the top plate the base (5 M KOH), the feed (8.3.2.6 Feed Medium), the acid (10 % H_2SO_4), the antifoam solution (Struktol) and the harvesting-module (Figure 1) were connected to the bioreactor. A manually adjustable pressure relief valve that opened when the bioreactor reached a certain threshold (1.5 bar overpressure) was placed on the top of the bioreactor. The harvesting-module (Figure 1) consisted of a riser pipe, a pump and a waste barrel. The pump was connected to the balance (2151WC), on which the bioreactor was placed to achieve constant dilution rate during a chemostat experiment (see 8.4.4 Continuous Fermentation). When the bioreactor weight rose up to +10 g (0.65 % of working volume) during a continuous fermentation, the pump was turned on to compensate the excess weight. The acid and the base were also located on balances (PM6100 and PM600), to give an overview of consumption.
Pumps were used for the acid, the base, the antifoam, the feed and for the waste. All of them were peristaltic pumps (120U und 101U/R). The tube diameters were selected to meet the requirements for accurate pump capacities (depending on the pump).
Within the bioreactor shell the pH and pO_2 probe (408-DPAS-SC-K8S/200 and INGOLD), the sampling-module, which was electrically operated and had adjustable sampling times and the filtrate-module were located on the shell of the bioreactor. The manually openable filter-module consisted of a ceramic filter and a pump. It allowed passage of particles smaller than 0.22 µm.

On the bottom plate of the bioreactor an outlet valve was located, to release liquids out of the bioreactor. The heating element and the water cooler (both connected to the temperature sensor (Pt 100)) were located at the bottom of the bioreactor as well.
The bioreactor was operated either with compressed air or with a gas-mixture of nitrogen, oxygen and carbon dioxide. These in-gas flows were set by mass flow controllers (GFC171S).
The inlet gas must flow through a 0.2 µm PTFE filter before it entered the bioreactor through a frit placed underneath the agitator shaft (Figure 1).
The exhaust-gas-module (Figure 1) consisted of two sensors: one for CO_2 and one for O_2 (BlueSens RS232). Before the exhaust-gas reached the sensors, it must flow through a counter-flow-cooler, so that the moisture condensed. Then the flow passed a cellulose filter (Midisart2000) and another cooler with integrated water trap, which equilibrated the gas temperature. Finally, the gas reached the sensors (Figure 1).
The CO_2 sensor was limited to 100 000 ppm maximum concentration. An interposed gas mixer (Figure 1) (Digamix M300a) provided sufficient dilution (1:10) to shift CO_2 exhaust-gas concentration from over 500 000 ppm back to sensor range.
The facility was furnished with temperature, pressure and pH control. The pH probe, pressure sensor (PR-35 X HAT), temperature sensor and the pO_2 probe (InPro® 6800) were connected to the process control system (based on LabVIEW 8.2).

Parallel to the fermentations of this work (always in reactor 1) other fermentations were performed using the same gas-mixture than for these fermentations (reactor 2) (Figure 1).

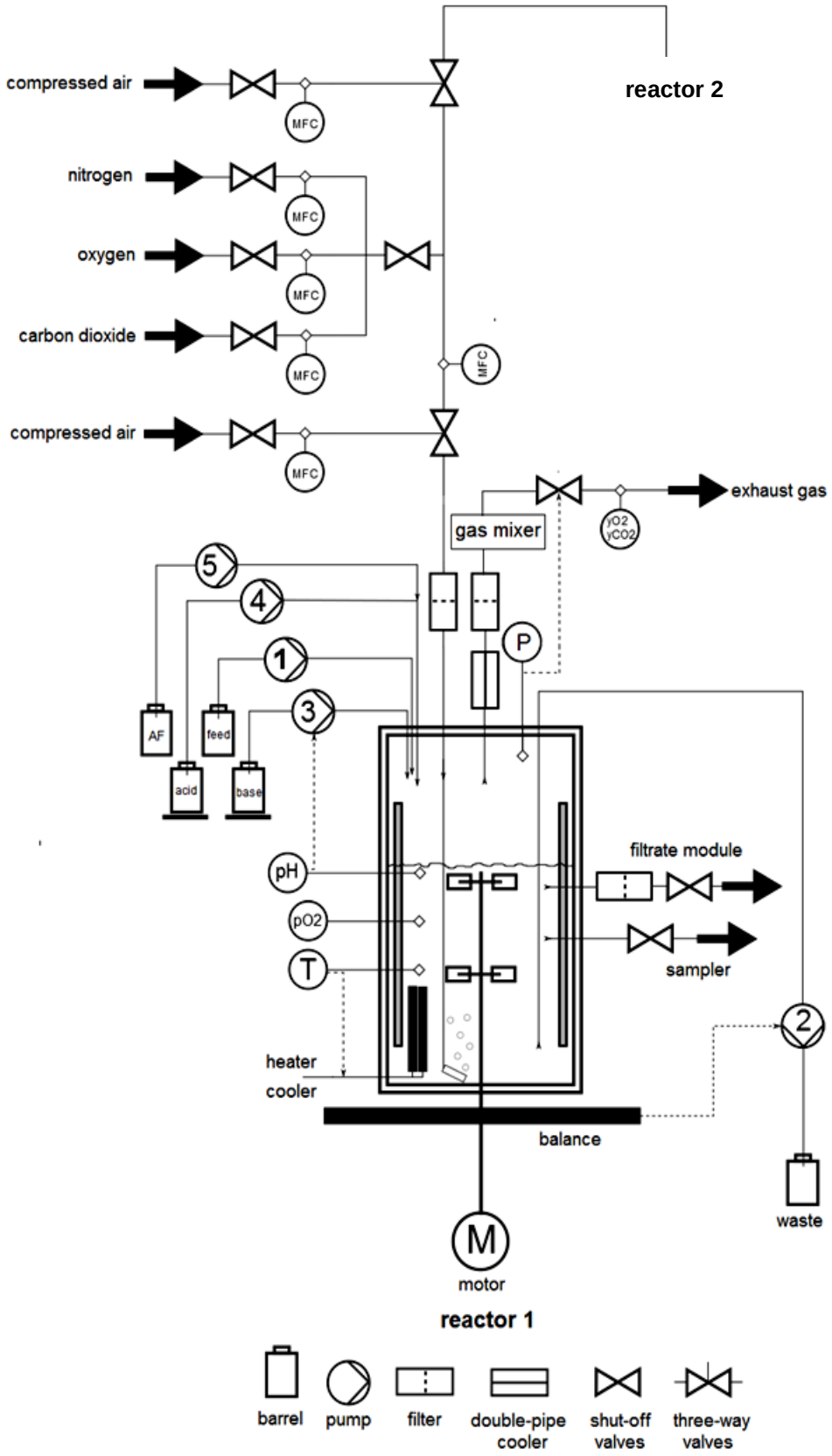

Figure 1 : Bioreactor setup: including bioreactor, exhaust-gas-module (yO_2 yCO_2), the process control system, the in-gas-module and the harvesting-module. Peristaltic pumps: 1 for the feed, 2 for the waste, 3 for the base, 4 for the acid and 5 for the antifoam (AF). Gas-mixture (nitrogen, oxygen and carbon dioxide) or compressed air as inflow gas were controlled by a mass flow controller (MFC) and entered the bioreactor through a sterile filter. The system was furnished with a pH probe and control, a pO_2 probe, a temperature (T) sensor and control and pressure (P) sensor and control. (inspired by [132]).

8.2.1 COMPOSITION OF MEDIA AND ELUENTS

Table 6: Composition of trace element solution (SEL) for every medium according to [133].

Substance	Final concentration [g/L]
Na_2EDTA	15
$ZnSO_4 \times 7H_2O$	4.5
$MnCl_2 \times 2H_2O$	1
$CoCl_2 \times 6H_2O$	0.3
$CuSO_4 \times 5H_2O$	0.3
$Na_2MoO_4 \times 2H_2O$	0.4
$CaCl_2 \times 2H_2O$	4.5
$FeSO_4 \times 7H_2O$	3
H_3BO_3	1
KI	0.1

Table 7: Composition of the vitamin solution for every medium [modified after [133].

Substance	Final concentration [g/L]
biotin	0.05
Ca-pantothenate	1
nicotinic acid	1
thiamine HCl	1
pyridoxol HCl	1
p-aminobenzoic acid	0.2
myo-inositole	25

Table 8: Composition of YPG-medium for the initial cultivation of strain CEN.PK 113-7D. Prepared in demineralized water.

Substance	Final concentration [g/L]
glucose	40
peptone	5
yeast extract	5
agar (solid medium only)	15

Table 9: Composition of pre-cryo medium, prepared in demineralized water.

Substance	Final concentration
$(NH_4)_2SO_4$	30 g/L
K_2HPO_4	5 g/L
KH_2PO_4	12 g/L
SEL	4 mL/L
vitamin solution	4 mL/L
glucose	40 g/L
$MgSO_4$	2 g/L

Table 10: Composition of cryo-medium prepared in demineralized water.

Substance	Final concentration
glucose	10 g/L
$(NH_4)_2SO_4$	7.5 g/L
K_2HPO_4	1.25 g/L
KH_2PO_4	3 g/L
SEL	1 mL/L
vitamin solution	1 mL/L
glycerin	15 g/L
MgSO4	0.5 g/L

Table 11: Composition of pre-culture medium prepared in demineralized water.

Substance	Final concentration
$(NH_4)_2SO_4$	5 g/L
K_2HPO_4	3 g/L
KH_2PO_4	1.25 g/L
SEL	1 mL/L
vitamin solution	1 mL/L
glucose	10 g/L
$MgSO_4$	0.5 g/L

Table 12: Composition of the batch medium, prepared in demineralized water.

Substance	Final concentration
$(NH_4)_2SO_4$	6.67 g/L
KH_2PO_4	4 g/L
SEL	1.33 mLl/L
vitamin solution	1.33 mLl/L
glucose	40 g/L
$MgSO_4$	0.67 g/L

Table 13: Composition of the feed medium. Compounds of section A are dissolved, adjusted to pH 5 and sterilized. Solutions of section B are separately sterilized in demineralized water and added to the cooled down mixture of section A.

	Substance	Final concentration	
A	$(NH_4)_2SO_4$	15 g/L	pH 5 (5 M KOH)
	K_2HPO_4	9 g/L	
B	SEL	3 mL/L	
	vitamin solution	3 mL/L	
	glucose	22.5 g/L	
	$MgSO_4$	1.5 g/L	

Table 14: Composition of eluent A for amino acid quantification by RP- HPLC

Substance	Eluent A
$Na_2HPO_4*2H_2O$	3.6 g
$Na_2B_4O_7*10H_2O$	7.6 g
NaN_3	65 mg
50 % (v/v) HCl	to pH 8.2
Final volume (ddH_2O)	**2 L**

Table 15: Composition of eluent B for amino acids quantification by RP-HPLC

Substance	Eluent B
acetonitrile	450 mL
methanol	450 mL
ddH_2O	100 mL

Table 16: Composition of the eluent for the quantification of sugars, organic acids and ethanol.

Substance	Eluent
50% H_2SO_4 (v/v)	3.5 mL
Final volume (ddH_2O)	**1 L**

8.3 METHODS

8.3.1 PROCESS OVERVIEW

The fermentation process consisted of several stages (Figure 2): preparation of the cryo-culture from the dried culture, the pre-culture inoculated by the cryo-culture, the batch fermentation to generate biomass, the continuous fermentation conducted with compressed air for comparison and finally shift to the continuous fermentation conducted with the gas- mixture (50 % CO_2, 29 % N_2 and 21 % O_2). The amounts of O_2, N_2 and CO_2 in the in-flow were adjusted by the mass flow controllers. The composition of the gas-mixture described below and the dilution rate of 0.05 1/h was chosen, due to preliminary tests (not shown).
The operation conditions for the batch and the continuous fermentation using compressed air and the gas-mixture are listed in Table 17.

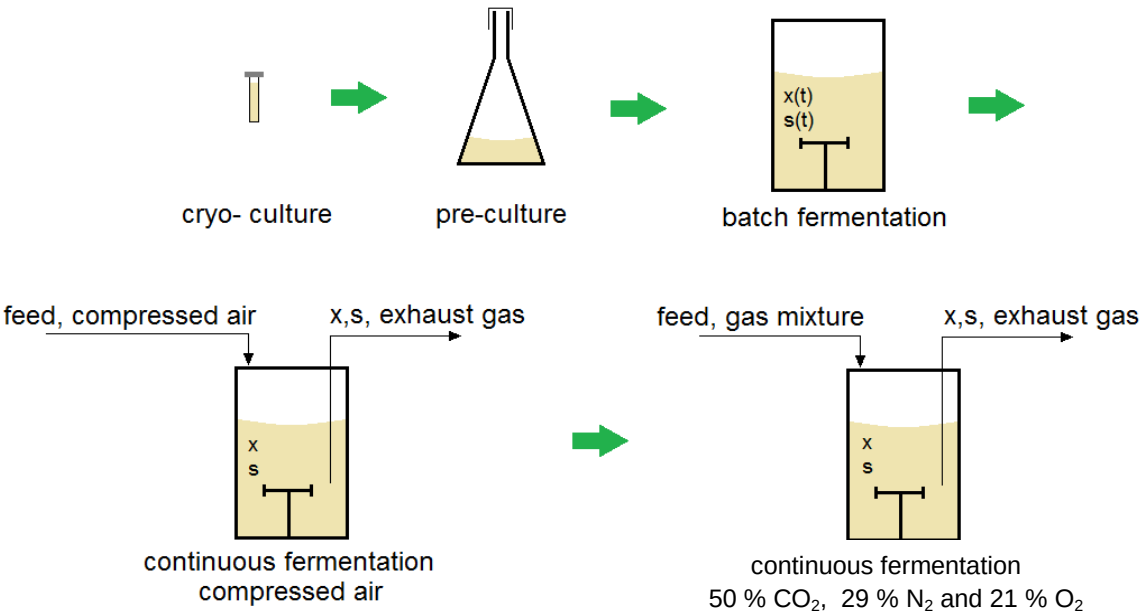

Figure 2: Process overview: the purchased dried *S. cerevisiae* strain CEN.PK 113-7D strain was used to produce the cryo-culture, which was applied for inoculation of the pre-culture. After reaching the exponential phase the pre-culture was transferred together with the batch medium to the fermenter, to start the batch process. Then the process is moved to a continuous fermentation with compressed air. After six residence times the gas inflow was shifted from compressed air to the gas-mixture (50 % CO_2, 29 % N_2 and 21 % O_2) and after six additional residence times the process was finished. (x = biomass and s = substrate)

Table 17: Operation conditions for batch and continuous fermentation.

dilution rate [1/h]	0.05±0.005	
volume of reaction [L]	1.5±0.05	
biomass dry weight concentration [gCDW/L]	~11	
temperature [°C]	30±1	
pH	5±0.1	
agitator speed [rpm]	800±5	
$k_L a$ O_2 [1/h]	700	
pO_2 [%]	70±10	
excess pressure [bar]	0.5±0.005	
gas flow [L/h]	45±2	49.14±3
	air	**gas-mixture**
CO_2 [%]	0.06	50
O_2 [%]	20.93	21
N_2 [%]	79.01	29

8.3.2 PREPARATION OF MEDIA

8.3.2.1 Trace Element Solution (SEL)

The trace element solution was a component of all applied media. The compounds were added in the given order and amount listed in Table 6: after every addition of a chemical the pH was adjusted to 6 (0.1 M NaOH) and finally the pH is adjusted to 4 and filled-up to the final volume with demineralized water. The SEL was sterilized by filtration (0.2 µm) and stored at 4 °C for maximum 4 weeks (ERN16510) [133].

8.3.2.2 Vitamin Solution

The vitamin solution was a component of the all used media. Biotin was dissolved in 0.1 M NaOH and then Ca-pantothenate, nicotinic acid, thiamine HCl, pyrodoxol HCl and p-aminobenzoic acid were added and filled-up to the final volume with demineralized water as listed in Table 7 [modified after 133]. The solution was sterilized by filtration (0.2 µm) and stored at -20 °C (Comfort NoFrost or Liebherr Premium).

.

8.3.2.3 Cryo-Media

The YPG-, pre-cryo and the cryo media were used for the preparation of the storable liquid cryo-culture from the *S. cerevisiae* strain CEN.PK 113-7D (see 8.1.4 Organism). The YPG-medium (Table 8) was prepared by mixing peptone, yeast extract and agar (for solid medium only) with demineralized water and following sterilization in the autoclave (PACS 2000 or DX-23). After the mixture was cooled down the separately sterilized glucose solution was added. The pre-cryo and the cryo-medium on the other hand were prepared by mixing the separately sterilized stock solutions (Table 9 and Table 10). The media were prepared right before use.

8.3.2.4 Pre-Culture Medium

The medium is used for the pre-culture for inoculation of the batch and for producing new cryo-cultures out of old ones. In Table 11 the composition of the media is listed, which is prepared by mixing separately sterilized stock solutions in demineralized water. The pre-culture is storable at 4 °C for maximum 4 weeks.

8.3.2.5 Batch Medium

The separately sterilized stock solutions (prepared in demineralized water), were mixed together (Table 12) to form the batch medium. It was stored at 4 °C for maximum 4 weeks.

8.3.2.6 Feed Medium

For the preparation of 50 L of feed medium 750 g of $(NH_4)_2SO_4$ and 450 g of K_2HPO_4 were dissolved in about four liters of demineralized water to adjust the pH to 5 by using 5 M KOH. After about 30 minutes the pH was checked again and adjusted when necessary. The solution was transferred to a pre-sterilized 50 L barrel to fill it up with demineralized water to a final mass of 46 kg. After sterilization (sterility control: 50 L barrel with the same amount of

water including temperature probe) the barrel was cooled down and the separately prepared sterile supplement solutions were added under the clean bench: 150 mL of SEL (8.3.2.1 Trace Element Solution (SEL)), 150 mL of vitamin solution (8.3.2.2 Vitamin Solution), 2.5 L of a 450 g/L glucose solution and 250 mL of a 300 g/L $MgSO_4$ solution. Finally the missing 950 mL of demineralized water were added to purge all the equipment used and to reach the mass of 50 kg (Table 13).

8.3.3 PREPARATION OF THE BIOREACTOR

After the bioreactor was assembled as it is described in 8.2 Assembling of the Bioreactor, the peripheral devices such as the acid, the base and the antifoam vessels, the feed barrel and the harvesting-module were sterilized separately. Also parts of the bioreactor were sterilized separately: the sampling-module and the filter of the exhausting-gas-module (Figure 1). The needles necessary for the connection of the peripheral devices and the bioreactor by puncturing the septa were packed into sterile metal cases and are autoclaved together with their vessels and tubes.
The bioreactor was assembled and all the connectors awere sealed with plugs and/or septa. Then a pressure test was conducted to check the tightness of the construction. The pH and the pO_2 probes were then calibrated outside of the bioreactor at the operation temperature of 30°C. On the one hand, the pH probe was calibrated by using buffer solutions of pH 4 and 7, and on the other hand, the pO_2 probe was calibrated by using mixed and aerated demineralized water as set point for 100 % and by adding a tip of spatula of sodium sulfate to the demineralized water as set point for 0 %. Then the probes were connected to the bioreactor.

The calibration of the exhaust-gas system was conducted with compressed air (two point calibration) and then checked with standardized gas (5.01 % (v/v) CO_2, 15.00 % (v/v) O_2 and 79.99 % (v/v) N_2).
For further calculations the gas flow was necessary, and therefore it was measured by using a flow meter (TG 3/5). The device determines the volume passed through. The gas meter was connected to the gas flow and after a minimum of 30 minutes the volume was noted. The average of a triplicate divided by the time represents the gas flow of the system.

2 L of a 1 M potassium phosphate buffer pH 7 were prepared by adding 120 mL of 1 M K_2HPO_4 solution and 80 mL of a 1 M KH_2PO_4 solution to a final volume of 2 L with demineralized water and transferred into the bioreactor.

According to the manual of the bioreactor, the mechanical seal at the bottom of the bioreactor was incubated for 30 minutes with buffer before switching on the stirrer. Then the bioreactor was autoclaved by excess pressure of 1.2 bars and 121 °C for at least 30 minutes.

After the bioreactor was sterilized, the in-gas-module (Figure 1) including a 0.2 µm PTFE filter was connected by puncturing the septum with the aid of a flame. Then the filled antifoam, base and acid vessels (the base and acid do not need to be autoclaved, because their sterility is guaranteed by their extreme pH values) were connected and their tubes were filled up with its liquid and locked. The outlet device as the bottom of the bioreactor was sterilized with hot steam before it was opened to drain out the buffer used for sterilization. After additional sterilization of the outlet divice was closed, so that the batch medium were able to be transferred into the bioreactor.

8.4 CONDUCTION OF A FERMENTATION PROCESS

8.4.1 CRYO-CULTURE

To isolate a single colony, the purchased dried yeast strain was cultivated in 10 mL YPG-medium at 30°C, 150 rpm and streaked out on a solid YPG plate, which was incubated until single clones were visible (2-3 days 30°C). Then a single colony was used to inoculate 20 mL of pre-cryo medium. After the exponential phase was reached, the cell suspension was used to inoculate 200 mL of pre-cryo media (Table 9) to a final OD_{600} of 1-2. The culture was harvested by centrifugation at 4 °C, 4000 rpm for 10 minutes (Avanti J-25). From the OD_{600} value of the culture, the amount of cryo-medium need to reach OD_{600} 30 in the final cry-culture was calculated. The needed amount of cryo-medium (Table 10) was then added to suspend the pellet. Finally the suspensions were aliquoted (1mL) into cryo-vessels and stored at -70 °C.
After a cryo-culture was available, it could be used for the generation of further cryo-cultures: the culture was used for inoculation of pre-culture medium (Table 11). When the exponential phase was reached the procedure described above was continued (starting with streaking out the culture on YPG agar plate).

8.4.2 PRE-CULTURE

Two 0.5 L baffled shake flaks were filled with 150 mL pre-culture medium (Table 11) and 0.4 and 0.6 mL of cryo-culture (OD_{600} = 30) were used to inoculate the two flasks (start OD_{600} =0.08 and 0.12). The pre-culture was incubated at 30 °C and 150 rpm until OD_{600} reached values between 1 and 2 within (exponential phase). The pure medium was incubated as well, as sterility control.

8.4.3 BATCH FERMENTATION

The batch phase of the fermentation process was required to produce necessary amount of biomass (14 gCDW/L) for the following continuous fermentation.
The pre-culture with OD_{600} of 1-2 was transferred into the bioreactor, were 1.35 L of batch medium was already adapted at the operation conditions (Table 17). The final volume in the bioreactor was then 1.5 L. The batch was conducted with compressed air as oxygen source and at the mentioned process conditions (Table 17). The passage from compressed air source to the bioreactor was cleared by switching the 3-way valve to the suitable position, while the passage to the gas-mixture was closed.

The batch was finished when all of the glucose of the batch media was consumed. The following starvation phase (5-10 hours) synchronized the start of continuous phase and ensured the complete consumption of secondary carbon sources, which prevented early oscillation in continuous phase.

8.4.4 CONTINUOUS FERMENTATION USING COMPRESSED AIR AND GAS-MIXTURE

The continuous fermentation was conducted in glucose-limited conditions with compressed air as oxygen source, at the general operation conditions listed in Table 17.
After the starvation phase of the batch, the harvesting-module was installed to remove discontinuously fermentation broth during continuous fermentation. The steered feed barrel (
Table 13) (40 rpm) was then connected to the bioreactor to start the continuous fermentation by setting the pumping speed to a value so that the desired flow rate of 0.05 1/h with around 11 gCDW/L

was reached (approximation procedure). In parallel the harvesting- module regulation was switched on. After five residence times (100 hours) a stable steady state was assumed.
After that, the gas mixer was interposed after the first cooling element (Figure 1).Then the 3-way valve was turned into the position, which clears the passage of the gas-mixture (and locks the passage of the compressed air). The inlet gas tubes were separated from the bioreactor to get purged with the gas-mixture (achieved by the three mass flow controllers). The shift started after the inlet gas tubes were connected again with the bioreactor (time point zero). The physiological change of the culture was monitored until a new steady state was assumed after additional six residual times.

8.5 OFFLINE MEASUREMENTS

During conduction of the pre-culture and the batch, only the optical density was measured, while during continuous fermentation the dilution rate, the density of the fermentation broth and the optical density were analyzed, which are described in more detail in the following paragraphs.

8.5.1 DILUTION RATE AND DENSITY

Before a sampling process was conducted, the dilution rate and the density of the fermentation broth were determined. For this purpose a weighted cylinder was used to collect the drained fermentation broth for minimum 30 minutes. The procedure started and terminated after the pump of the harvesting-module turned on. The dilution rate was then calculated from the mass of the fermentation broth, the time and the density of the fermentation broth measured with a density areometer:

$$D = \frac{m_{\text{cylinder full}} - m_{\text{cylinder empty}}}{\rho_{\text{susp.}}\ t\ V_R} \qquad \textbf{Eq. 3}$$

where D [1/h] is the dilution rate, $m_{\text{cylinder full}}$ [g] is the mass of cylinder with fermentation broth, $m_{\text{cylinder empty}}$ [g] is the mass of the empty cylinder, $\rho_{\text{susp.}}$ [g/mL] is the density of the fermentation broth, t [h] is the time of the measurement and V_R [mL] volume of fermentation broth in the bioreactor. V_R was always held constant and controlled by a manually attached marker at the bioreactor and additionally checked at the end of every fermentation externally by a cylinder.

8.5.2 OPTICAL DENSITY (OD_{600})

The optical density delivers a fast estimation of the biomass concentration in the fermentation broth. With the known cx/OD_{600} (biomass dry weight concentration [gCDW/L] per optical density at 600 nm [ ]) relation the cx can be calculated.
First the absorbance of a 0.9 % NaCl solution was measured (triplicate) as blank at 600 nm (Dr. Lange DR 2800). Then the samples were measured in triplicates at 600 nm. When the OD_{600} value was not within the photometer dependent linear correlation of cell count and measured value at 600 nm (0.05-0.3) the sample was diluted in 0.9 % NaCl. The OD_{600} was then calculated from the difference of the arithmetic mean of the blank and the sample, multiplied by the dilution factor of the sample:

$$OD_{600} = (\overline{OD}_{sample} - \overline{OD}_{NaCl}) \cdot F \qquad \textbf{Eq. 4}$$

where $\overline{OD}_{sample}$ [ ] is the arithmetic mean (triplicate) of the absorbance of the sample, $\overline{OD}_{NaCl}$ [ ] is the arithmetic mean (triplicate) of the absorbance of the 0.9 % NaCl solution, both at 600 nm and F [ ] is the dilution factor of the sample.

8.6 Sampling and Sample Preparation during Continuous Fermentation conducted with Compressed Air and Gas-Mixture

In Figure 3 the time points of sampling and the type of samples are shown. There were six types of samples: the methanol quenching samples, glycogen and trehalose samples, biomass dry weight samples, the filtrate, the total inorganic carbon samples and the transcript samples. At residence time five and six of the continuous fermentation with compressed air and with gas-mixture, the same amount of samples was withdrawn (see

Figure 3 for more details). Because of intense sampling during the CO_2 shift, the number of samples was reduced, to ensure a constant bioreactor volume. Therefore at the shift from compressed air to the gas-mixture samples were withdrawn every 10 min until 60 min (process 1 and 2) and then every 20 minutes until 180 min (only process 2).

Before the sampling process was conducted, the sampling times of the electrically operated switch of the sampling-module was determined to sample 1, 2 and 4 mL. For this purpose a weighted vessel was used to sample three times per sampling time the fermentation broth. The average volume and its standard deviation were then calculated by multiplying the density and the mass obtained.
The first fraction was always discarded before sampling to avoid inaccuracies.

In the following, the six types of samples are described in more detail.

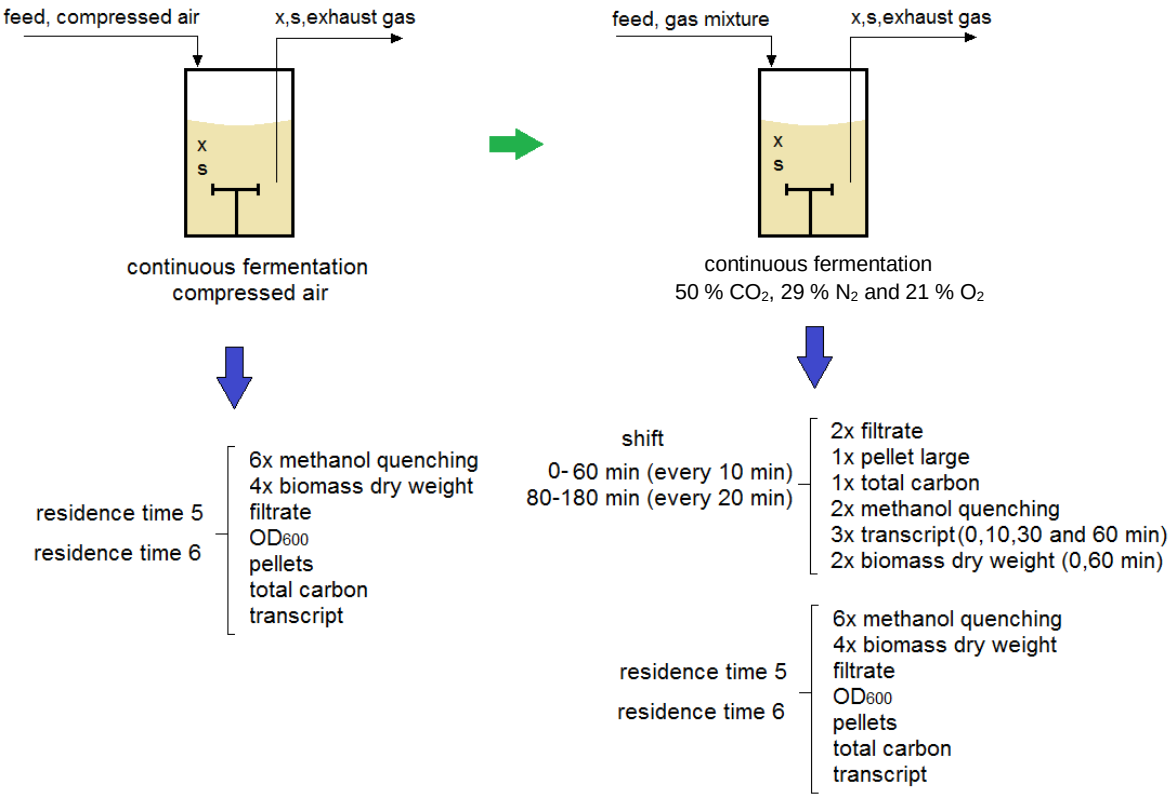

Figure 3: Sampling overview: at the continuous fermentation using compressed air, samples were withdrawn at residence time (RT) 5 and 6. At the continuous fermentation with gas-mixture (50 % CO_2, 29 % N_2 and 21 % O_2) samples were withdrawn during the shift from compressed air and gas-mixture (0-180 min) and at RT 5 and 6.

8.6.1 METHANOL QUENCHING SAMPLES

The quenching solution was produced by mixing 300 mL of methanol with 200 mL of ddH_2O including 7.5 mM γABA (gamma-aminobutyric acid), which resulted in a 60 % methanol solution including 3 mM γABA (as internal standard). Then 6 mL quenching solution per 10 mL vessel were transferred. The exact mass of the quenching solution in the vessels were recorded manually and stored at -70 °C.

3-4 mL of the fermentation broth were transferred into one vessel including 6 mL of quenching solution (used directly after removal out of the freezer) to a final volume of 9-10 mL. After recording the weight the sample was centrifuged at 7 000 rpm at -20 °C for 5 minutes (Avanti J-25). 2 mL of supernatant were kept for further analysis, the remains were discarded. The final pellet was then stored at -70 °C.

Whenever it was possible, the vessels were held in ice or in the cryostat at -20°C. Due to short time intervals during the shift from compressed air to the gas-mixture, only a duplicate was conducted. At steady state conditions the methanol quenching was carried out sixfold.

8.6.2 BIOMASS DRY WEIGHT

The determination of the biomass dry weight was conducted fourfold per sample. The glass vessels (LP41.1) were stored in a drying chamber at 120 °C until the mass was constant. Before sampling, the vessels were stored in ice and then 5 mL of fermentation broth were transferred per vessel and centrifuged at 4000 rpm, at 4 °C for 5 minutes (Avanti J-25). The supernatant was discarded and the pellet was washed three times with 5 mL of 0.9 % (w/v) NaCl solution (same centrifugation conditions than before). The washed biomass pellets were then stored in the drying chamber at 120 °C for two days to remove the water. After cooling in the desiccator to reach room temperature, the vessels were weighted again.

The concentration of biomass dry weight per liter and the standard deviation was calculated from these data (8.8.1 Biomass Dry Weight).

8.6.3 FILTRATE OF THE FERMENTATION BROTH

The filtrate was sampled by using the filtrate-module. The connection between bioreactor and module was opened and the pump was switched on manually. The fermentation broth then passed the ceramic filter, where the biomass was separated from the filtrate. The first 2 mL of filtrate were discarded and the next 2 mL were sampled and stored at – 20°C.

8.6.4 BIOMASS PELLETS FOR GLYCOGEN AND TREHALOSE ASSAY AND THE DETERMINATION OF NITROGEN TO CARBON RATIO

2 mL of fermentation broth was sampled into a 2 mL ice cold vessel and centrifuged for 5 minutes at 14 000 rpm and 4 °C (5417 R). The pellets were washed twice afterwards with 0.9% NaCl solution at the same operation parameters than before and stored at -20 °C. The pellets were used for glycogen and trehalose assay and for the determination of the total carbon and total nitrogen amount with the C/N-analyzer.

8.6.5 Samples for Total Inorganic Carbon (TIC) Measurement

500 µL of 5 M KOH were transferred into a 10 mL graduated flask filled-up with 5-8 mL of demineralized water. Then 1 mL of fermentation broth was transferred through a tube directly in the bottom of the liquid. The KOH captures the carbon dioxide in the liquid, for accurate measuring of inorganic carbon with the C/N-analyzer [134]. The suspension was then filled-up to 10 mL, mixed and transferred into 2 mL vessels and frozen quickly by holding the filled vessel into liquid nitrogen for a few seconds. Then the vessels were stored at -70 °C. The procedure was conducted in duplicates at steady state conditions. During the shift from compressed air to the gas-mixture only one TIC sample was withdrawn per sampling.

8.6.6 Transcript

0.5 mL of fermentation broth was transferred into a cooled 1.5 mL vessel and centrifuged quickly for five seconds at 14 000 rpm. The rotor of the centrifuge was stored at -20°C for 30 minutes before use. After centrifugation the supernatant was discarded and the biomass pellets in the vessels were shock-frozen in liquid nitrogen and stored at -70 °C.
The sample preparation for transcript analysis was conducted in duplicates.
Within the scope of a master thesis, the transcript samples and their data evaluation were not investigated.

8.7 Analysis of the Filtrate, the Quenching samples and the Biomass Pellets from Continuous Fermentation conducted with Compressed Air and Gas-Mixture

8.7.1 Quantification of the Intracellular Amino Acids

Amino acids were quantified from the quenched pellets. The metabolite fraction was extracted first, and then the methanol was evaporated before the amino acids were quantified by RP-HPLC using a fluorescence detector.

8.7.1.1 Extraction of the Metabolites from the Quenching Samples

First of all the extraction solution was prepared. 250 mL of methanol was mixed with the same amount of a 600 µmol/L norvaline solution (as internal standard in ddH_2O), which resulted in a 50 % (v/v) methanol solution including 300 µmol/L norvaline. The second liquid used for the extraction was chloroform, which was stored at -20 °C along with the methanol solution.

The quenched pellets were stored in the cryostat at -20°C during the metabolite extraction. Then 1 mL of ice cold 50 % (v/v) methanol solution including 300 µmol/L norvaline was added to each pellet. After mixing, 1 mL of ice cold chloroform was added to form a two-phase mixture, which was incubated for 2 hours at -20 °C in a rotation shaker. After incubation the vessels were centrifuged at -20 °C and 7 000 rpm for 10 minutes (Avanti J-25) to form three phases: the chloroform phase on the bottom, cell debris in the middle and on top the methanol phase including most of the metabolites. The upper phase was transferred into a previously weighted 1.5 mL vessel (on ice) for evaporation. The weight of the methanol phase was than determined for following evaporation.

After removing the upper methanol phase a second extraction was performed to identify the quality of extraction. For this purpose again 1 mL of ice cold 50 % (v/v) methanol solution including 300 µmol/L norvaline once again added to the remaining chloroform-cell debris phases. The further procedure was equal to the first extraction described above.

8.7.1.2 Evaporation of the Metabolite Extracts

The metabolites in the methanol phase were quantified by a RP-HPLC. But methanol is a disturbing component for this methodology and therefore needed to be separated. For this purpose the samples were evaporated at 40 mbar at 30 °C (RVC 2-33 IR) as long as the volume was reduced by 50 %, identified by weight.

The supernatant formed by centrifugation of the quenched samples to generate the pellets (8.6.1 Methanol Quenching Samples) were evaporated as well in order to identify the leakage out of the cells during quenching.

The extraction solution (50 % (v/v) methanol including 300 µM norvaline) and the quenching solution (60 % (v/v) methanol including 3 mM γABA) are evaporated as well for further quantification of the internal standards by RP-HPLC.

8.7.1.3 Quantification of Amino Acids by RP-HPLC

The amount of amino acids was determined from the quenching supernatants and from the processed quenching pellets (extracted and evaporated) according to [154]. Additionally the internal standards norvaline and γABA were analyzed in every sample and also in the evaporated extraction- and quenching solutions.

The RP-HPLC for amino acid quantification consisted of an auto-sampler, a pre-column (Zorbax Eclipse Plus C18, Guard Columns, 4.6 x 12.5 mm, 5 µm), a main column (Zorbax Eclipse Plus C18, 4,6 x 250 mm, 5 µL, Agilent, Germany) and an fluorescence detector (G1321A).

1 µL of the sample were injected, derivatized and then separated at the following operation conditions: flow rate of 1.5 mL/min and 40°C. The method worked with a gradient elution, and therefore two eluents were used. Eluents A consisted of 3.6 g Na_2HPO_4 $2H_2O$, 7.6 g $Na_2B_4O_7$ $10H_2O$ and 65 mg NaN_3 filled-up to two liters, with a pH of 8.2 (Table 14). Eluent B consisted of 450 mL acetonitrile, 450 mL methanol and 100 mL ddH2O (45 % :45 % :10%) (Table 15). Both eluents were degassed by using a sonicator bath (Sonorex super RK 510) for 15 minutes.

8.7.1.3.1 Derivatisation

The non-fluorescent ortho-phthaldialdehyde (OPA) forms a fluorescent cyclic isoindole system when in presence of organo-sulphur compounds with primary amino acids under alkaline conditions. Secondary amino acids cannot react with OPA; instead, they react with fluorenylmethyloxycarbonyl chloride (FMOC-Cl) to a fluorescent carbamate derivate. These derivatization reactions were conducted in the pre-column. 36 different amino acids can be detect with this method in one run [135].

The metabolite extracts were diluted 1:20 and the supernatants 1:2 in ddH2O. Additionally AIBA (2-aminoisobutyric acid) was added as internal standard to a final concentration of 100 µM.

8.7.1.3.2 Calibration

For the calibration an 18-amino acid (AA) mix was used for the stock solution, the three missing AA (L-glutamine, L-asparagine and L-tryptophane) were added to the mix, as well as L-ornithine, γABA and L-norvaline to cover the spectrum of amino acids may present in the samples. The final concentration of every AA in the stock solution was 400 µM. The stock solution was then used to prepare concentration levels from 400-1 µM including 100µM AIBA as internal standard (Table 18).

Table 18: Composition of the concentration levels for quantification of amino acids by RP-HPLC.

c(AA) [µM]	V(stock AA-mix, 400 µM) [µL]	V(ddH_2O) [µL]	V(AIBA, 10mM) [µL]	V(total) [µL]
400	375.00	120.00	5	500
300	281.25	213.75	5	500
200	187.50	307.00	5	500
100	93.75	401.25	5	500
50	46.88	448.13	5	500
25	23.44	471.56	5	500
15	14.06	480.94	5	500
10	9.38	485.63	5	500
5	4.69	490.31	5	500
3	2.81	492.19	5	500
2	1.87	493.13	5	500
1	0.94	494.06	5	500

8.7.2 QUANTIFICATION OF GLYCOGEN AND TREHALOSE IN CELL PELLETS

The biomass pellets (8.6.4 Biomass Pellets for Glycogen and Trehalose assay and the Determination of Nitrogen to Carbon Ratio) were used to quantify the amount of glycogen and trehalose in the cells. For this purpose they were disrupted and then degraded enzymatically with trehalase or amyloglycosidase to glucose (trehalose fraction) or glucose and trehalose (glycogen fraction) [136]. These final products were then quantified by using reversed phase high performance liquid chromatography (RP-HPLC) with a diode array detector.

8.7.2.1 Cell Disruption

For the quantification of glycogen and trehalose only 1.5 10^8 cells from each pellet were used [137]. The volume containing this amount of cells was removed in duplicates from the resuspended biomass pellet and centrifuged at 14 000 rpm for 5 minutes (5417 R) and the supernatants were discarded. The volume of the cell suspension including 1.5 10^8 cells was calculated by using the volume of the suspension, the cell count per mL and OD_{600} (20226539 yeast cells/mL/OD_{600} [137]) and the sampling volume out of the bioreactor (Eq. 5).

$$V_{1.5\ 10^8} = \frac{1.5\ 10^8 \text{cells}\ V_{\text{suspension}}}{N\ OD_{600} V_{\text{sampling}}} 1000 \qquad \text{Eq. 5}$$

where $V_{1.5\ 10^8}$ [µL] is the volume of cell suspension including 1.5 10^8 cells, $V_{\text{suspension}}$ [mL] is the volume of biomass pellet suspension, V_{sampling} [mL] is the volume of fermentation broth sampled,

OD_{600} [ ] is the optical density at 600 nm of 1 mL fermentation broth and N [cell count/mL /OD_{600}] is the cell count per mL and OD_{600} (20226539 cells/mL/OD_{600}).

The pellets including 1.5 10^8 cells were mixed afterwards with 500 µL of 0.25 M Na_2CO_3 and were incubated for 2 hours at 100 °C in the water bath (MS / M6 Lauda). Then 300 µL of 1 M acidic acid was added to reach pH 5.2±0.2 and 400 µL of 0.2 M sodium acetate was added to a final volume of 1.2 mL. The obtained suspension was mixed carefully overhead and then 300 µL were transferred into two fresh vessels for the following enzyme degradation.
The cell disruption was performed in duplicates for each pellet.

8.7.2.2 Enzymatic Degradation of Glycogen and Trehalose

Two out of the four vessels including 300 µL disrupted cell suspension were mixed with 2 µL trehalase, which cleaves trehalose into two molecules of glucose. The mixture was incubated for minimum 12 h at 37 °C in the thermomixer (10 x 100/min) (Eppendorf Thermomixer 5436).
The disrupted cell suspension of the two remaining vessels were mixed with 5 µL amyloglycosidase solution (1:100 in 0.2 M sodium acetate), which cleaves the glycogen macromolecule into glucose molecules. The mixture was incubated for minimum 12 h at 57 °C in a thermomixer (10 x 100/min) (Eppendorf Thermomixer 5436).
After the enzymatic cleavage all the suspensions were centrifuged for 5 minutes at 14 000 rpm (5417 R) and the supernatants were directly used for quantification by RP-HPLC.

8.7.2.3 Quantification of Glucose and Trehalose by RP-HPLC

To quantify the glucose (trehalose fraction and glycogen fraction) and trehalose (glycogen fraction) in the samples, reversed phase high performance liquid chromatography was used. The HPLC consisted of an auto sampler (G1329A ALS), a pre-column (Rezex ROA-Organic Acid H+ 50 7.8 mm),t he main column (Rezex ROA-Organic Acid H+ 300x7.8 mm, 8 µm) and an refracting index detector (Agilent G1315B DAD, λ= 360nm). 10 µL of the sample were injected and separated with a flow rate of 0.4 mL/min, at 50°C and 26 bar.

The elution mode was isocratic, therefore just a 5 mM H_2SO_4 solution as eluent was used: 3.5 mL of a 50 % (v/v) H_2SO_4 were filled up to 1 L with ddH2O and subsequently degassed by using a sonicator bath for 15 minutes.

8.7.2.3.1 Calibration

A stock solution including 10 mM glucose (0.1803 g glucose (99.9 % in 10 mL ddH_2O) and 10 mM trehalose (0.3783 g trehalose 2 H_2O in 10 mL ddH_2O) was used to prepare concentration levels from 0.05-2 mM (Table 19).

Table 19: Composition of concentration levels for glucose and trehalose quantification by RP- HPLC.

c(glc and tre) [mM]	V(stock, 10 mM) [µL]	V(ddH_2O) [µL]
2	200	800
1	100	900
0.5	50	950
0.4	40	960
0.3	30	970
0.2	20	980
0.1	10	990
0.05	5	995

*glc = glucose, tre = trehalose, stock = stock solution of glucose and trehalose

The samples were analyzed undiluted in duplicates, without any internal standard. Finally the software (ChemStation for LC 3D Systems) generated a chromatogram, by using the calibration, which was then used for data analysis in the end (8.8.6 Glycogen und Trehalose Assay) to calculate the intracellular concentrations of glycogen and trehalose.

8.7.3 Quantification of Sugars, Organic Acids and Ethanol present in the Filtrate (and the Feed)

8.7.3.1 Phosphate Precipitation

High phosphate concentrations in the samples lowers the life cycle of the used column. Therefore the phosphate is precipitated (Eq. 6), when the concentration was estimated to be higher than 5 mM in the samples before performing RP-HPLC analysis.

200 µL of the sample (samples were diluted in ddH_2O before, when phosphate amount was higher than 100 mM) were mixed with 9 µL of 4 M NH_3 (pH 10.2), then 20 µL of 1.2 M $MgSO_4$ were added. After 5 minutes of incubation the mixture was centrifuged for 5 minutes and 13 000 rpm at 4°C (5417 R) to get rid of the precipitate ($MgNH_4PO_4$). 100 µL of the supernatant (pH minimum 9) were mixed with 100 µL 0.1 M H_2SO_4 (final pH < 3) and then incubated for another 15 minutes before it was centrifuged again at 13 000 rpm, at 4°C for 15 minutes. During the procedure the samples got diluted 1:2.29 and were ready for RP-HPLC analysis.

$$3\ NH_3 + 2\ MgSO_4 + K_2HPO_4 + KH_2PO_4 \rightarrow 2\ MgNH_4PO_4 \downarrow + K_2SO_4 + KNH_4SO_4 \qquad \textbf{Eq. 6}$$

Depending on the concentration of the components in the sample, dilution (ddH_2O) was necessary to reach a concentration within the calibration.

8.7.3.2 Quantification of Sugars, Organic Acids and Ethanol by RP-HPLC

For the quantification of sugars, organic acids and ethanol by RP-HPLC the same methodology described in 8.7.2.3 Quantification of Glucose and Trehalose by RP-HPLC was used.

Two stock solutions were prepared for the calibration. The first stock solution contained 1 mM glucose, trehalose, myo-inositole, malate, succinate, lactate, glycerin, acetate and ethanol. The second

contained 10 mM lactate, myo-inositole, malate, succinate, acetate and ethanol. The 1 mM stock was used to prepare the concentration levels for 0.05-1 mM, the second for 5 and 10 mM (Table 20).

Table 20: Composition of stock solution A and B for quantification of organic acids, sugars and ethanol out of the filtrate

	c [mM]	Substances
A	**0.05**	glucose, trehalose, myo-inositole, malate, succinate, lactate, glycerin, acetate, ethanol
	0.1	
	0.2	
	0.3	
	0.4	
	0.5	
	1.0	
B	**5**	lactate, myo-inositole, malate, acetate, ethanol, succinate
	10	

8.7.4 Quantification of Carbon Species and Nitrogen by C/N- analyzer

Quantification of the different carbon species: total inorganic carbon (TIC), total organic carbon (TOC), total carbon (TC) and total nitrogen (TN) were determined from the samples for total inorganic carbon quantification and the biomass pellets by using the C/N-analyzer (Multi N/C 2100s).
The concentration levels were generated with phenylalanine, as source of organic carbon and nitrogen and Na_2CO_3 as source of inorganic carbon. First stock solutions of 2 g/L phenylalanine and 5 g/L Na_2CO_3 in ddH_2O were prepared. The phenylalanine stock consisted of 1.3088 g/L organic carbon and 0.1696 g/L nitrogen, while the Na_2CO_3 stock included 0.5666 g/L inorganic carbon. From the stock solutions concentration levels from 5-1000 mg/L for organic and inorganic carbon and 0.65-129.57 mg/L nitrogen were diluted (Table 21).

Table 21: Composition of concentration levels to quantify TIC, TC, TOC and TN by N/C-analyzer.

conc. level	c (org. and inorg. carbon) [mg/L]	c (N) [mg/L]	V (phenylalanine stock) [µL]	V (Na_2CO_3 stock) [µL]	V (ddH2O) [µL]
13	1000	129.57	1528.14	-	471.86
12	750	97.18	1146.10	-	853.90
11a	500*	64.79	764.07	-	1235.93
11b	500*	-	-	1764.88	235.12
10	250	32.39	382.03	882.44	735.52
9	200	25.91	305.63	705.95	988.42
8	150	19.44	229.22	529.46	1241.31
7	100	12.96	152.81	352.98	1494.21
6	50	6.48	76.41	176.49	1747.10
5	40	5.18	61.13	141.19	1797.68
4	30	3.89	45.84	105.89	1848.26
3	20	2.59	30.56	70.60	1898.84
2	10	1.30	15.28	35.30	1949.42
1	5	0.65	7.64	17.65	1974.71

*only this solutions include either organic or inorganic carbon

Out of these concentration levels, calibration lines for TC, TIC and TN were generated and their linear equations were used to calculate the concentrations of the samples. The concentrations of TOC were always calculated out of the TIC and TC values, by subtracting TIC from TC.

The total carbon samples generated in 8.6.5 Samples for Total Inorganic Carbon (TIC) were thawed and determined undiluted. The pellets generated in 8.6.4 Biomass Pellets for Glycogen and Trehalose assay and the Determination of Nitrogen to Carbon Ratio were suspended in 2 mL of ddH_2O. 200 µL and 100 µL of the suspension were mixed with 1800 µL and 1900 µL ddH_2O (1:10 and 1:20 dilution) to a final volume of 2 mL. All the samples were transferred into C/N-analyzer vessels including a magnetic agitator and analyzed by the C/N-analyzer.

8.8 DATA ANALYSIS

8.8.1 BIOMASS DRY WEIGHT

The samples for the biomass dry weight were conducted fourfold. The average and the standard deviation were calculated out of the four masses and divided by the sampling volume ($V_{sampling}$ [L]), which was 0.005 L to calculate the biomass dry weight concentration of the fermentation broth (cx) in g/L:

$$c_x = \frac{(m_{full} - m_{empty})}{V_{sampling}} \qquad \textbf{Eq. 7}$$

where m_{full} and m_{empty} are the masses [g] of the glass vessels with and without the dried biomass.

8.8.2 DETERMINATION OF THE INTRACELLULAR AMINO ACID POOLS

Because of the complex sample preparation multiplication factors (MF) were specified to calculate the real concentrations of intracellular amino acids. The MF1 was 20, because the samples were diluted 1:20 for HPLC measurement. The MF2 was calculated separately for every value by dividing the mass of the evaporated liquid by the mass of the liquid before the evaporation, therefore MF2 takes the loss of methanol during evaporation into account.
The cells in the quenched biomass pellets contained about 60 % intracellular water and some quenching solution in the cellular interspaces. Because of this additional volume, the norvaline concentration (c^0_{Nor}) of the 50 % methanol solution was up to 25 % higher than the norvaline concentration in the extraction solution of the sample (c^{sample}_{Nor}). This concentration change of the internal standard norvaline mirrors the dilution quantified individually for each sample as MF3 (Eq. 8):

$$MF3 = \frac{c_{norvalin\ solution} - (MF1\ MF2\ c_{norvalin\ sample})}{(MF1\ MF2\ c_{norvalin\ sample})} + V_{susp.} \qquad \textbf{Eq. 8}$$

where $MF3$ [ ] considers the reduction of the amino acid concentration by volume increase , $c_{norvalin\ solution}$ [µM] is the concentration of norvaline in the extraction solution (50 % methanol) before evaporation, $c_{norvalin\ sample}$ [µM] is the concentration of norvaline in the final sample solution of the HPLC quantification (after evaporation) and $V_{susp.}$ is the volume of suspension (1 mL).

The last factor (F) considers the biomass dry weight of the fermentation broth sampled in the 60 % methanol quenching solution:

$$F = c_X \frac{m_{sample}}{\rho_{sample}\ 1000} \quad \textbf{Eq. 9}$$

where m_{sample} [g] is the mass of fermentation broth sampled into the quenching solution, c_X [gCDW/L] is the biomass dry weight concentration in the fermentation broth and ρ_{sample} [g/mL] is the density of the fermentation broth.

Finally the intracellular concentrations of the amino acid were calculated using the four factors:

$$c_{amino\ acid\ real} = \frac{MF1\ \ MF2\ \ MF3\ \ \frac{c_{amino\ acid}}{1000}}{F} \quad \textbf{Eq. 10}$$

where $c_{amino\ acid\ real}$ [mmol/gCDW] is the intracellular concentration of one amino acid per g cell dry weight and $c_{amino\ acid}$ [µM] is the concentration of one amino acid in the sample injected into the HPLC, calculated by using the calibration line [µM].

Table 22: Retention times of the amino acids analyzed by RP-HPLC

Substance	Retention time [min]
aspartate	2.90
glutamate	4.70
asparagine	8.40
serine	9.00
glutamine	10.13
histidine	10.56
glycine	11.24
threonine	11.60
arginine	13.31
alanine	13.97
γABA	14.43
AIBA	14.98
tyrosine	16.25
valine	19.91
methionine	20.31
norvaline	21.00
tryptophane	21.91
phenylalanine	22.69
isoleucine	23.08
ornithine	23.35
leucine	24.34
lysine	24.91
proline	32.06

8.8.3 Determination of Nitrogen to Carbon Ratio (N/C) in the Biomass Pellets and the Total Inorganic Carbon (TIC) in the TIC Samples

Four measurements were conducted by the N/C-analyzer and four areas therefore obtained. The arithmetic mean of the obtained areas for the calibration lines of TC, TIC and TN were subtracted by their corresponding zero samples (ddH_2O) and the linear equations were created.
The areas of the samples were also averaged and subtracted by its zero samples (ddH_2O) and then used to calculate the concentrations from the linear equations. The received concentrations were then converted into the initial bioreactor concentration. The dilution of the sample was therefore considered by multiplication with 10 or 20. The concentration was adjusted as well because the pellets were not diluted in their original sampling volume. The TOC was then calculated by subtracting TIC from TC. The following equation was used to calculate the nitrogen to carbon ration (C/N-ratio) [mNmol/mCmol]:

$$\frac{N}{C} = \frac{\frac{TN}{M_N}}{\frac{TOC}{M_C}} \qquad \textbf{Eq. 11}$$

where the TN [mg/L] is the total nitrogen in the sample, M_N [mg/mNmol] is the molar mass of nitrogen, TOC [mg/L] is the total organic carbon in the sample and M_C [mg/mCmol] is the molar mass of carbon.

8.8.4 Determination of the Henry Coefficient

The Henry coefficient of CO_2 is calculated as stated below:

$$H = \frac{c^L_{CO_2}}{p_{total}\, y_{CO_2}} \qquad \textbf{Eq. 12}$$

where H [mmol/L/bar] is the Henry Coefficient, $c^L_{CO_2}$ [mmol/L] is the concentration of CO_2 in the fermentation broth obtained by the N/C-analyzer ,p_{total} [bar] is the total pressure of the system and y_{CO_2} [ ] is the mole volume fraction of CO_2 in the exhaust-gas above the fermentation broth.

p_{total} was constant and therefore H was obtained graphically with $c^L_{CO_2}$ as the y-axis and y_{CO_2} as the x-axis, where the slope represents the Henry coefficient.

8.8.5 Determination of Sugars Organic Acids and Ethanol in the Filtrate

The peaks generated by the RP-HPLC were integrated by the program (ChemStation for LC 3D Systems) and corrected manually, when the program integrated incorrect. The retention times of all the analyzed substances are listed in Table 23.

Table 23: Retention times of sugars , organic acids and ethanol analyzed by RP-HPLC

Substance	Retention time [min]
trehalose	12.76
glucose	15.26
myo-inositole	15.91
malate	16.36
succinate	20.05
lactate	21.09
glycerin	21.83
acetate	24.70
ethanol	33.47

The program calculated the concentrations of the samples with the data of the calibration line and the areas of the substance peaks. The filtrate samples were measured undiluted.

8.8.6 GLYCOGEN UND TREHALOSE ASSAY

With the data of the calibration line and the areas of the glucose and trehalose peaks the program calculated the concentrations of the samples.
In the trehalose samples the glucose concentration in mM (digested trehalose) and the trehalose concentration in mM (if not completely digested) and in the glycogen samples the glucose concentration in mM (digested glycogen) and the trehalose concentration in mM (not digested by amyloglycosidase) were measured.

In Eq. 13 calculation of % trehalose per g cell dry weight (w_{Tre} [%]) is shown:

$$w_{Tre} = \frac{(c_{Tre\ undig.} + \frac{c_{Glc}}{2})\ V_{1.5\ 10^8}^{dil.}\ M_{Tre}}{c_x\ V_{1.5\ 10^8}}\ 100 \qquad \textbf{Eq. 13}$$

where $c_{Tre\ undig.}$ [mM] is the concentration of undigested trehalose during enzymatic digestion, c_{Glc} [mM] is the concentration of glucose delivered from enzymatic digestion of trehalose, $V_{1.5\ 10^8}^{dil.}$ [L] is the volume in which 1.5 10^8 cells were diluted during the assay (1.2 mL), M_{Tre} [mg/mmol] is the molar mass of trehalose, c_x[mg/mL] is the concentration of biomass dry weight in the fermentation broth and $V_{1.5\ 10^8}$ is the volume of cell suspension including 1.5 10^8 cells [mL].

In Eq. 14 the calculation of % glycogen per g biomass dry weight w_{Gly} [%] is shown

$$w_{Gly} = \frac{c_{Glc}\ V_{1.5\ 10^8}^{dil.}\ M_{Gly}}{c_x\ V_{1.5\ 10^8}}\ 100 \qquad \textbf{Eq. 14}$$

where c_{Glc} [mM] is the concentration of glucose delivered from enzymatic digestion of glycogen and M_{Gly} [mg/mmol] is the molar mass of glycogen.

The specific glycogen degradation/building rate q_{Gly} [mmolGlc/gCDW/h] is calculated as shown in Eq. 15:

$$q_{Gly} = \frac{\left(c_{Gly}^2 - c_{Gly}^1\right)}{(t_2 - t_1)\bar{c_x}} = \frac{\left(w_{Gly}^2 - w_{Gly}^1\right)}{(t_2 - t_1)M_{Gly}} \cdot 1000 \quad \textbf{Eq. 15}$$

where c_{Gly}^1 and c_{Gly}^2 [mM] are the concentrations of glycogen at time point t_1 and t_2 [h], $\bar{c_x}$ [gCDW/L] is the average mean of the biomass dry weight concentration of the two time points. w_{Gly}^1 and w_{Gly}^2 [%] are the percentage of glycogen per g cell dry weight at the two time points (1 and 2).

Analogous to the specific glycogen degradation/building rate, the specific trehalose degradation/building rate q_{Tre} [mmolGlc/gCDW/h] is calculated:

$$q_{Tre} = \frac{(c_{Tre}^2 - c_{Tre}^1)}{(t_2 - t_1)\bar{c_x}} = \frac{(w_{Tre}^2 - w_{Tre}^1)}{(t_2 - t_1)\frac{M_{Tre}}{2}} 1000 \quad \textbf{Eq. 16}$$

8.8.7 MASS-BALANCE OF A CONTINUOUS PROCESS

The mass-balance is based on the law of conservation of mass, which means that the mass entering and leaving the system are equal. The general mass-balance equation is shown in Eq. 17. The equation consists of the mass entering and leaving the system and the mass consumed or generated within the system.

$$\begin{Bmatrix} mass \\ accumulated \\ within\ system \end{Bmatrix} = \begin{Bmatrix} mass\ entering \\ the\ system \\ boundaries \end{Bmatrix} - \begin{Bmatrix} mass\ leaving \\ the\ system \\ boundaries \end{Bmatrix} + \begin{Bmatrix} mass \\ generated \\ within\ system \end{Bmatrix} - \begin{Bmatrix} mass \\ consumed \\ within\ system \end{Bmatrix} \quad \textbf{Eq. 17}$$

In a continuous process the mass accumulation over time is zero, because all properties of the system are constant over time and therefore the system cannot accumulate mass. The general mass-balance equation can be based on rates to form a differential balance:

$$\frac{dm_i}{dt} = \dot{m}_i^{in} - \dot{m}_i^{out} \pm \sigma_i \quad \textbf{Eq. 18}$$

where $\frac{dm_i}{dt}$ [g/h] is the change in mass of compound i over time, $\dot{m}_i^{in}$ [g/h] is the inlet mass flow rate of compound i, $\dot{m}_i^{out}$ [g/h] is the outlet mass flow rate of compound i and σ_i [g/h] is the term for generation or consumption of the mass of compound i. Further m_i and σ_i can be expressed as:

$$m_i = c_i V_R \quad \textbf{Eq. 19}$$

$$\sigma_i = Q_i V_R \quad \textbf{Eq. 20}$$

where c_i [g/L] is the concentration of compound i in the bioreactor, Q_i [g/L/h] is the volumetric generation/consumption rate of compound i and V_R [L] is the reaction volume. In general Q_i can be expressed as:

$$Q_i = q_i\, c_x \quad \textbf{Eq. 21}$$

where q_i is the biomass specific uptake/consumption rate of the compound i [g/gCDW/h].

By inserting Eq. 21 into Eq. 18, Eq. 22 is formed:

$$\frac{dm_i}{dt} = \frac{d(c_i V_R)}{dt} = \frac{dc_i}{dt} V_R + \frac{dV_R}{dt} c_i \qquad \textbf{Eq. 22}$$

In a continuous fermentation the volume of reaction over time is constant, therefore $\frac{dV_R}{dt}$ is zero. And so $\frac{dm_i}{dt}$ is equal $\frac{dc_i}{dt} V_R$.

Further it is assumed that the volumetric flow rate of the inflow $\dot{V}^{in}$ [L/h] and the outflow $\dot{V}^{out}$ [L/h] is equal and donated as F [L/h]. Therefore Eq. 23 is formed:

$$\frac{dc_i}{dt} V_R = F c_i^{in} - F c_i^{out} \pm Q_i V_R \qquad \textbf{Eq. 23}$$

which is the general balance equation for continuous fermentations and is used for further calculations. c_i^{in} [g/L] is the concentration of compound i in the inflow and c_i^{out} [g/L] is the concentration of compound i in the outflow.

Then Eq. 23 is divided by the volume, which leads to:

$$\frac{dc_i}{dt} = \frac{F}{V} \left(c_i^{in} - c_i^{out}\right) \pm Q_i \qquad \textbf{Eq. 24}$$

The term $\frac{F}{V}$ is the dilution rate D [1/h], which is inversely proportional to the average residence time Θ [h]. And finally Eq. 25 is formed:

$$\frac{dc_i}{dt} = D\left(c_i^{in} - c_i^{out}\right) \pm Q_i \qquad \textbf{Eq. 25}$$

Eq. 25 was used as a basis for the calculation of the specific growth rate μ [1/h], the specific substrate uptake rate q_s [g/gCDW/h] and the specific by-product formation rate q_P [g/gCDW/h].

8.8.8 SPECIFIC GROWTH RATES

8.8.8.1 Specific Growth Rate in General

In a closed system (batch or shake flask culture) the change in the biomass concentration over time *cx* [gCDW/L] is described as

$$\frac{dc_x}{dt} = \mu\, c_x \qquad \textbf{Eq. 26}$$

Eq. 27 is formed by integration of Eq. 26 with constant specific growth rate μ [1/h] and with the initial conditions (t_0, c_x^0). It is used for the calculation of the biomass growth in the exponential phase of a certain time.

$$c_x = c_x^0 \, e^{\mu \, t - t_0)} \qquad \textbf{Eq. 27}$$

If the natural logarithm is applied to Eq. 27 and the equation is solved for μ Eq. 28 is formed and used to calculate the growth rate between two certain time points:

$$\mu = \frac{\ln\left(\frac{c_x}{c_x^0}\right)}{t - t_0} \qquad \textbf{Eq. 28}$$

8.8.8.2 Specific Growth Rate in a Continuous Fermentation

If Eq. 25 is applied to biomass, the volumetric biomass production or consumption rate Q_x [gCDW/L/h] is inserted as the product of the specific growth rate μ (=q_x) [g/gCDW/h] and the concentration of the biomass dry weight in the bioreactor cx [gCDW/L] :

$$\frac{dc_x}{dt} = D\left(c_x^{in} - c_x^{out}\right) + \mu \, c_x \qquad \textbf{Eq. 29}$$

where c_x^{in} and c_x^{out} are cell dry weight concentrations of the in- and the outflow of the biomass [gCDW/L]. In this work, no biomass was present in the inflow, therefore c_x^{in} is zero and the equation becomes:

$$\frac{dc_x}{dt} = -Dc_x^{out} + \mu \, c_x \qquad \textbf{Eq. 30}$$

In a continuous fermentation the change in biomass over time at steady state condition is zero and therefore

$$Dc_x^{out} = +\mu \, c_x \qquad \textbf{Eq. 31}$$

and by assuming that the biomass dry weight concentration of the outflow is equal to the biomass dry weight concentration within the bioreactor, it finally leads to

$$D = \mu \qquad \textbf{Eq. 32}$$

8.8.9 SUBSTRATE UPTAKE RATE

The substrate uptake rate is based on the mass-balance described before. Eq. 25 is therefore transformed into:

$$\frac{dc_s}{dt} = D\left(c_s^{in} - c_s^{out}\right) + Q_s \qquad \textbf{Eq. 33}$$

where c_s^{in} and c_s^{out} [g/L] are the concentrations of the substrate of the in- and outflow and Q_s is the volumetric substrate uptake rate [g/L/h].

The volumetric rate of substrate uptake can be generally described as a function of the biomass concentration and the specific substrate uptake rate:

$$Q_s = -q_s\, c_x \qquad \textbf{Eq. 34}$$

It is negative because the substrate is consumed and not produced (see general mass- balance). The Eq. 33 and Eq. 34 are combined to

$$\frac{dc_s}{dt} = D\left(c_s^{in} - c_s^{out}\right) - q_s c_x \qquad \textbf{Eq. 35}$$

In a continuous system the change in concentration of the substrate over time is zero and therefore the equation leads to

$$D\left(c_s^{in} - c_s^{out}\right) = q_s c_x \qquad \textbf{Eq. 36}$$

and after solving for q_s the equation is

$$q_s = \frac{D\left(c_s^{in} - c_s^{out}\right)}{c_x} \qquad \textbf{Eq. 37}$$

where c_s^{out} can also be the concentration of the substrate in the bioreactor at a certain time point.

8.8.10 PRODUCT FORMATION RATE

The product formation rate is based on the mass-balance and therefore Eq. 25 is transformed into:

$$\frac{dc_P}{dt} = D\left(c_P^{in} - c_P^{out}\right) \pm Q_P \qquad \textbf{Eq. 38}$$

where c_P^{in} and c_P^{out} [g/L] are the product concentrations in the in- and the outflow and Q_P [g/L/h] is the volumetric production rate of a certain product. There is no product in the inflow, c_P^{in} is zero and by inserting the specific production rate q_p [g/gCDW/h] multiplied by *cx* for Q_P the equation is transformed into:

$$\frac{dc_P}{dt} = -D\, c_P^{out} + q_p c_x \qquad \textbf{Eq. 39}$$

By assuming that c_P^{out} is equal to c_P inside of the bioreactor and by using the average mean of the two product concentrations at two certain time points ($\overline{c_p^{1,2}}$) instead of c_P and after solving for q_p , the equation becomes:

$$-q_P = \frac{\frac{(c_P^2 - c_P^1)}{(t_2 - t_1)} + D\,\overline{c_p^{1,2}}}{\overline{c_x^{1,2}}} \qquad \textbf{Eq. 40}$$

If there are two different biomass dry weight concentrations at two certain time points, the average mean is used ($\overline{c_x^{1,2}}$).

8.8.11 BIOMASS TO SUBSTRATE YIELD AND MAINTENANCE

The biomass to substrate yield is the amount of biomass formed per amount of substrate consumed. The true (Y_{xs}^{true} , theoretical or stoichiometric) and the apparent (Y_{xs}^{app} , observed) yields are distinguished:

$$Y_{xs}^{true} = \frac{total\ mass\ \ of\ biomass\ formed}{mass\ of\ substrate\ used\ to\ form\ biomass} \quad \textbf{Eq. 41}$$

$$Y_{xs}^{app} = \frac{mass\ \ of\ biomass\ present}{total\ mass\ \ of\ substrate\ consumed} \quad \textbf{Eq. 42}$$

The volumetric substrate uptake rate can also be described as:

$$Q_s = \frac{1}{Y_{xs}} D c_x \quad \textbf{Eq. 43}$$

The substrate taken up in a cell culture may be used for biomass production, product production and for maintenance activities. The specific substrate uptake rate for maintenance activity is defined as the maintenance coefficient ms [gGlc/gCDW/h]. In the mass-balance for the substrate the maintenance is inserted to form:

$$\frac{dc_s}{dt} = D\left(c_s^{in} - c_s^{out}\right) - \frac{1}{Y_{xs}} D c_x - ms\ c_x \quad \textbf{Eq. 44}$$

As mentioned earlier $\frac{dc_s}{dt}$ is zero in a continuous process, therefore the equation is transformed into

$$D\left(c_s^{in} - c_s^{out}\right) = \frac{1}{Y_{xs}} D c_x + ms\ c_x \quad \textbf{Eq. 45}$$

and by solving for cx the equation becomes:

$$c_x = \frac{D\left(c_s^{in} - c_s^{out}\right)}{ms + \frac{D}{Y_{xs}}} \quad \textbf{Eq. 46}$$

Dividing Eq. 46 by $(c_s^{in} - c_s^{out})$, Y_{xs}^{app} is received and is transformed to

$$Y_{xs}^{app} = \frac{c_x}{c_s^{in} - c_s^{out}} = \frac{D}{ms + \frac{D}{Y_{xs}}} = \frac{D Y_{xs}}{ms Y_{xs} + D} \quad \textbf{Eq. 47}$$

The reciprocal of Eq. 47 is therefore

$$\left(\frac{1}{Y_{xs}^{app}}\right) = \frac{ms Y_{xs} + D}{D Y_{xs}} = \frac{m_s}{D} + \frac{1}{Y_{xs}} \quad \textbf{Eq. 48}$$

And by solving for *ms* the equation becomes:

$$ms = \frac{D}{Y_{xs}^{app}} - \frac{D}{Y_{xs}^{true}} \quad \textbf{Eq. 49}$$

which was used to calculate the maintenance in this work. For Y_{xs}^{true} the value of 0.55 was used [161].

8.8.12 OXYGEN UTILIZATION RATE (OUR)

The oxygen utilization rate [mmol/L/h] is based on the mass-balance for oxygen:

$$\dot{V}_G(c_{O_2}^{in})_G = \dot{V}_G(c_{O_2}^{out})_G + Q_{O_2}V_R \quad \textbf{Eq. 50}$$

where $\dot{V}_G$ [L/h] are the volumetric gasflow rates of the in- and outflow, $(c_{O_2}^{in})_G$ and $(c_{O_2}^{out})_G$ [mmol/L] are the concentrations of gaseous oxygen in the in- and outflow, Q_{O_2} is the volumetric oxygen uptake rate [mmol/L/h] and V_R [L] is the reaction volume. By solving Eq. 50 for Q_{O_2}, the following equation is

$$Q_{O_2} = \frac{\dot{V}_G}{V_R}((c_{O_2}^{in})_G - (c_{O_2}^{out})_G) \quad \textbf{Eq. 51}$$

And by inserting the ideal gas law:

$$p\,\dot{V}_G = \dot{n}\,R\,T \quad \textbf{Eq. 52}$$

where p [kg/dm/s^2] is the pressure, $\dot{V}_G$ [L/h] is the volumetric gas flow rate, $\dot{n}$ [mol/h] is the mass flow, R [(kg dm^2)/(s^2 mol K)] is the universal gas constant (8.31 (kg dm^2)/(s^2 mol K)) and T [K] is the temperature. $\dot{n}$ divided by $\dot{V}_G$ is the concentration of oxygen in the gas phase $(c_{O_2})_G$ [mol/L] and by inserting the oxygen volume fraction y_{O_2} [ ] the equation is transformed into:

$$(c_{O_2})_G = \frac{y_{O_2}p}{RT} \quad \textbf{Eq. 53}$$

By inserting Eq. 53 in Eq. 51 the following equation is formed

$$Q_{O_2} = \frac{p}{V_R RT}(\dot{V}_G y_{O_2}^{in} - \dot{V}_G y_{O_2}^{out}) \quad \textbf{Eq. 54}$$

When the volumetric gas in and outflow are not equal Eq. 54 would lead to large errors. Because N_2 is an inert gas, it is not consumed or produced within the bioreactor. Therefore the balance for N_2 is

$$\dot{n}_{N_2}^{in} = \dot{n}_{N_2}^{out} \quad \textbf{Eq. 55}$$

and by inserting the ideal gas law the equation is transformed into

$$\frac{p^{in}}{T^{in}}\dot{V}_G^{in}y_{N_2}^{in} = \frac{p^{out}}{T^{out}}\dot{V}_G^{out}y_{N_2}^{out} \quad \textbf{Eq. 56}$$

Because p and T are equal in the in- and the outflow the equation is transformed into

$$\dot{V}_G^{in}\, y_{N_2}^{in} = \dot{V}_G^{out}\, y_{N_2}^{out} \quad \textbf{Eq. 57}$$

In consideration of oxygen and carbon dioxide as main compounds of the gas phase the mole volume fractions of nitrogen are expressed as

$$y_{N_2}^{in} = 1 - y_{O_2}^{in} - y_{CO_2}^{in} \quad \textbf{Eq. 58}$$

$$y_{N_2}^{out} = 1 - y_{O_2}^{out} - y_{CO_2}^{out} \quad \textbf{Eq. 59}$$

By inserting Eq. 58 and Eq. 59 in Eq. 57 results in:

$$\dot{V}_G^{out} = \dot{V}_G^{in} \left(\frac{1 - y_{O_2}^{in} - y_{CO_2}^{in}}{1 - y_{O_2}^{out} - y_{CO_2}^{out}} \right) \quad \textbf{Eq. 60}$$

and by inserting Eq. 54 results in the final equation

$$OUR = \; Q_{O_2} = \frac{p\dot{V}_G^{in}}{V_R RT} \left[y_{O_2}^{in} - y_{O_2}^{out} \left(\frac{1 - y_{O_2}^{in} - y_{CO_2}^{in}}{1 - y_{O_2}^{out} - y_{CO_2}^{out}} \right) \right] \quad \textbf{Eq. 61}$$

which was used to calculate OUR in this work and the specific oxygen uptake rate was calculated by the following equation

$$q_{O_2} = \frac{OUR}{c_x} \quad \textbf{Eq. 62}$$

8.8.13 CARBON DIOXIDE EVOLUTION RATE (CER)

The carbon dioxide evolution rate [mmol/L/h] is calculated analogous the oxygen utilization rate, where the mass-balance is

$$\dot{V}_G^{in}\, (c_{CO_2}^{in})_G + Q_{CO_2} V_L = \dot{V}_G^{out}\, (c_{CO_2}^{out})_G \quad \textbf{Eq. 63}$$

and by inserting the ideal gas law the equation is transformed into

$$Q_{CO_2} = \frac{p}{V_L RT} \left(\dot{V}_G^{out} y_{CO_2}^{out} - \dot{V}_G^{in} y_{CO_2}^{in} \right) \quad \textbf{Eq. 64}$$

and finally by inserting the inert gas balance the following equation is formed

$$CER = \; Q_{CO_2} = \frac{p\dot{V}_G^{in}}{V_L RT} \left[y_{O_2}^{out} \left(\frac{1 - y_{O_2}^{in} - y_{CO_2}^{in}}{1 - y_{O_2}^{out} - y_{CO_2}^{out}} \right) - y_{O_2}^{in} \right] \quad \textbf{Eq. 65}$$

which was used to calculate CER in this work and the specific carbon dioxide evolution rate was calculated by the following equation

$$q_{CO_2} = \frac{CER}{c_x} \quad \textbf{Eq. 66}$$

8.8.14 RESPIRATORY QUOTIENT (RQ)

The respiratory quotient [ ] was calculated by using the following equation

$$RQ = \frac{OUR}{CER} \quad \textbf{Eq. 67}$$

RQ changes by utilization of different substrates and indicates therefore the physiological situation of microorganisms.

8.8.15 ELEMENTAL CARBON-BALANCE (C-BALANCE)

The elemental C-balance represents a powerful tool to validate the obtained data of the conducted experiments. Substances containing carbon, which are entering or leaving defined system boundaries (bioreactor), are considered in the C-balance:

$$C_{C-source} = C_{biomass} + C_{by-product} + C_{CO_2} \quad \textbf{Eq. 68}$$

All of the compounds of the C-balance are recorded, when 100% of the C-source can be found in the biomass, the by-products and CO_2.
If all of the incoming carbon atoms of the C-source can be recovered by biomass, by-products and CO_2 the balance is fulfilled and this ensures that all by-products and substrates are recorded in the balance and so the process took place in a defined way. The C-balance provides the possibility to discover new by-products or measure errors. It is a quality criterion of the experiment.

Carbon exists in different species, therefore the molecule i, with its number of carbon atoms α must be considered in the balance in Cmol units. For a continuous fermentation the dilation rate is considered as well to form the following equation

$$c_{Glc}\, V_R\, \alpha_{Glc} D = \frac{c_x}{M_x} V_R D + \sum_i^N (c_i V_R\, \alpha_i D) \;\; + Q_{CO_2} V_R \quad \textbf{Eq. 69}$$

where c [mmol/L] is the concentration of glucose in the feed media and M_x [g/Cmol] the molar mass of the biomass.

In a continuous fermentation the in- and the outflows of biomass, by-products and CO_2 are not equal. In this work there was no biomass and no by-products in the inflow and therefore only the outflows were considered. Glucose entered the bioreactor as C-source, but since the cells do not take up all of it, some glucose remained. In this work, the fermentations were conducted C-limited, therefore the glucose remains were low. So finally Eq. 70 is formed:

$$c_{Glc}^{in}\, V_R\, \alpha_{Glc} D = \frac{\left(c_x^{out} - c_x^{in}\right)}{M_x} V_R D + \sum_i^N \left[\left(c_P^{out} - c_P^{in}\right) V_R\, \alpha_i D\right] + Q_{CO_2} V_R + c_{Glc}^{out}\, V_R\, \alpha_{Glc} D \qquad \textbf{Eq. 70}$$

8.8.16 STATISTICAL DATA ANALYSIS

Error estimation is an essential part in data evaluation. If there are more than two of the same data sets (repeats) the arithmetic average $\bar{x}$ is calculated:

$$\bar{x} = \frac{1}{N} \sum_{i=1}^{N} x_i \qquad \textbf{Eq. 71}$$

where N is the number of measurements and x_i is the value of a single measurement.

Another important statistical term is the variance σ, which describes the quadratic distribution of data values x_i around the arithmetic mean $\bar{x}$. It is calculated as following

$$\sigma = \frac{1}{N-1} \sum_{i=1}^{N} (x_i - \bar{x})^2 \qquad \textbf{Eq. 72}$$

If the variance becomes zero, it means that the measured values are equal to the arithmetic mean. In this work the arithmetic mean was calculated together with its standard deviation, which was calculated by using the square root of the variance:

$$s = \sqrt{\sigma} \qquad \textbf{Eq. 73}$$

Terms were often calculated of several arithmetic means with their standard deviations. In this case the propagation of error according to Gauß was used. F is a function of 1,2-k arithmetic means:

$$F = f(\overline{x_1}, \overline{x_2} \ldots \overline{x_k}) \qquad \textbf{Eq. 74}$$

The final standard deviation was then calculated by the root of the sum of the squares of the partial derivatives of function F with all of its arithmetic means multiplied by the corresponding standard deviations:

$$s_F = \sqrt{\left(\frac{\partial F}{\partial \overline{x_1}}\, s_1\right)^2 + \left(\frac{\partial F}{\partial \overline{x_2}}\, s_2\right)^2 + \cdots + \left(\frac{\partial F}{\partial \overline{x_k}}\, s_k\right)^2} \qquad \textbf{Eq. 75}$$

9 RESULTS

9.1 PROCESS OVERVIEW: BATCH AND CONTINUOUS FERMENTATION BEFORE AND AFTER CO_2 SHIFT

Two continuous fermentations (process 1 and 2) with a dilution rate of 0.05 1/h were conducted with compressed air until reaching steady state. Then a shift from compressed air to the gas-mixture containing 50 % CO_2 was conducted until a new steady state was reached. In the following, the whole process is described by using the operation parameters of process 2 (Figure 4: A, B and C).

Each process started with a batch cultivation (Figure 4: A, B and C, process time = 0 h), which ended after 38.6 h (Figure 4: C, marker 1). During the overnight batch cultivation the in-gas tube detached itself from the bioreactor. Therefore the process started aerobic and became anaerobically (Figure 4: C, between marker 0 and 1), due to missing air supply. The glucose available in the batch medium was consumed anaerobic and the next day the in-gas tube was reconnected and the agitator speed was increased (Figure 4: A, around 40 h) until ethanol was depleted. Yeast is a facultative anaerobic organism, which is highly tolerant towards high ethanol concentrations, thus the technical failure had no negative effect on the process. The batch phase was not investigated and because it delivered enough biomass for the conduction of the following continuous fermentation, it was not necessary to repeat it.

After the batch was conducted, the starvation phase (Figure 4: C, marker 2) was performed to ensure that all of the secondary metabolites were depleted. Then at process time 46.15 h, the continuous fermentation with compressed air was conducted (Figure 4: C, marker 3). After reaching steady state (five retention times) the gas mixer was interposed before the off-gas analyzer to dilute the off-gas 1:10 (Figure 4: C, marker 4). Finally the shift from compressed air to the gas-mixture was conducted at process time 164 h (Figure 4: C, marker 5) and ended after reaching steady state at 281.2 h (Figure 4: C, marker 6).

During the process the volume of fermentation broth was checked, therefore the agitator was switched off, which is visible in Figure 4, B. The pO_2 values during the process are equivalent the yO_2 values (Figure 4: compare A and C).

During the whole process the operation parameters (Table 17) stayed constant (except for the air supply and the agitator speed mentioned above). The data confirms successful conduction of the experiment: the operation parameters were constant during the continuous fermentation and steady state was reached either with compressed air or with the gas-mixture.

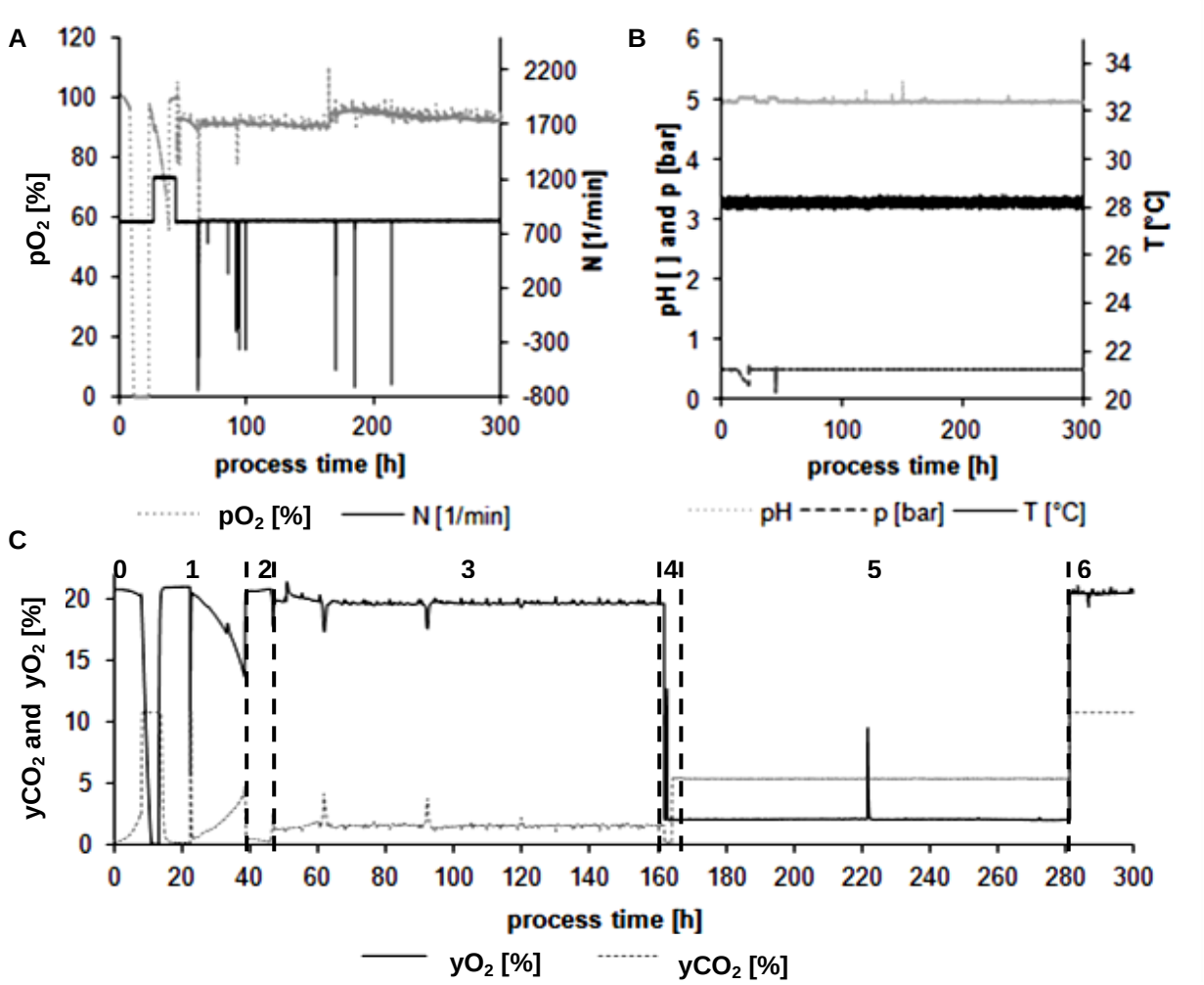

Figure 4 : Process overview of process 2: in A the pO_2 [%] and the rotation number N [1/min], in B the temperature T [°C], pH [ ] and overpressure p [bar] and in C the yCO_2 and yO_2 [%] values are blotted against the process time [h]. 0: start of batch fermentation, 1: batch fermentation, 2: starvation phase, 3: continuous fermentation with compressed air, 4: interpose of gas mixer, 5: continuous fermentation with gas-mixture containing 50 % CO_2, 6: end of process.

9.2 Carbon-balance and General Physiological Parameters During Steady State Conditions Before and After CO_2 Shift

9.2.1 General Physiological Parameters Before and After CO_2 Shift

In Figure 5 *qs* (biomass specific uptake rate, A), *Yxs* (biomass to substrate yield, B), *cx* (cell dry weight concentration, C) and *ms* (maintenance, D) are shown at time point 0, which is the steady state condition before CO_2 shift, time point 1, which is 1 hour after CO_2 shift and time point 100, which is the average of retention time five and six (steady state). The values are calculated as described in 8.8.9 Substrate Uptake Rate, 8.8.11 Biomass to Substrate Yield and Maintenance and 8.8.1 Biomass Dry Weight.

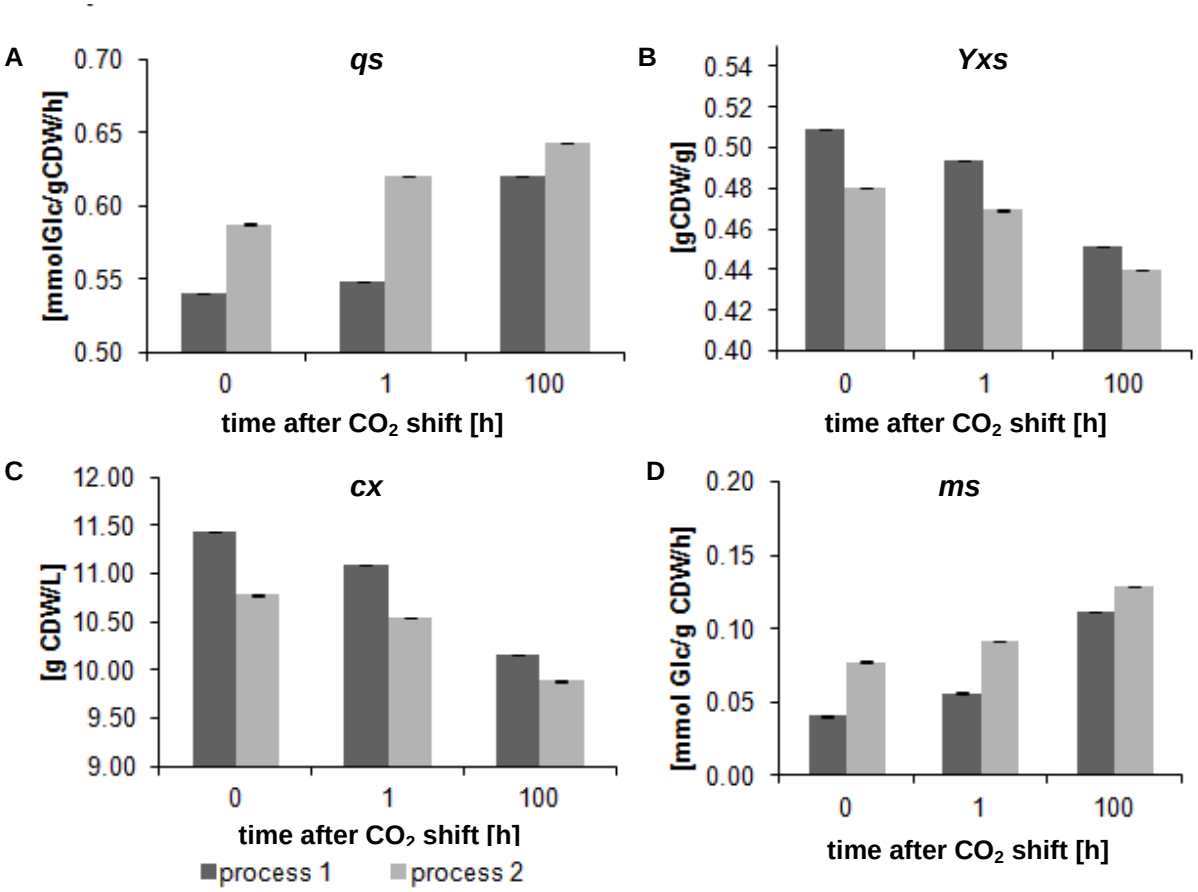

Figure 5: Biomass specific glucose uptake rate (*qs*, A), biomass-substrate yield (*Yxs*, B), cell dry weight concentration (*cx*, C) and maintenance (*ms*, D) during CO_2 shift of process 1 and 2. *qs* and ms were increasing, while *cx* and *Yxs* were decreasing during the shift.

qs increased during the CO_2 shift by 15 and 9 % for process 1 and 2, when comparing the reference condition to 100 h after CO_2 shift (Figure 5, A). Also the ms showed increased values: in average it doubled in process 1 and 2 (Figure 5, D). In contrast, *cx* and *Yxs* were decreasing at elevated CO_2 concentrations. *Cx* increased from time point zero to 100 h after CO_2 shift by 11 and 8 % (Figure 5, C), while *Yxs* increased by 12 and 8 % (Figure 5, B), for process 1 and 2.

The data show clearly that the CO_2 shift has an effect on *qs*, *ms*, *Yxs* and *cx*. Process 1 and 2 are not equal, they already differ before the CO_2 shift, although they had the same starting conditions. At steady state conditions during gassing with the gas-mixture, the differences between process 1 and 2 are lower in comparison to the differences before the CO_2 shift.

9.2.2 Carbon-balance Before and After CO_2 Shift

A carbon-balance was set up to ensure that the collected data are complete and valid, as described in 8.8.15 Elemental Carbon-Balance (C-balance). The balance achieves 100 %, when all of the carbon present in the inflow (glucose in feed and CO_2 in the in-gas) can be recovered in the outflow (biomass, the off-gas, by-products, glucose residue and CO_2 in off-gas).
In Figure 6 the carbon-balance of process 1 and 2 before and after CO_2 shift at steady state conditions are displayed. At reference conditions (Figure 6, first two bars on the left) nearly 100 % of carbon was recovered considering the standard deviations: 105.01±4.07 % and 101.28±2.32 % for process 1 and 2. In contrast the carbon-balances at elevated CO_2 conditions (average of residence time five and six) had very high standard deviations concerning the CER and therefore no statement can be made concerning the carbon recovery and the comparison of the CER values before and after shift. As it is

mentioned in the previous chapter the biomass dry weight concentration decreased and the by-product formation increased as well (no by-product formation was measured at reference conditions) after CO_2 shift. In Table 24 the data of the carbon-balances including their standard deviations are shown in detail.

Table 24: Carbon-balances of process 1 and 2 in % regarding to the carbon inflow of the feed.

	% biomass	% products and glucose residue	% CO_2
Process 1			
0 % CO_2	58.42	0.38	46.21
stdev	0.03	0.01	4.07
6000 and 7000 min, 50 % CO_2	51.86	0.95	49.41
stdev	0.01	0.12	14.38
Process 2			
0 % CO_2	55.08	0.45	45.75
stedev	2.10	0.07	0.98
6000 and 7000 min, 50 % CO_2	50.52	0.84	48.69
stdev	0.02	0.02	7.83

*stdev = standard deviation

Two reasons for the increased standard deviations of the yCO_2 values during CO_2 treatment should be mentioned: the gas mixer interposed before the off-gas analyzer leaded to higher standard deviations in yCO_2 values and yO_2 values. Additionally the CO_2 treatment itself triggered an increased oscillation behaviour in oxygen uptake and carbondioxide release. The corresponding oscillation of CO_2 and O_2 contents in the off-gas were also mirrored by the oxygen saturation signal in the liquid phase. In this case, a simple measurement artefact was improbable (Figure 7). The period duration and the amplitude was calcuated as an average out of five oscillations. The average of the period duration was 49±4 min and the average of the amplitude was 0.015±0.002 %. Therfore the minimal standard deviation of yCO_2, yO_2 and pO_2 values became equal to the amplitude of the oscillation.

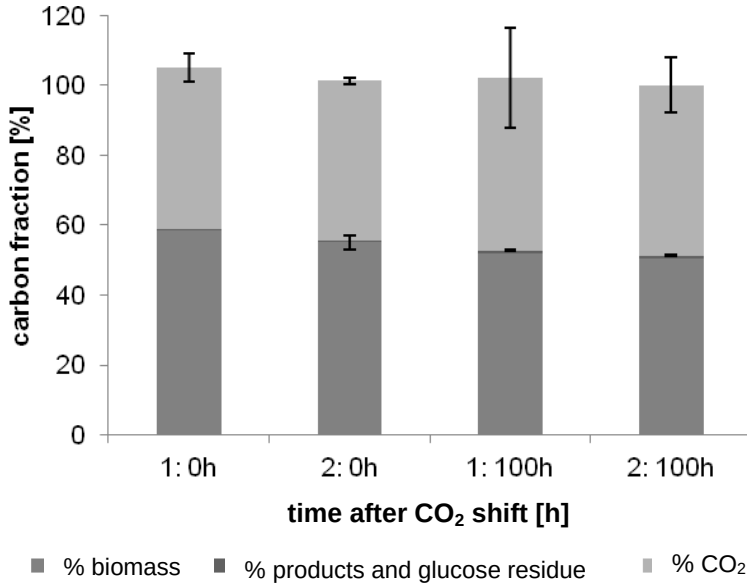

Figure 6: Carbon-balance before and after CO_2 shift at steady state conditions of process 1 and 2. Biomass fraction was decreasing, while by-products were increasing. Because of high standard deviation during off-gas measurement, limited accuracy about the CO_2 production can be made.

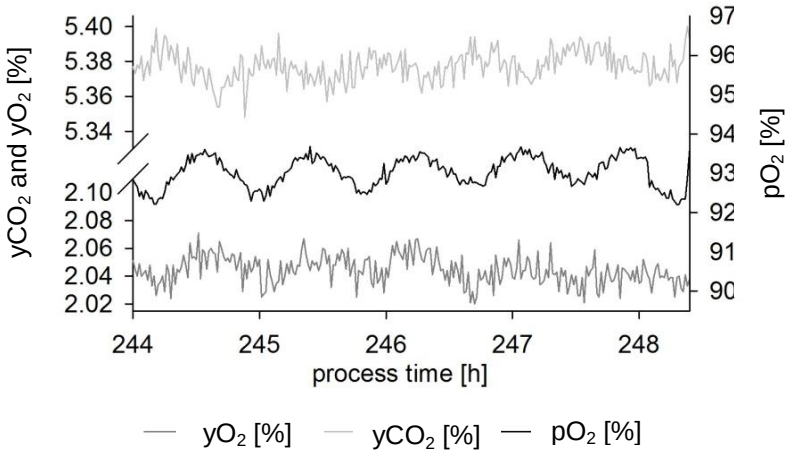

Figure 7: Oscillation behavior of yCO_2 [%], yO_2 [%] and pO_2 [%] during CO_2 treatment of process 2.

9.2.3 DETERMINATION OF THE HENRY COEFFICIENT

Estimation of the Henry coefficient from the CO_2 in the off-gas measurement and the TIC values representing the sum of CO_2, H_2CO_3, HCO_3^-, and CO_3^{2-} in the biomass suspension. The dissociation equilibrium of H_2CO_3 depends on the cultivation pH. The concentration of bicarbonate at pH 5 represents less than 5 % (v/v) of the CO_2 concentration. Therefore, the TIC value represents mainly CO_2. The Henry coefficient was calculated according to 8.8.4 Determination of the Henry Coefficient.
Figure 8 shows a graphical evaluation of the Henry coefficient compared to calculated dissolved CO_2 concentration at 30 °C and 1.5 bar by using the Henry coefficient of 0.029 mol/L/bar in water from the literature considering temperature dependency [138] and yCO_2 values of 0, 21 and 50 % (v/v). The slope of the trend line is 0.044 mol/L/bar. Values obtained from this study were in excellent agreement with reported data(the Henry coefficient of 0.029 mol/L/bar is 0.044 mol/L/bar for 1.5 bar).

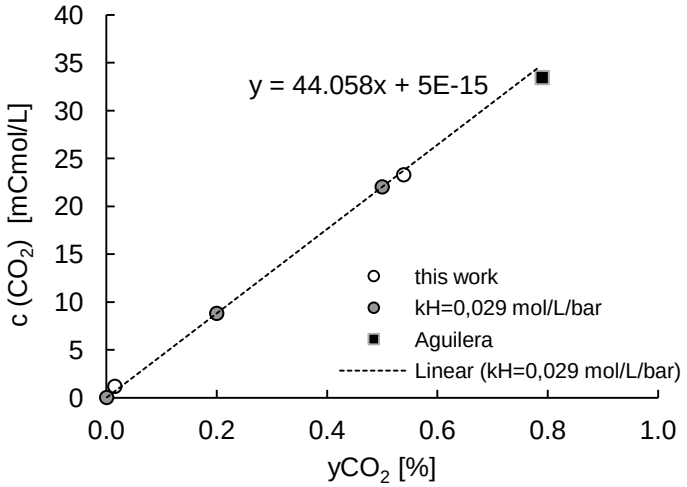

Figure 8: Determination of Henry coefficient during continuous fermentation with compressed air and gas-mixture (this work) in comparison to calculated concentrations of CO_2 by using the Henry coefficient for 30°C an 1.5 bar, which is 0.029 mol/L/bar (0.044 for the pressure of 1.5 bar) and the published data by Aguliera et al. (2005) [1]. The slope of the line is the Henry coefficient (44.06 mmol/L/bar).

9.3 BY-PRODUCT EXCRETION INTO THE FILTRATE OF THE FERMENTATION BROTH DURING CO_2 SHIFT

Switching from 0.06 to 50 % (v/v) CO_2 in the in-gas leaded to by-product formation. Acetate showed the highest extracellular concentration among the by-products. It was present between 10 and 180 min after CO_2 shift (Figure 9: A and B). Acetate was produced within the first hour of CO_2 treatment (Figure 10, C) until maximum concentrations above 6 mM (Figure 9: A and B) were reached in the two processes. At the dilution rate of 0.05 1/h and for a reaction volume of 1.5 L, a wash out up to 5 % (v/v) of the by-products per hour can be estimated. The acetate concentration returned to an amount near to zero at the end of the short-term time frame.
In this case, ethanol - the redox-neutral product of the fermentative metabolism - is produced in minor amounts compared to acetate. However, the production progress was similar to acetate: it was also produced within the first hour (Figure 10, B) until it reached a maximum concentration of 2 mM (Figure 9: A and B) and also returned to zero at the end of the short-term time frame. In contrast, succinate was present in the filtrate during the whole fermentation process with CO_2 treatment (Figure 9: A and B) until a maximum concentration of 2 mM (Figure 9: A and B). Within the first three hours of CO_2 treatment, succinate was continuously produced (Figure 10, A), where the highest production rate was reached after 30 minutes.

The by-products found in the filtrate of the fermentation broth, were similar in process 1 and 2 according to the amount and time after CO_2 shift. Little variations were found in the ethanol concentrations of the two processes. However, according to the big picture of process reproducibility with over 70 measurements this single case seems arguable.

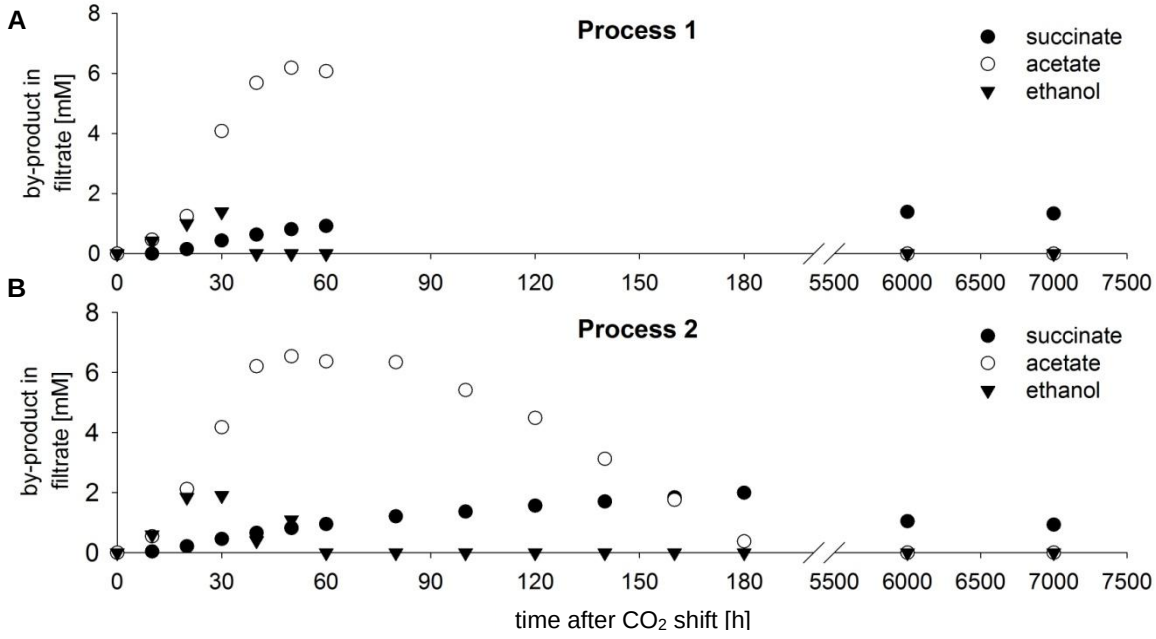

Figure 9: By-product content in filtrate during CO_2 shift of process 1 and 2. Succinate, acetate and ethanol were detected extracellular, where acetate and ethanol were produced short-term and succinate short- and long-term. In process 1 sampling was only conducted between 0-60 minutes and long-term, while in process 2 sampling was extended from 60 -180 min every 20 minutes, due to the results obtained from process 1.

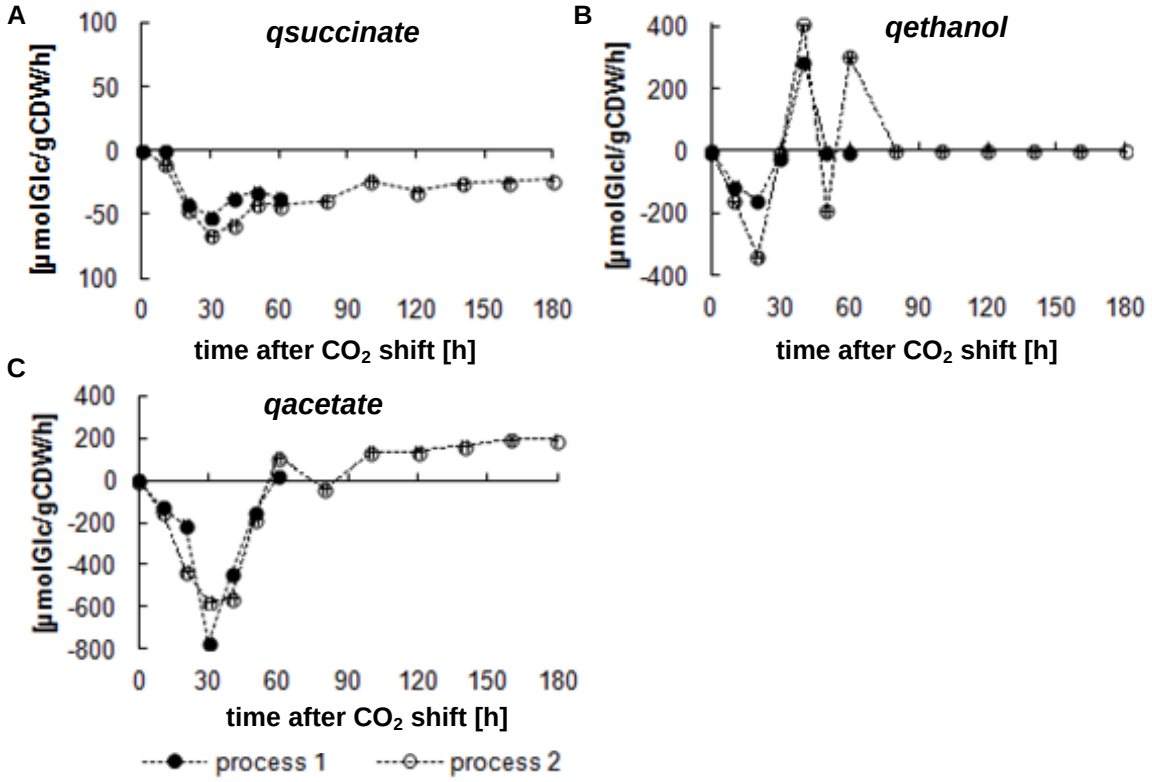

Figure 10: Biomass specific rates of succinate (*qsuccinate*), ethanol (*qetahnol*) and acetate (*qacetate*) [µmolGlc/gCDW/h] during CO_2 shift of process 1 and 2. Succinate was produced during the whole CO_2 treatment, while ethanol and acetate were produced in the first hour and consumed afterwards. (negative rate = production and positive rate = consumption)

9.4 GLYCOGEN AND TREHALOSE CONTENT DURING CO_2 SHIFT

Glycogen and trehalose content in the biomass pellets were analyzed as described in 8.8.6 Glycogen und Trehalose Assay.

Figure **11** shows the glycogen and trehalose content in % per g cell dry weight (CDW) blotted over time after CO_2 shift. The data demonstrates a short-term decrease of both sugar storages during the shift from compressed air to the gas-mixture including 50 % CO_2. The glycogen content was 7.6 % per g CDW and the trehalose content was 7.1 % per g CDW at time point zero for both processes. After the first 30 min most of the glycogen and trehalose were degraded: decrease of 4.1 % per g CDW of glycogen and 2.05 per g CDW trehalose for both processes. After 30 min the degradation proceeded, but not as strongly as in the first 30 min. At retention times five and six (6000 and 7000 min), glycogen and trehalose contents stayed at the same level than they were at 180 min. In total a decrease of 77.5 % glycogen and 82.8 % trehalose was determined in both processes.

Process 1 showed a faster sugar storage degradation than process 2, but both ended up in a similar amount of glycogen and trehalose per g CDW in the long-term.

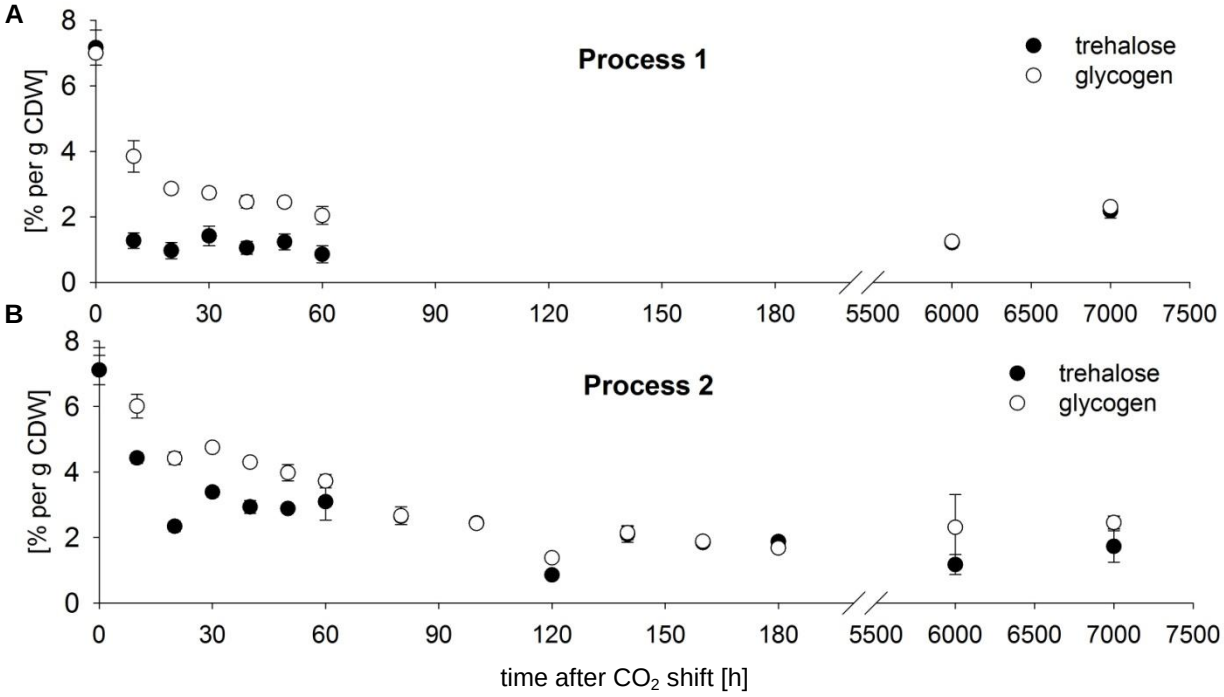

Figure 11: Intracellular glycogen and trehalose content during CO_2 shift of process 1 and 2. During CO_2 shift carbon storage was degraded and stayed at a low level even when exposed long-term (6000 and 7000 min) to elevated CO_2 concentrations. Breakdown was highest at the first 30 minutes and happened more intensely for trehalose than for glycogen.

9.5 N/C-RATIO IN BIOMASS AFTER CO_2 SHIFT

The nitrogen to carbon ratio (N/C) in the biomass was calculated as it is described in 8.8.3 Determination of Nitrogen to Carbon Ratio (N/C) in the Biomass Pellets and the Total Inorganic Carbon (TIC) in the TIC Samples. In this work an increase of N/C ratio in the biomass was recognized as response of elevated CO_2 concentrations. Before the CO_2 shift the N/C-ratio was 0.139±0.003 mNmol/mCmol and 0.134±0.002 mNmol/mCmol for process 1 and 2. Then the values increased long-term to 0.160±0.004 and 0.151±0.003 mNmol/mCmol for process 1 and 2 at six retention times (7000 min).

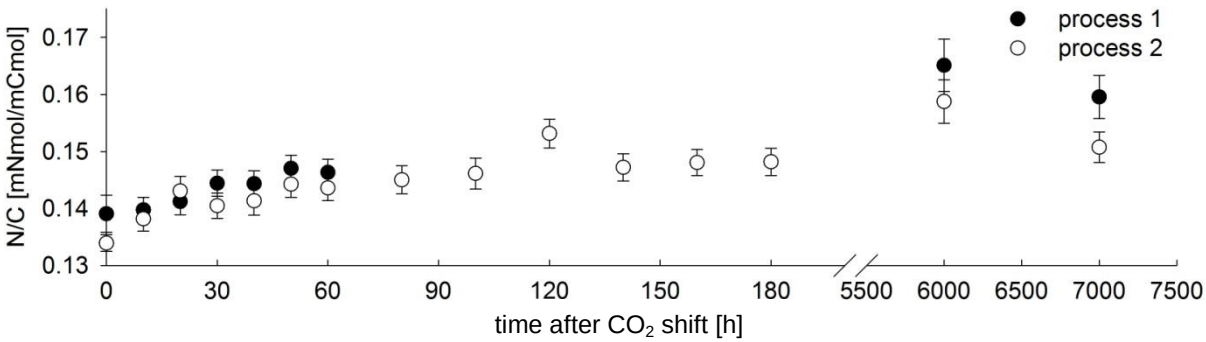

Figure 12: Nitrogen to carbon ratio (N/C) from biomass during CO_2 shift of process 1 and 2. N/C-ratio increased during CO_2 shift in process 1 and 2

9.6 ESTIMATION OF RESPIRATIONAL AND FERMENTATIONAL *qCO₂*

The results shown above indicate that there was a respirational and a fermentational metabolism in *S. cerevisiae* during CO_2 shift. To get more detailed information the mass-balance for carbon was applied:

$$\frac{dm_c}{dt} = \dot{m}_C^{in} - \dot{m}_C^{out} + \dot{m}_C^{generated} - \dot{m}_C^{consumed} \quad \textbf{Eq. 76}$$

Then the equation was adapted to this work, by adding the carbon mass flows of the feed ($\dot{m}_C^{feed}$), CO_2 ($\dot{m}_{CO2}$), biomass ($\dot{m}_C^{bio}$), by-products ($\dot{m}_C^{by-prod}$) and the carbon available due to glycogen and trehalose degradation ($\dot{m}_C^{glytre}$):

$$\frac{dm_C}{dt} = \dot{m}_C^{feed} - \left(\dot{m}_{CO2}^{ferm} + \dot{m}_{CO2}^{resp}\right) - \dot{m}_C^{bio} - \dot{m}_C^{by-prod} + \dot{m}_C^{glytre} \quad \textbf{Eq. 77}$$

where the mass flow of CO_2 consists of fermentational CO_2 ($\dot{m}_{CO2}^{ferm}$) and respirational CO_2 ($\dot{m}_{CO2}^{resp}$).

In a continuous fermentation the change in the mass of carbon over time is zero:

$$\frac{dm_c}{dt} = 0 \quad \textbf{Eq. 78}$$

and therefore Eq. 76 is transformed into Eq. 79:

$$\dot{m}_{CO2}^{ferm} + \dot{m}_{CO2}^{resp} + \dot{m}_C^{bio} = \dot{m}_C^{feed} - \dot{m}_C^{byprod} + \dot{m}_C^{glytre} \quad \textbf{Eq. 79}$$

Then Eq. 79 is scaled to biomass specific glucose equivalents (the dilution rate is neglected):

$$q_s + q_{glytre} - \frac{q_{succ} + q_{ace} + q_{eth}}{2} = q_{bio} + q_{CO2}^{resp} \quad \textbf{Eq. 80}$$

where q_s [mmolGlc/gCDW/h] is the biomass specific glucose uptake rate, q_{glytre} [mmolGlc/gCDW/h] is the biomass specific glucose production rate by degradation of glycogen and trehalose, q_{succ}, q_{ace}, q_{eth} [mmolGlc/gCDW/h] are the biomass specific production rates of succinate, acetate and ethanol, q_{bio} [mmolGlc/gCDW/h] is the biomass production rate [mmolGlc/gCDW/h] and q_{CO2}^{resp} [mmolGlc/gCDW/h] is the biomass specific production rate of respirational CO_2.

The *q*-values of the by-products are divided by two, to scale them to glucose equivalents. The biomass specific production rate of fermentation CO_2 is included in the by-product terms.

The data for the left part of Eq. 80 is available and can be calculated, which is graphically represented in Figure 13.

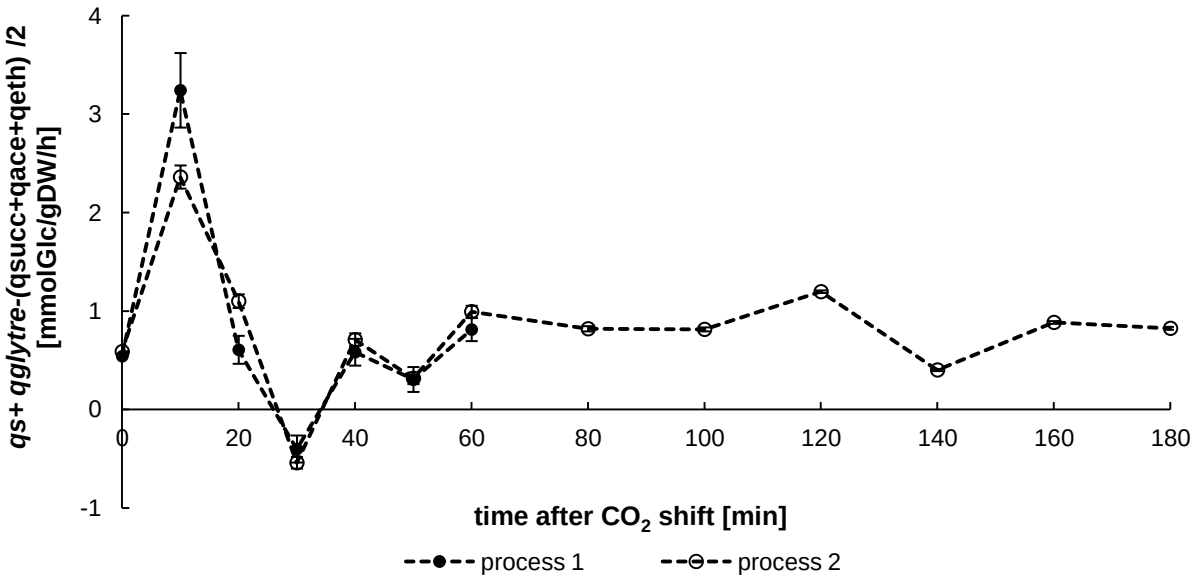

Figure 13: Carbon-balance of biomass specific yields during CO_2 shift of process 1 and 2. Biomass specific rates of the substrate added by biomass specific rates of glycogen and trehalose and subtracted by biomass specific rates of the by-products in glucose equivalents ($q_s + q_{glytre} - \frac{q_{succ}+q_{ace}+q_{eth}}{2}$). The balance is negative at 30 minutes, which indicates that the released glucose molecules are stored in the cell before being converted into by-products.

At time point zero 0.56 mmolGlc/gCDW/h were available in both processes. After 10 minutes of CO_2 shift the highest amount of glucose equivalents were available for process 1 and 2: 3.24±0.38 and 2.36±0.12 mmolGlc/gCDW/h. Then at 30 min the balance became negative: -0.40±0.14 and -0.54±0.06 mmolGlc/gCDW/h, which is in fact not possible, but may be explained, when the cells were not using all of the released glucose from the glycogen and trehalose degradation at the time it is released, it was stored at 10 min and degraded at 30 min. Therefore the degradation of storage sugars were faster than metabolism of their released glucose. The addition of *qglytre* to *qby-products* (Table 25) results in an excess of glucose equivalents: 1.86 and 1.39 mmolGlc/gCDW/h for process 1 and 2, meaning that not all of the glucose molecules delivered from glycogen and trehalose degradation were used for by-product formation.

Table 25: Biomass specific glucose production rate ($q_{excess\ glucose}$) of process 1 and 2

	q_{glytre} [mmolGlc/gCDW/h]	$q_{by\text{-}products}$ [mmolGlc/gCDW/h]	$q_{excess\ glucose}$ [mmolGlc/gCDW/h]
Process 1 (0-60min)	3.75±0.48	-1.89±0.00	**+1.86**
Process 2 (0-60min)	3.38±0.14	- 2.04±0.00	**+1.37**

The right part of Eq. 80 consists of the biomass production rate and the biomass specific production rate of respirational CO_2. For the calculation of q_{CO2}^{resp}, q_{bio} is needed, but sampling for the cell dry weight were only conducted at time point zero and at 60 minutes, therefore not enough data was available for the calculation. To overcome the lack of data the N/C-ratio of the biomass was used, because samples at every time point were analyzed (see Figure 12).

In the purpose of calculating q_{bio} it was assumed that the moles of nitrogen do not change and only the moles of carbon decreased over time, which is the maximum possible change in carbon moles:

$$\frac{dn_N}{dt} \rightarrow 0 \qquad \textbf{Eq. 81}$$

and

$$\frac{dn_C}{dt} \rightarrow max \qquad \textbf{Eq. 82}$$

By considering the balance for the moles of carbon over time ($\frac{dn_C}{dt}$), Eq. 83 is formed:

$$\frac{dn_C}{dt} = \frac{dn_C^{feed}}{dt} - \frac{dn_C^{bio}}{dt} - \frac{dn_{CO2}^{resp}}{dt} - \frac{dn_C^{by-prod}}{dt} - \frac{dn_{CO2}^{ferm}}{dt} \qquad \textbf{Eq. 83}$$

where the moles of carbon in the feed, in the biomass, in the by-products and CO_2 (fermentational and respirational) over time are considered. In a continuous fermentation $\frac{dn_C}{dt}$ is zero and by solving after $\frac{dn_{CO2}^{resp}}{dt}$ the following equation is formed:

$$\frac{dn_{CO2}^{resp}}{dt} = \frac{dn_C^{feed}}{dt} - \frac{dn_C^{bio}}{dt} - \frac{dn_C^{by-prod}}{dt} - \frac{dn_{CO2}^{ferm}}{dt} \qquad \textbf{Eq. 84}$$

where the $\frac{dn_C^{bio}}{dt}$ is missing, but which can be calculated from the data received from the N/C-analyzer. The moles of carbon at time point zero were therefore subtracted from the moles of carbon at a certain time point, which can be calculated from the moles of nitrogen at time point zero (assumed to stay unchanged) divided by the N/C-ratio of a certain time point. The formula for the calculation is shown in Eq. 85:

$$\frac{dn_C^{bio}}{dt} = \left(n_C^{t=0} - \frac{n_N}{\left(\frac{n_N}{n_C}\right)^t} \right) \frac{1}{dt} \qquad \textbf{Eq. 85}$$

where $n_C^{t=0}$ is calculated by the mass of carbon at time point zero [g] divided by the molar mass of carbon M_C [g/mol]:

$$n_C^{t=0} = \frac{c_x \frac{\%\ C\ in\ CDW}{100}}{M_C} \qquad \textbf{Eq. 86}$$

and the $n_N^{t=0}$ is calculated by multiplying $n_C^{t=0}$ by the N/C ratio at time point zero:

$$n_N^{t=0} = \left(\frac{n_N}{n_C}\right)^{t=0} n_C^{t=0} \qquad \textbf{Eq. 87}$$

After $\frac{dn_C^{bio}}{dt}$ is calculated, Eq. 84 is scaled to biomass specific glucose equivalents to form the following equation:

$$q_{CO2}^{resp} = q_s + q_{bio}^{release} - \frac{q_{succ} + q_{ace} + q_{eth}}{2}$$ **Eq.88**

Then the q_{CO2}^{resp} values were balanced in intervals of 30 minutes. In Figure 14 the results of this procedure are shown. The following values representing the averages for both process: qCO_2 respirational was -0.26 mmolGlc/gCDW/h at reference conditions and increased at 30 min to -0.13 mmolGlc/gCDW/h followed by an additional decrease at 60 min to -1.06 mmolGlc/gCDW/h. *qby-products* and *qs + qglytre* are also shown: at reference conditions there was no by-product formation and the available glucose (*qs + qglytre*) was 1.69 mmolGlc/gCDW/h. At 30 minutes the by-product formation rate and the available glucose (*qs + qglytre*) were the highest: 1.59 and 4.82 mmolGlc/gCDW/h. At 60 minutes *qs + qglytre* decreased to 2.18 mmolGlc/gCDW/h and *qby-products* decreased as well to -0.09 mmolGlc/gCDW/h.

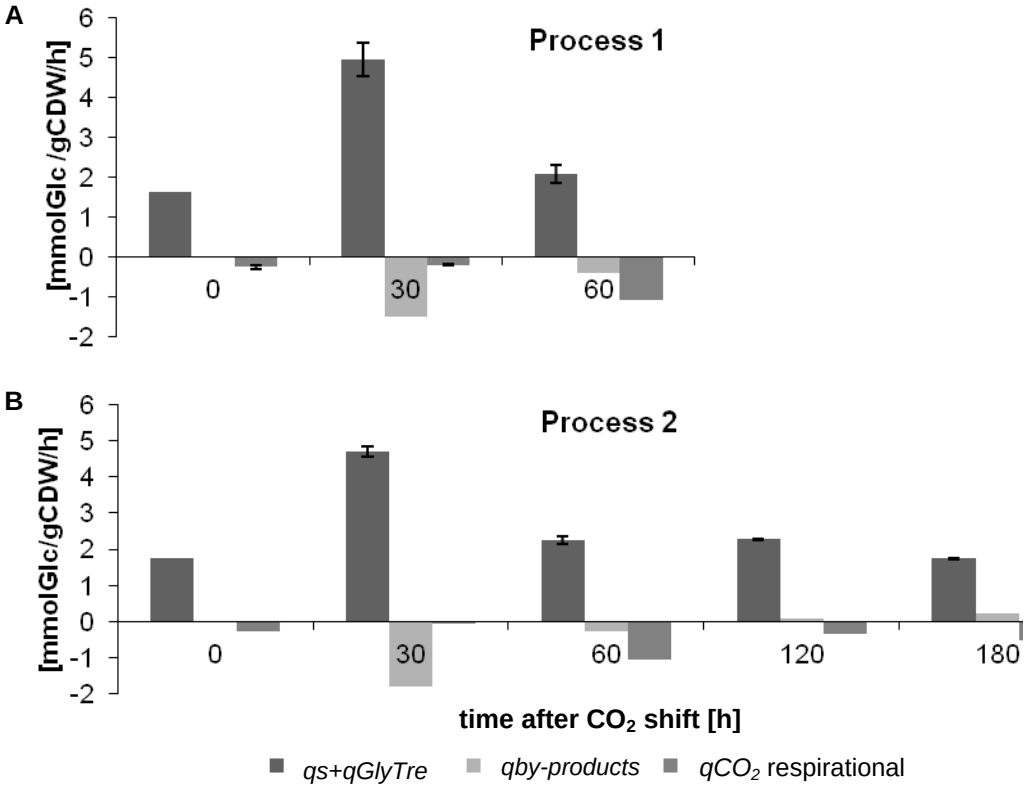

Figure 14: Estimation of biomass specific respirational CO_2 production rate in comparison to the biomass specific rates of by-product, substrate and glycogen and trehalose during CO_2 shift of process 1 and 2. *qCO_2* respirational decreased at 30 minutes and increased at 60 minutes after CO_2 shift.

$q_{CO_2}^{ferm}$ was calculated as well for comparison with $q_{CO_2}^{resp}$. The biomass specific production rates of by-product formation (acetate, ethanol or succinate) were divided by six to scale them to glucose equivalents:

$$q_{CO_2}^{ferm} = \frac{q_{CO_2}^{ace} + q_{CO_2}^{succ} + q_{CO_2}^{eth}}{6}$$ **Eq. 88**

In Figure 15 $q_{CO_2}^{ferm}$ and $q_{CO_2}^{resp}$ are balanced in intervals of 30 minutes for comparison. The $q_{CO_2}^{ferm}$ was highest at 30 (-0.44 mmolGlc/gCDW/h in average for both processes) and 60 minutes (-0.48 mmolGlc/gCDW/h for both processes) and increased afterwards to -0.09 mmolGlc/gCDW/h at 120 min and 0.17 mmolGlc/gCDW/h at 180 min in process 2.

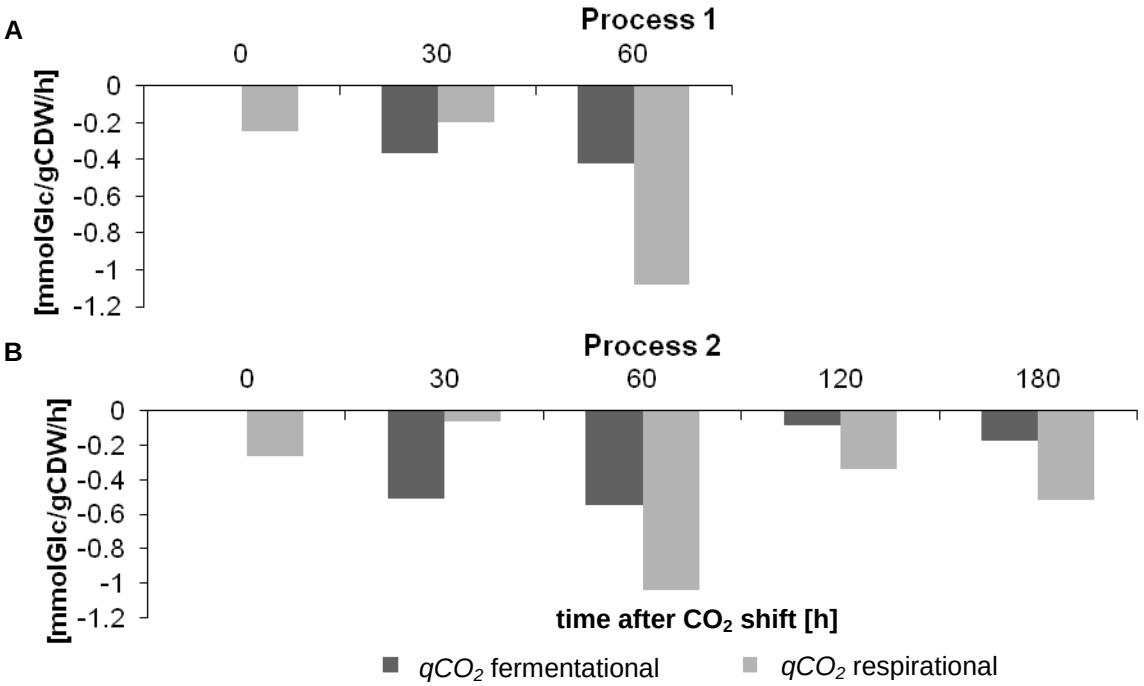

Figure 15: Comparison of biomass specific rates of respirational CO_2 and fermentational CO_2. The fermentational CO_2 rate is highest at 30 and 60 minutes and increases afterwards, while the respirational CO_2 rate is increasing at 30 minutes and decreasing at 60 minutes of CO_2 shift.

9.7 INTRACELLULAR AMINO ACID CONTENT BEFORE AND AFTER CO_2 SHIFT

The intracellular amino acid pools were calculated according to section 8.8.2 Determination of the Intracellular Amino Acid Pools. Only 19 out of the 20 proteinogenic amino acid could be measured by RP-HPLC, only cysteine was missing. From the calibration standard mix cysteine was also not measurable. In Figure 16-19 the intracellular concentration in µmol/gCDW of the remaining 19 amino acids are blotted against time after CO_2 shift are shown. Additionally norvaline and γABA were used for internal standardization (8.8.2 Determination of the Intracellular Amino Acid Pools).

The two processes showed in most cases very similar results. Three amino acids showed no significant differences with and without elevated CO_2 concentrations: asparagine, methionine and isoleucine (Figure 15: C, D and E). And some showed only very slight changes: histidine (Figure 15, B), tyrosine (under detection limit, not shown), tryptophan (under detection limit, not shown) and phenylalanine (Figure 15, A).

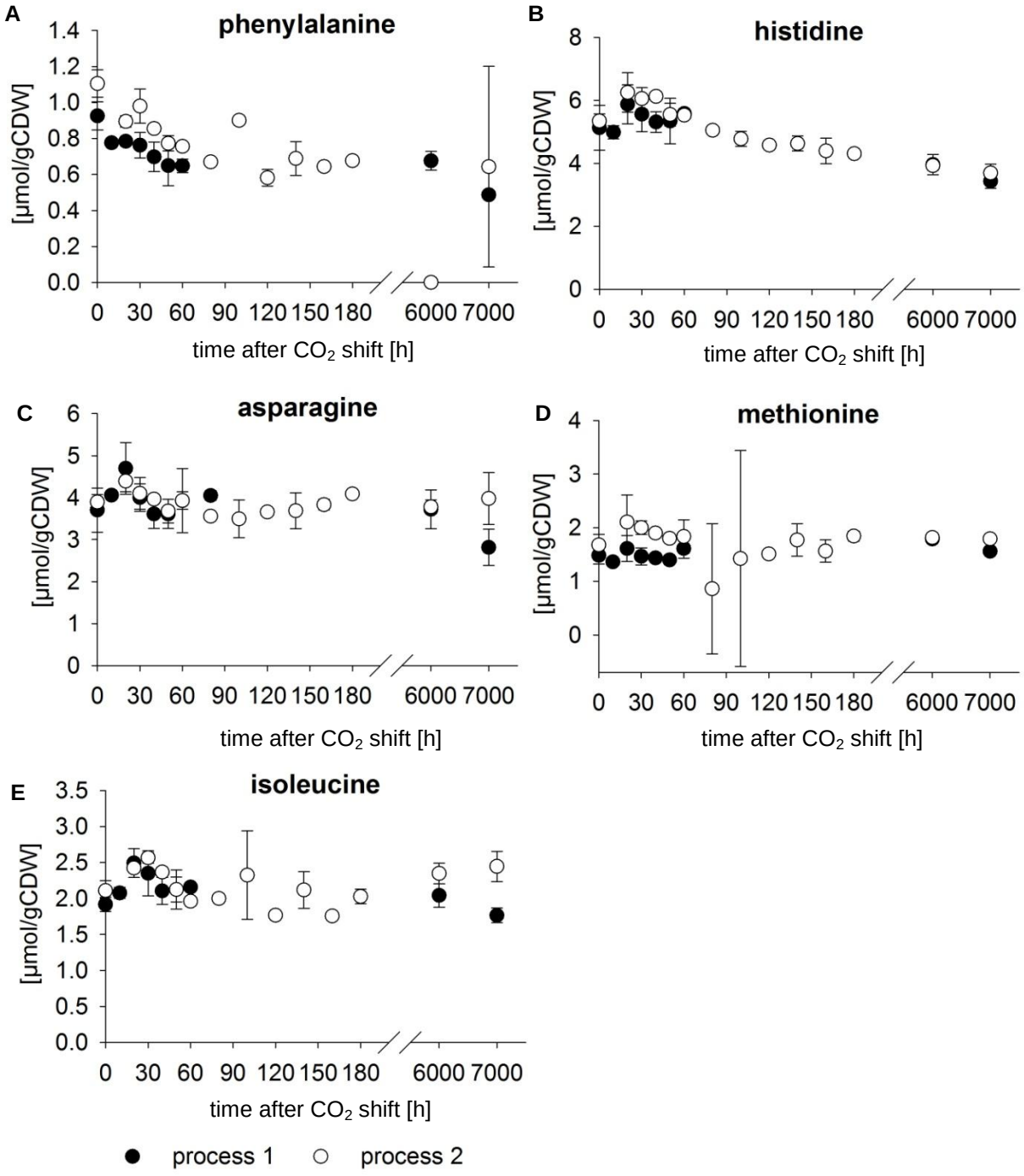

Figure 16: Intracellular amino acid content during CO_2 shift of process 1 and 2 (part 1/4): no significant change was measured for asparagine, methionine and isoleucine and slight changes were measured for phenylalanine and histidine.

Decrease of intracellular acid pool size was determined for aspartate, arginine, glutamate and glutamine. 10 minutes after CO_2 shift a strong decrease in intracellular aspartate concentration of about 65 % was detected (Figure 17, A). Then the concentration increased and reached at 40 minutes the initial concentration again, which was constant till long-term conditions. 50 % of the intracellular glutamate concentration was decreased within 100 minutes after CO_2 shift (Figure 17, B). The initial concentration was not reached again, instead the concentration stayed even long-term at this low level.

The glutamine concentration increased slightly in the first 30 minutes of about 10 %, but then the concentration decreased about 60 % at long-term CO_2 treatment (Figure 17, C). In the short-term no

specific change in arginine concentration in comparison to the reference was measurable, but at long-term treatment with CO_2 the concentration decreased about 80 % (Figure 17, D).

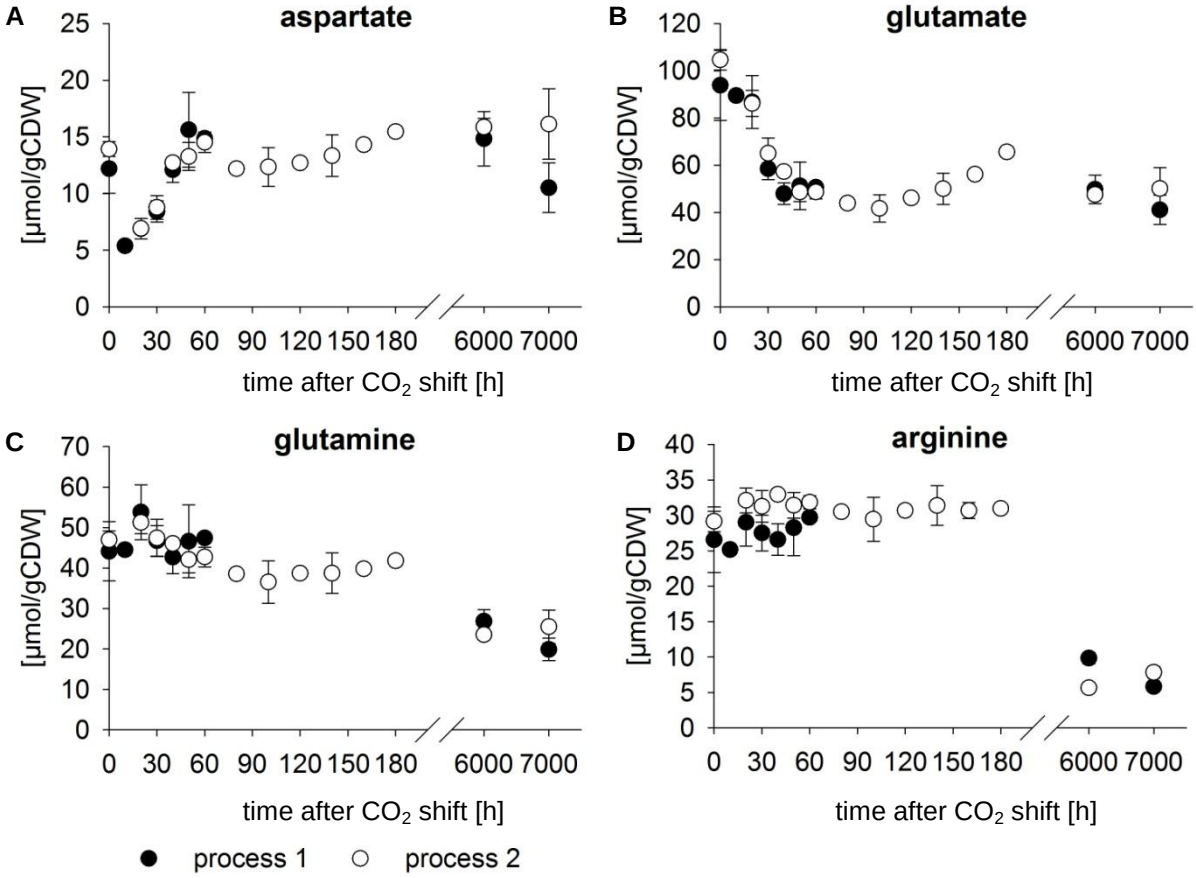

Figure 17: Intracellular amino acid content during CO_2 shift of process 1 and 2 (part 2/4). Descriptions see text.

An increase of intracellular amino acid concentration during CO_2 shift was measured for serine, glycine, threonine, alanine, leucine, lysine, proline and valine (Figure 18 and Figure 19). Serine, alanine, threonine and valine showed very similar progression during CO_2 shift: their concentrations increase during the first 20 minutes (serine +150 %, threonine +350 %, alanine +100 % and valine +100 %) and decreasing till retention time six (long-term) to values that are still higher than the initial ones (serine -40 % , threonine of -30 %, alanine -40 % and valine of -30 %) (Figure 18: A, B, C and D)

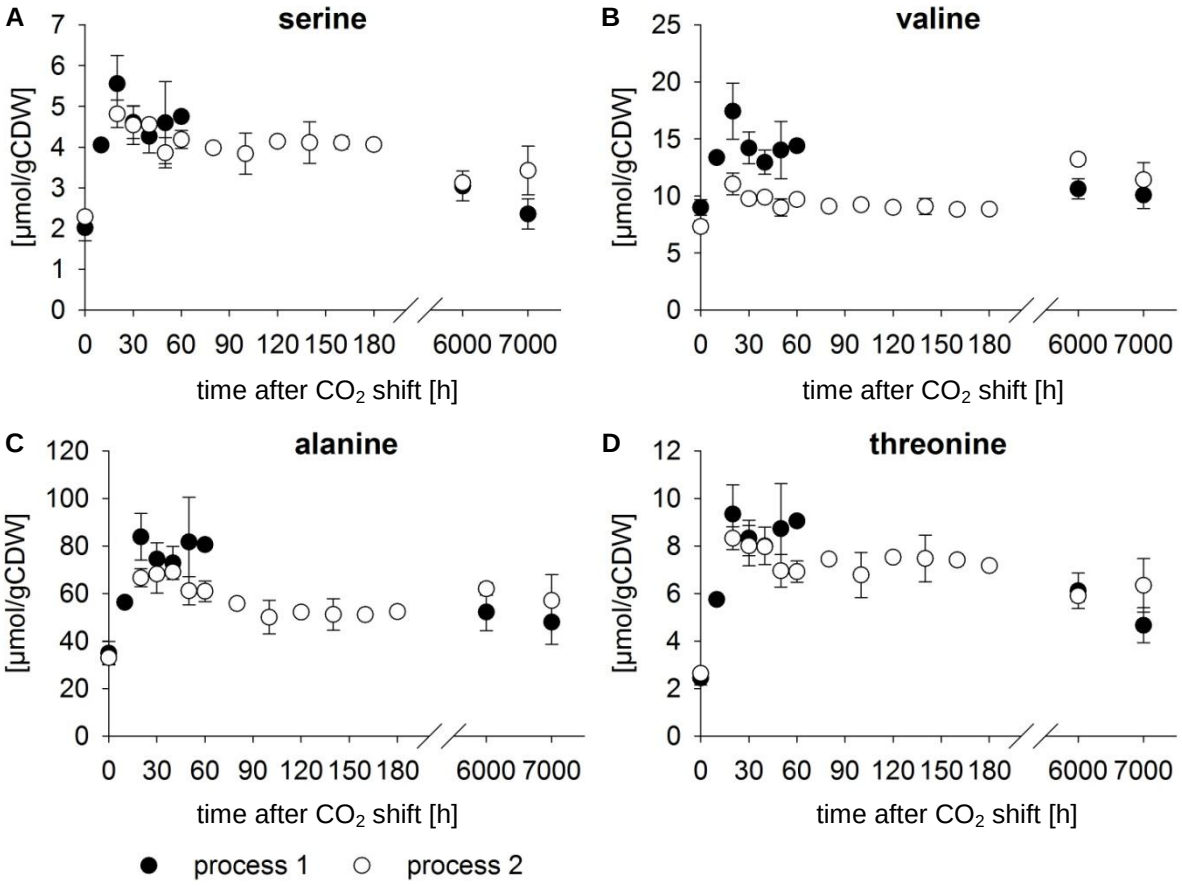

Figure 18: Intracellular amino acid content during CO_2 shift of process 1 and 2 (part 3/ 4). Descriptions see text.

Proline and leucine also showed an increased concentration during the first 20 minutes of CO_2 shift of about 100 %, but their concentration was almost the same than the initial one in the long-term (Figure 19: A and B). The intracellular concentration of glycine and lysine increased constantly for long- and short-term exposes to CO_2 to final values that were fourfold and threefold higher than the initial concentrations (Figure 19: C and D). .

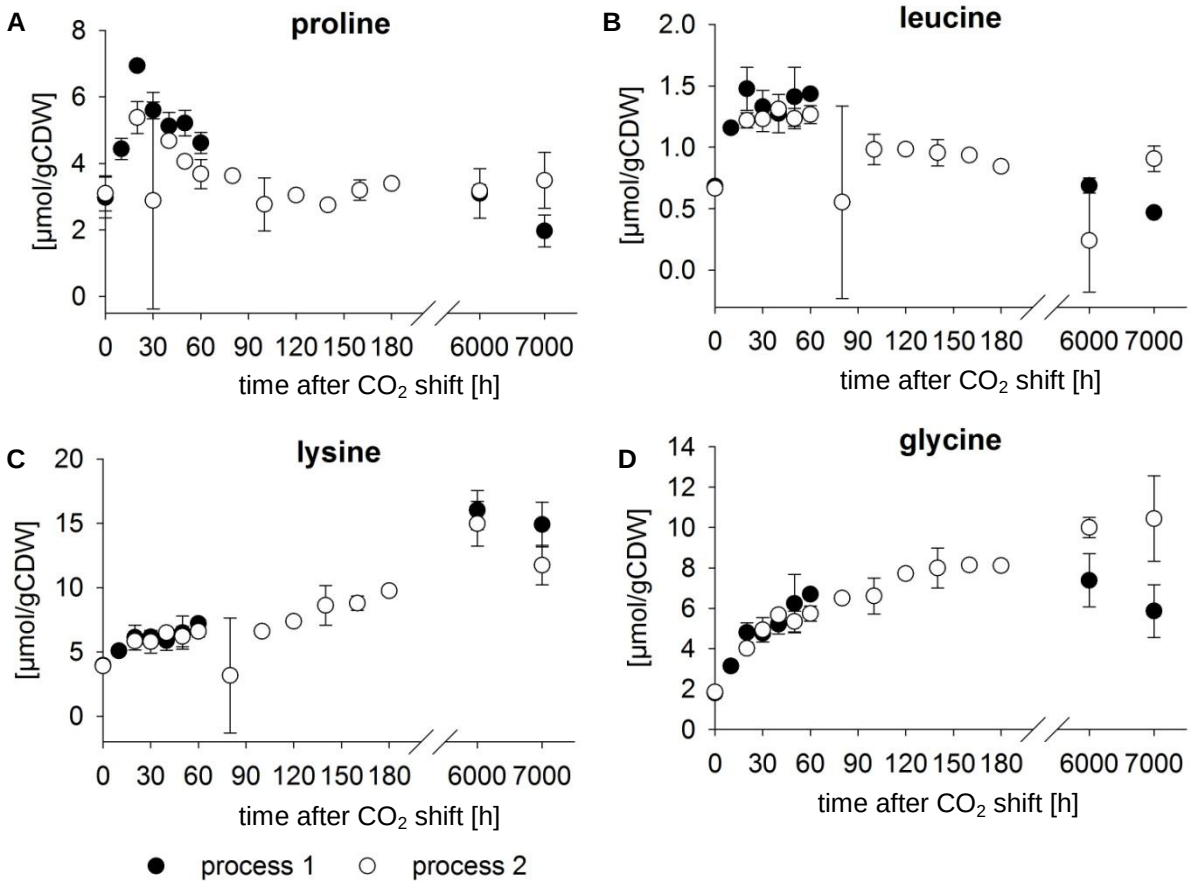

Figure 19: Intracellular amino acid content during CO_2 shift of process 1 and 2 (part 4/ 4). Descriptions see text.

10 DISCUSSION

10.1 OSCILLATING BEHAVIOR DURING CO_2 TREATMENT

Oscillating behavior in aerobic, glucose-limited chemostat cultures of yeast is a well-known phenomenon. It has been monitored even when the operation conditions kept constant [69]. As reviewed by Patnaik in 2003 [139], oscillations are noticed for dissolved oxygen tension (DOT), CER, OUR, the concentration of the carbon source and the concentration of the products ethanol and acetate, storage sugars and pH. Oscillations of CER, OUR, were also mentioned from Richards et al [29] as short time result of certain shifts with different CO_2 concentration in the in-gas phase.

10.2 CHANGES IN PHYSIOLOGICAL PARAMETERS

A decreasing biomass yield in a continuous fermentation of yeast under CO_2-stress was also reported by other authors [1,29]. Richards et.al [29] observed a decrease in biomass yield of 6.6 and 13.5 %, while dissolved CO_2 concentration was increased from 1.49 to 6.76 mM and from 1.43 to 17.20 mM in the long-term. Aguilera et al. [1] also reported a decrease of 24 %, by increasing dissolved CO_2 concentration from 0.22 mM to 22.30 mM. These data are comparable to the obtained values in this work of 8.82 % (process 1) and 11.22 % (process 2) loss in cell dry weight concentration under CO_2-stress (increasing dissolved CO_2 concentration from 1.18 to 23.29 mM). Interestingly, Richards worked with lower CO_2 concentrations and a higher dilution rate (0.13-0.166 1/h), but delivered a similar decrease of biomass yield than in this work, while Aguilera et al. worked with similar CO_2 concentrations and also higher dilution rate (0.1 1/h) and delivered a higher biomass yield decrease than in this work. This indicates that the effect of elevated CO_2 concentrations is depended on the CO_2 concentration and also on the dilution rate respectively the specific substrate rate.
The loss of glycogen and trehalose content short-term is lowering *cx*, when the released glucose is consumed. Delayed these glucose molecules may be used for by-product synthesis, but there is still glucose left afterwards and therefore the remaining molecules must be used for energy generation.

The existing long-term loss of *cx* is thus explained by an energy drain, which affects the energy homeostasis [29]. Additionally Richards et. al. and Aguilera et al. found an increased specific oxygen rate, which was increased, but not significantly altered in this work. Aguilera mentioned that elevated levels of CO_2 may be associated with an metabolic uncoupling of electron transport and ATP synthesis [1,140]. A reason for the uncoupling may be that the energy needs at elevated CO_2 levels are higher. This theory is supported by the significant increase of *qs* and *ms* measured in this work and by the fact that bicarbonate is found to activate ATP hydrolysis by the mitochondrial F_1/F_0 ATPase/synthase [140], which fits to the results of Richards, who showed that the ATP to biomass yield is reduced linearly at increased dissolved CO_2 levels [29].
Other reasons for higher energy needs may rely in the maintenance of pH homeostasis during CO_2-stress. The impact of CO_2 on the intracellular pH is well known [141]. To maintain the pH homeostasis, Pma1p ATPase located on the cell membrane mostly used [120]. It transfers 1 proton out of the cell by the usage of 1 ATP [142]. While the H^+ is able to be transferred outside of the cell, HCO_3^- remains in the cell, because no transporter is found to exist [143], therefore the intracellular concentration of bicarbonate ions increases and may change the electric potential of the cell membrane [144].

10.3 BY-PRODUCT FORMATION

At CO_2-stress, released sugar by storage sugar degradation, lead to an overflow metabolism, where acetate and ethanol is produced, which was also shown by Richards et al. [29]. Additionally succinate was produced, which was also published by Aguilera et al. and Richards at al. [29]. In fact, it is already known that bicarbonate stimulate the production of organic acid, especially succinate [128]. It may be due to an inhibition of succinate dehydrogenase in the TCA [29,1]. In this work, the respirational qCO_2 was estimated. At 30 minutes a drain in respirational qCO_2 was calculated, which may match to the presumption that the SDH is inhibited. In fact, when the SDH activity is lower, anaplerotic activities are necessary [1]. Due to published transcriptional data PEPCK (phospoenolpyruvate carboxykinase) and PYC (pyruvate carboxylyase) are known to work as anaplerotic enzymes during gassing with elevated CO_2 levels [1]. A minor inhibition of SDH may be compensated by acetate synthesis. The advantage of acetate over ethanol is the production of cytosolic reduction equivalents, which can be used for ATP synthesis via respiratory chain.

10.4 DEGRADATION OF GLYCOGEN AND TREHALOSE

A significant decrease in glycogen and trehalose content was could be identified in this work. A similar trend was also reported by Richards et al. [29]. The degradation of storage sugars, due to CO_2-stress may be explained by the following hypothesis: when CO_2 enters the yeast cell it dissociates and forms HCO_3 and H^+, which is lowering the internal pH [145]. An intercellular acidification activates the adenylate cyclase via RAS protein, the resulting cAMP activates the PKA, which leads to the degradation of the storage sugars [146]. The adenylate cyclase was also found to be activated by $HCO3^-$ directly, but only in mammalian cells [145]. When glycogen and trehalose are degraded, high glucose levels are released, which may activate the adenylate cyclase as well, via G-Proteins Gpr1-Gpa2 [27] or by passing over to the next cell cycle [74]. In case of the yeast that is passing another cell cycle, the energy from the degradation of the storage sugars is used for budding or cell deviation [72]. In this work, the glycogen and trehalose pools stayed at a low level at long-term treatment with CO_2, which may have a negative effect on the cell deviation. There might be two possibilities why the glycogen and trehalose storage are not built up again: their degradation could be as fast as the build up or the enzymes for the synthesis of the sugars storages are inhibited by CO_2 and therefore the built up is not conducted.
As mentioned above, cAMP plays an important role in glycogen and trehalose degradation, but it also has an influence on the plasma membrane ATPase [147] and mitochondrial ATPase [148], cAMP may therefore be one of the key metabolites in CO_2-stress response.

10.5 INCREASE OF N/C-RATIO OF THE BIOMASS

An increasing N/C-ratio is usually received, when the dilution rate is increased in *S. cerevisiae* [149]. The correlation is approximately linear (see Figure 20). The initial value of N/C-ratio is similar to the published data of Lange and Heijnen [149], but the final N/C-ratio after six retention times after CO_2 shift, is as high as the dilution rate of about 0.15 1/h. In the paper the different mass fractions of the cell compounds are stated at different dilution rates. At a dilution rate of 0.158, protein content and RNA content are increasing, while carbohydrates and lipid content are decreasing, when compared to dilution rate 0.05 1/h. Nevertheless DNA were mentioned to stayed constant at every dilution rate between 0.022 and 0.211 1/h.

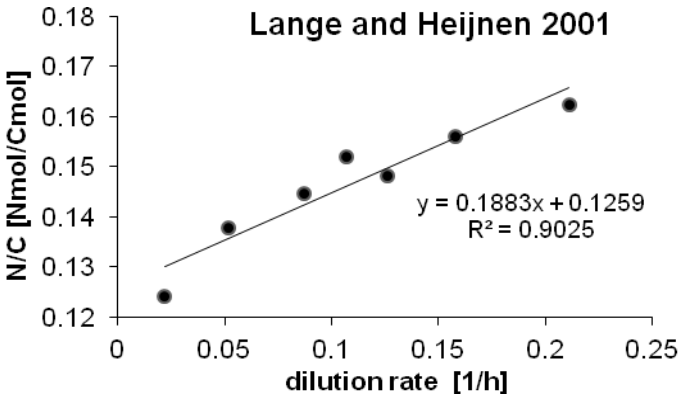

Figure 20: Correlation between N/C-ratio and dilution rate according to Lange and Heijnen, 2001 [149].

Furthermore there are three possibilities why the N/C is increasing: first only the nitrogen content is increasing and the carbon content stays constant; second only the carbon content is decreasing and the nitrogen content stays constant or third nitrogen content increased, while carbon content decreased at the same time. The available data cannot indicate which case is true, but it can be assumed that the carbon ratio might be decreased because of glycogen and trehalose degradation and by-product formation.

10.6 CHANGES IN INTRACELLULAR AMINO ACID POOLS

Transient degradation within the first minutes led to an increased flux through glycolysis. Metabolite pool sizes are highly flux dependent. Changes in the intracellular amino acid contents are explainable by the glucose equivalents from storage carbohydrate degradation. The intracellular concentrations of two derivates from TCA intermediates aspartate and glutamate are decreased during the treatment. The cellular aspartate level is restored immediately whereas the glutamate pool decreases much slower but stayed permanently low. The response of the aspartate pool to CO_2 level may show a limited pyruvat carboxylyase activity [1] associated with a decrease in TCA flux. The increased N/C-ratio of the biomass provides an important indicator for cellular ammonia assimilation. The glutamate pool as the main allocator of assimilated nitrogen may be affected due to increased cellular protein and nucleotide synthesis [149]. Amino acid contents, delivered from glycolysis intermediates, like alanine, glycine, threonine and serine are permanently increased. These facts show that only the amino acids, which derived close to the central carbon metabolism, are affected by CO_2-stress. Nevertheless, it is possible, that changes in intracellular amino acid pools, do not have any impact on the cell, because only aspartate, glutamate, leucine and isoleucine pools are found in high concentrations located in the cytoplasm and the remaining are mostly located in the vacuole [150]. So if the total intracellular amino acid concentration changes, it does not necessarily mean that the concentration changes a lot - for example in the cytoplasm - due to a dynamic behavior between the pools in the compartments by the transporters [151].

This work demonstrates the complexity of the impact of CO_2-stress on *S. cerevisiae* and delivers an overview about the processes taking place during a CO_2 shift. The effect of CO_2 on yeast is still not fully understood and further investigation is therefore needed.

11 ACKNOWLEDGMENTS

Hiermit möchte ich mich bei all denen Bedanken, die mir auf dem Weg bis hin zu dieser Arbeit zur Seite standen:
Vielen Dank Herr Prof .Dr. Ralf Takors, dass Sie es mir möglich machten, an Ihrem Institut meine Arbeit zu verrichten.
Vielen Dank Dipl.-Ing. Dr.nat.techn. Univ.-Doz. Mario Klimacek, für die Betreuung seitens der TU Graz. Besonders dafür, dass Sie immer so schnell zur Stelle waren, wenn ich Sie gebraucht hab.
Vielen Dank Gerhard, für all die unzähligen Dinge die ich lernen durfte und für die viele Zeit die nötig war sie mir beizubringen.
Danke Attila für die Co-Betreuung so mancher arbeiten. Danke für die ausgiebige Erklärung der LC-MS und auch für viele interessante Diskussionen und die unzähligen „leisen" Stunden mit Dir.
Vielen Dank an alle, die bei den Shift-Experimenten mitgeholfen haben, es wäre unmöglich ohne euch gegangen: Salahddine Laghrami, Maria Rahnert, Attila Teliki und seine Praktikantin Angelika, Michael Kraml und sein Praktikant Moritz, Johannes Wutz, Tobias Vallon, Alexander Nies , Jurek Failmezger, Michael Löffler und Frederike Froriep.
Vielen Dank an Alle am Institut der Bioverfahrenstechnik der Universität Stuttgart, Ihr habt dieses Jahr in Stuttgart unvergesslich schön gemacht! Besonderen Dank geht hierbei Annette die für mich da war, als ich mir Verbrühungen zu gezogen habe, an Frederike, für die gegenseitige mentale Unterstützung, an Mira für die Hilfe und die Erklärungen an der HPLC. Danke auch an Eugenia und Jenny, für die lustigen Mittagspausen. Auch dem Herrn Marathonius Kramel viel Dank, für die stetige Bereitschaft zu helfen und den guten Mokka. Danke an Frau Reu (auch für die lustigen Mittagspausen) und für all die Dinge die sie jeden Tag tun, die vieles leichter machen. Danke Maria, für die belebenden Pausen und das offene Ohr. Danke an die Fußball Crew, voll toll von euch mit „Mädchen" zu spielen☺. Auch danke an Maike, die als zweites „Mädchen" standhaft gegen die Männer gespielt hat. Danke an Branka, die coolste deutsche Kroatin, die ich kenne. Danke auch an die Koch-Gruppe, es war mir eine Gaumenfreude.
Danke Emily für die mühevolle Englischkorrektur dieser Arbeit und den damit verbundenen Zeitaufwand!
Vielen Dank Astrid und Martin, für die Unterstützung in allen Lebenslagen. Es ist toll solche „Schwiegereltern" zu haben! Großen Dank besonders an Clemens. Und jetzt wird's schwer, das Ganze in ein- zwei Sätze auszudrücken: Danke, dass Du da bist, mich unterstützt und dass du mich durch die Höhen und Tiefen während meines Studiums begleitet hast!
Danke an meine Freunde, für tolle gemeinsame reisen, die lustige Zeit und für intensive Gespräche, was die Zeit zwischen dem Studium versüßt hat. Besonderen Dank hierfür an Deniza, die mich immer wieder aufgebaut hat, an mich geglaubt hat und mir zeigte, dass die Dinge oft nur halb so schlimm sind, wie sie scheinen.
Danke an meine Familie für die Unterstützung, besonders meiner kleinsten Schwester Patricia und meiner Tante (Tanne) Eveline, die mich mental stets aufgebaut haben. Danke auch an meine Eltern für die Ermöglichung meines Werdeganges.

Zuletzt möchte ich mich für jeden Stein, der mir in den Weg gelegt wurde bedanken, rückblickend sind diese Hindernisse genau das Gegenteil gewesen.

12 REFERENCES

[1] Aguilera J., Petit T., De Winde, Johannes H, and Pronk J. T., 2005,"Physiological and genome-wide transcriptional responses of Saccharomyces cerevisiae to high carbon dioxide concentrations," FEMS Yeast Research, **5**(6-7), pp. 579–593.

[2] Blombach B., and Takors R., 2015,"CO_2 - Intrinsic Product, Essential Substrate, and Regulatory Trigger of Microbial and Mammalian Production Processes," Frontiers in bioengineering and biotechnology, **3**, p. 108.

[3] Takors R., 2012,"Scale-up of microbial processes: impacts, tools and open questions," Journal of biotechnology, **160**(1-2), pp. 3–9.

[4] Gebhardt G., 2010,"Reaktionstechnische Untersuchungen von rekombinanten Saccharomyces cerevisiae zur Bernsteinsäureherstellung," https://books.google.at/books?id=PZpFmwEACAAJ.

[5] Goffeau A., Barrell B. G., Bussey H., Davis R. W., Dujon B., Feldmann H., Galibert F., Hoheisel J. D., Jacq C., Johnston M., Louis E. J., Mewes H. W., Murakami Y., Philippsen P., Tettelin H., and Oliver S. G., 1996,"Life with 6000 genes," Science (New York, N.Y.), **274**(5287), pp. 546, 563-7.

[6] Suter B., Auerbach D., and Stagljar I., 2006,"Yeast-based functional genomics and proteomics technologies: the first 15 years and beyond," BioTechniques, **40**(5), pp. 625–644.

[7] Borodina I., and Nielsen J., 2014,"Advances in metabolic engineering of yeast Saccharomyces cerevisiae for production of chemicals," Biotechnology Journal, **9**(5), pp. 609–620.

[8] Nielsen J., and Jewett M. C., 2008,"Impact of systems biology on metabolic engineering of Saccharomyces cerevisiae," FEMS Yeast Research, **8**(1), pp. 122–131.

[9] van Maris, Antonius J A, Luttik, Marijke A H, Winkler A. A., van Dijken, Johannes P, and Pronk J. T., 2003,"Overproduction of threonine aldolase circumvents the biosynthetic role of pyruvate decarboxylase in glucose-limited chemostat cultures of Saccharomyces cerevisiae," Applied and environmental microbiology, **69**(4), pp. 2094–2099.

[10] Geertman J.-M. A., van Maris, Antonius J A, van Dijken, Johannes P, and Pronk J. T., 2006,"Physiological and genetic engineering of cytosolic redox metabolism in Saccharomyces cerevisiae for improved glycerol production," Metabolic engineering, **8**(6), pp. 532–542.

[11] Yamano S., Ishii T., Nakagawa M., Ikenaga H., and Misawa N., 1994,"Metabolic engineering for production of beta-carotene and lycopene in Saccharomyces cerevisiae," Bioscience, biotechnology, and biochemistry, **58**(6), pp. 1112–1114.

[12] Wattanachaisaereekul S., Lantz A. E., Nielsen M. L., Andresson O. S., and Nielsen J., 2007,"Optimization of heterologous production of the polyketide 6-MSA in Saccharomyces cerevisiae," Biotechnology and bioengineering, **97**(4), pp. 893–900.

[13] Porro D., Bianchi M. M., Brambilla L., Menghini R., Bolzani D., Carrera V., Lievense J., Liu C. L., Ranzi B. M., Frontali L., and Alberghina L., 1999,"Replacement of a metabolic pathway for large-scale production of lactic acid from engineered yeasts," Applied and environmental microbiology, **65**(9), pp. 4211–4215.

[14] Zelle R. M., Hulster E. de, van Winden, Wouter A, Waard P. de, Dijkema C., Winkler A. A., Geertman J.-M. A., van Dijken, Johannes P, Pronk J. T., and van Maris, Antonius J A, 2008,"Malic acid production by Saccharomyces cerevisiae: engineering of pyruvate carboxylation, oxaloacetate reduction, and malate export," Applied and environmental microbiology, **74**(9), pp. 2766–2777.

[15] Raab A. M., Gebhardt G., Bolotina N., Weuster-Botz D., and Lang C., 2010,"Metabolic engineering of Saccharomyces cerevisiae for the biotechnological production of succinic acid," Metabolic engineering, **12**(6), pp. 518–525.

[16] Joe Whitworth, 2012,"Global yeast market to reach $5.1bn by 2016 - report: The worldwide yeast industry will grow 8.6% annually until 2016 to $5.1bn (€3.9bn), according to a new report.," http://www.bakeryandsnacks.com/Markets/Global-yeast-market-to-reach-5.1bn-by-2016-report.

[17] Grand View Research, 2015. *Yeast Ingredients Market Analysis By Product (Yeast Extracts, Yeast Autolysates, Yeast Beta-Glucan, Yeast Derivatives), By Application (Food, Feed) And Segment Forecasts To 2020*.

[18] Steensels J., Snoek T., Meersman E., Picca Nicolino M., Voordeckers K., and Verstrepen K. J., 2014,"Improving industrial yeast strains: exploiting natural and artificial diversity," FEMS Microbiology Reviews, **38**(5), pp. 947–995.

[19] Köhler G. J., 2005. *Funktionelle Charakterisierung der Kinetochorproteine Ame1p und Iml3p sowie des Folsäurebiosyntheseproteins Fol1p in der Hefe Saccharomyces cerevisiae: I n a u g u r a l - D i s s e r t a t i on zur Erlangung des Doktorgrades der Mathematisch-Naturwissenschaftlichen Fakultät der Heinrich-Heine-Universität Düsseldorf (Fachbereich Biologie)*.

[20] Krook D. ,Mashego M.R. ,van Gulik W.M. ,Heijnen J.J., 2004. *Effect of Dissolved Carbon Dioxide Concentration on the Metabolism oi Saccharomyces cerevisiae*, TU Delft.

[21] Schneider K., 2011. *Auswirkungen der MAE1-Gendeletion auf den Zentralstoffwechsel von Saccharomyces cerevisiae unter verschiedenen Physiologien: Dissertation zur Erlangung des Grades des Doktors der Ingenieurwissenschaften der Naturwissenschaftlich-Technischen Fakultät III Chemie, Pharmazie, Bio- und Werkstoffwissenschaften der Universität des Saarlandes*.

[22] Steensma H. Y., 1997. *pyruvate to acetyl-CoA and oxaloacetate. In: Yeast sugar metabolism – biochemistry, genetics, biotechnology, and applications.*, Technomic.

[23] Rodrigues, F., Ludovico, P. und Leao, C., 2006. *Sugar Metabolism in Yeasts: an Overview of Aerobic and Anaerobic Glucose Catabolism in Biodiversity and Ecophysiology of Yeasts*, Springer.

[24] Camarasa C., Grivet J.-P., and Dequin S., 2003,"Investigation by 13C-NMR and tricarboxylic acid (TCA) deletion mutant analysis of pathways for succinate formation in Saccharomyces cerevisiae during anaerobic fermentation," Microbiology (Reading, England), **149**(Pt 9), pp. 2669–2678.

[25] Arikawa Y., Kuroyanagi T., Shimosaka M., Muratsubaki H., Enomoto K., Kodaira R., and Okazaki M., 1999,"Effect of gene disruptions of the TCA cycle on production of succinic acid in Saccharomyces cerevisiae," Journal of bioscience and bioengineering, **87**(1), pp. 28–36.

[26] Enomoto K., Ohki R., and Muratsubaki H., 1996,“Cloning and sequencing of the gene encoding the soluble fumarate reductase from Saccharomyces cerevisiae,” DNA research an international journal for rapid publication of reports on genes and genomes, **3**(4), pp. 263–267.
[27] François J., Walther T., and Parrou J., 2012, Genetics and Regulation of Glycogen and Trehalose Metabolism in Saccharomyces cerevisiae, *Microbial Stress Tolerance for Biofuels*, Liu Z. L., ed., Springer Berlin Heidelberg, pp. 29-55.
[28] Lillie S. H., and Pringle J. R., 1980,“Reserve carbohydrate metabolism in Saccharomyces cerevisiae: responses to nutrient limitation,” Journal of Bacteriology, **143**(3), pp. 1384–1394.
[29] Richard L., Guillouet S. E., and Uribelarrea J.-L., 2014,“Quantification of the transient and long-term response of Saccharomyces cerevisiae to carbon dioxide stresses of various intensities,” Process Biochemistry, **49**(11), pp. 1808–1818.
[30] Wilson W. A., Roach P. J., Montero M., Baroja-Fernandez E., Munoz F. J., Eydallin G., Viale A. M., and Pozueta-Romero J., 2010,“Regulation of glycogen metabolism in yeast and bacteria,” FEMS Microbiology Reviews, **34**(6), pp. 952–985.
[31] Daran J. M., Bell W., and Francois J., 1997,“Physiological and morphological effects of genetic alterations leading to a reduced synthesis of UDP-glucose in Saccharomyces cerevisiae,” FEMS microbiology letters, **153**(1), pp. 89–96.
[32] Smith T. L., and Rutter J., 2007,“Regulation of glucose partitioning by PAS kinase and Ugp1 phosphorylation,” Molecular cell, **26**(4), pp. 491–499.
[33] Cid V. J., Duran A., del Rey F., Snyder M. P., Nombela C., and Sanchez M., 1995,“Molecular basis of cell integrity and morphogenesis in Saccharomyces cerevisiae,” Microbiological reviews, **59**(3), pp. 345–386.
[34] Montijn R. C., Vink E., Muller W. H., Verkleij A. J., Van Den Ende, H, Henrissat B., and Klis F. M., 1999,“Localization of synthesis of beta1,6-glucan in Saccharomyces cerevisiae,” Journal of Bacteriology, **181**(24), pp. 7414–7420.
[35] Huh W.-K., Falvo J. V., Gerke L. C., Carroll A. S., Howson R. W., Weissman J. S., and O'Shea E. K., 2003,“Global analysis of protein localization in budding yeast,” Nature, **425**(6959), pp. 686–691.
[36] Grose J. H., Smith T. L., Sabic H., and Rutter J., 2007,“Yeast PAS kinase coordinates glucose partitioning in response to metabolic and cell integrity signaling,” The EMBO journal, **26**(23), pp. 4824–4830.
[37] Melendez R., Melendez-Hevia E., and Canela E. I., 1999,“The fractal structure of glycogen: A clever solution to optimize cell metabolism,” Biophysical journal, **77**(3), pp. 1327–1332.
[38] Aklujkar, P. P., Sankh, S. N. and Arvindekar, A. U,“A simplified method for the isolation and estimation of cell wall bound glycogen in Saccharomyces cerevisiae,” J. Inst. Brew, **2008**(114), pp. 205–208.
[39] Gunja-Smith Z., Patil N. B., and Smith E. E., 1977,“Two pools of glycogen in Saccharomyces,” Journal of Bacteriology, **130**(2), pp. 818–825.
[40] François J., and Parrou J. L., 2001,“Reserve carbohydrates metabolism in the yeast Saccharomyces cerevisiae,” FEMS Microbiology Reviews, **25**(1), pp. 125–145.
[41] Cheng C., Mu J., Farkas I., Huang D., Goebl M. G., and Roach P. J., 1995,“Requirement of the self-glucosylating initiator proteins Glg1p and Glg2p for glycogen accumulation in Saccharomyces cerevisiae,” Molecular and cellular biology, **15**(12), pp. 6632–6640.
[42] Wilson W. A., Wang Z., and Roach P. J., 2002,“Systematic identification of the genes affecting glycogen storage in the yeast Saccharomyces cerevisiae: implication of the vacuole as a determinant of glycogen level,” Molecular & cellular proteomics MCP, **1**(3), pp. 232–242.
[43] Rutter J., Probst B. L., and McKnight S. L., 2002,“Coordinate regulation of sugar flux and translation by PAS kinase,” Cell, **111**(1), pp. 17–28.
[44] Baskaran S., Roach P. J., DePaoli-Roach A. A., and Hurley T. D., 2010,“Structural basis for glucose-6-phosphate activation of glycogen synthase,” Proceedings of the National Academy of Sciences of the United States of America, **107**(41), pp. 17563–17568.
[45] Francois J., and Hers H. G., 1988,“The control of glycogen metabolism in yeast. 2. A kinetic study of the two forms of glycogen synthase and of glycogen phosphorylase and an investigation of their interconversion in a cell-free extract,” European journal of biochemistry / FEBS, **174**(3), pp. 561–567.
[46] Pederson B. A., Wilson W. A., and Roach P. J., 2004,“Glycogen synthase sensitivity to glucose-6-P is important for controlling glycogen accumulation in Saccharomyces cerevisiae,” The Journal of biological chemistry, **279**(14), pp. 13764–13768.
[47] Teste M.-A., Duquenne M., Francois J. M., and Parrou J.-L., 2009,“Validation of reference genes for quantitative expression analysis by real-time RT-PCR in Saccharomyces cerevisiae,” BMC molecular biology, **10**, p. 99.
[48] Wang Z., Wilson W. A., Fujino M. A., and Roach P. J., 2001,“Antagonistic controls of autophagy and glycogen accumulation by Snf1p, the yeast homolog of AMP-activated protein kinase, and the cyclin-dependent kinase Pho85p,” Molecular and cellular biology, **21**(17), pp. 5742–5752.
[49] Colonna W. J., and Magee P. T., 1978,“Glycogenolytic enzymes in sporulating yeast,” Journal of Bacteriology, **134**(3), pp. 844–853.
[50] Clancy M. J., Smith L. M., and Magee P. T., 1982,“Developmental regulation of a sporulation-specific enzyme activity in Saccharomyces cerevisiae,” Molecular and cellular biology, **2**(2), pp. 171–178.
[51] Hwang P. K., Tugendreich S., and Fletterick R. J., 1989,“Molecular analysis of GPH1, the gene encoding glycogen phosphorylase in Saccharomyces cerevisiae,” Molecular and cellular biology, **9**(4), pp. 1659–1666.
[52] Sunnarborg S. W., Miller S. P., Unnikrishnan I., and LaPorte D. C., 2001,“Expression of the yeast glycogen phosphorylase gene is regulated by stress-response elements and by the HOG MAP kinase pathway,” Yeast (Chichester, England), **18**(16), pp. 1505–1514.
[53] Fosset M., Muir L. W., Nielsen L. D., and Fischer E. H., 1971,“Purification and properties of yeast glycogen phosphorylase a and b,” Biochemistry, **10**(22), pp. 4105–4113.
[54] Lerch K., and Fischer E. H., 1975,“Amino acid sequence of two functional sites in yeast glycogen phosphorylase,” Biochemistry, **14**(9), pp. 2009–2014.
[55] Lin K., Rath V. L., Dai S. C., Fletterick R. J., and Hwang P. K., 1996,“A protein phosphorylation switch at the conserved allosteric site in GP,” Science (New York, N.Y.), **273**(5281), pp. 1539–1542.
[56] Wilson W. A., Wang Z., and Roach P. J., 2005,“Regulation of yeast glycogen phosphorylase by the cyclin-dependent protein kinase Pho85p,” Biochemical and biophysical research communications, **329**(1), pp. 161–167.
[57] Becker J. U., Wingender-Drissen R., and Schiltz E., 1983,“Purification and properties of phosphorylase from baker's yeast,” Archives of biochemistry and biophysics, **225**(2), pp. 667–678.
[58] Pohlig G., Wingender-Drissen R., and Becker J. U., 1983,“Characterization of phosphorylase kinase activities in yeast,” Biochemical and biophysical research communications, **114**(1), pp. 331–338.

[59] Londesborough J., and Vuorio O. E., 1993,“Purification of trehalose synthase from baker's yeast. Its temperature-dependent activation by fructose 6-phosphate and inhibition by phosphate,” European journal of biochemistry / FEBS, **216**(3), pp. 841–848.
[60] Vandercammen A., Francois J., and Hers H. G., 1989,“Characterization of trehalose-6-phosphate synthase and trehalose-6-phosphate phosphatase of Saccharomyces cerevisiae,” European journal of biochemistry / FEBS, **182**(3), pp. 613–620.
[61] Neves M. J., Jorge J. A., Francois J. M., and Terenzi H. F., 1991,“Effects of heat shock on the level of trehalose and glycogen, and on the induction of thermotolerance in Neurospora crassa,” FEBS letters, **283**(1), pp. 19–22.
[62] Winderickx J., de Winde, J H, Crauwels M., Hino A., Hohmann S., van Dijck P., and Thevelein J. M., 1996,“Regulation of genes encoding subunits of the trehalose synthase complex in Saccharomyces cerevisiae: novel variations of STRE-mediated transcription control?,” Molecular & general genetics MGG, **252**(4), pp. 470–482.
[63] Jules M., Guillou V., Francois J., and Parrou J.-L., 2004,“Two distinct pathways for trehalose assimilation in the yeast Saccharomyces cerevisiae,” Applied and environmental microbiology, **70**(5), pp. 2771–2778.
[64] Panni S., Landgraf C., Volkmer-Engert R., Cesareni G., and Castagnoli L., 2008,“Role of 14-3-3 proteins in the regulation of neutral trehalase in the yeast Saccharomyces cerevisiae,” FEMS Yeast Research, **8**(1), pp. 53–63.
[65] Destruelle M., Holzer H., and Klionsky D. J., 1995,“Isolation and characterization of a novel yeast gene, ATH1, that is required for vacuolar acid trehalase activity,” Yeast (Chichester, England), **11**(11), pp. 1015–1025.
[66] He S., Bystricky K., Leon S., Francois J. M., and Parrou J. L., 2009,“The Saccharomyces cerevisiae vacuolar acid trehalase is targeted at the cell surface for its physiological function,” The FEBS journal, **276**(19), pp. 5432–5446.
[67] Guillou V., Plourde-Owobi L., Parrou J. L., Goma G., and Francois J., 2004,“Role of reserve carbohydrates in the growth dynamics of Saccharomyces cerevisiae,” FEMS Yeast Research, **4**(8), pp. 773–787.
[68] Kuenzi M. T., and Fiechter A., 1972,“Regulation of carbohydrate composition of Saccharomyces cerevisiae under growth limitation,” Archiv fur Mikrobiologie, **84**(3), pp. 254–265.
[69] Porro D., Martegani E., Ranzi B. M., and Alberghina L., 1988,“Oscillations in continuous cultures of budding yeast: a segregated parameter analysis,” Biotechnology and bioengineering, **32**(4), pp. 411–417.
[70] Martegani E., Porro D., Ranzi B. M., and Alberghina L., 1990,“Involvement of a cell size control mechanism in the induction and maintenance of oscillations in continuous cultures of budding yeast,” Biotechnology and bioengineering, **36**(5), pp. 453–459.
[71] Duboc P., Marison I., and Stockar U. von, 1996,“Physiology of Saccharomyces cerevisiae during cell cycle oscillations,” Journal of biotechnology, **51**(1), pp. 57–72.
[72] Müller D., Exler S., Aguilera-Vázquez L., Guerrero-Martín E., and Reuss M., 2003,“Cyclic AMP mediates the cell cycle dynamics of energy metabolism in Saccharomyces cerevisiae,” Yeast, **20**(4), pp. 351–367.
[73] Sillje H. H., ter Schure, E G, Rommens A. J., Huls P. G., Woldringh C. L., Verkleij A. J., Boonstra J., and Verrips C. T., 1997,“Effects of different carbon fluxes on G1 phase duration, cyclin expression, and reserve carbohydrate metabolism in Saccharomyces cerevisiae,” Journal of Bacteriology, **179**(21), pp. 6560–6565.
[74] Sillje H. H., Paalman J. W., ter Schure, E G, Olsthoorn S. Q., Verkleij A. J., Boonstra J., and Verrips C. T., 1999,“Function of trehalose and glycogen in cell cycle progression and cell viability in Saccharomyces cerevisiae,” Journal of Bacteriology, **181**(2), pp. 396–400.
[75] Paalman, Johannes W G, Verwaal R., Slofstra S. H., Verkleij A. J., Boonstra J., and Verrips C. T., 2003,“Trehalose and glycogen accumulation is related to the duration of the G1 phase of Saccharomyces cerevisiae,” FEMS Yeast Research, **3**(3), pp. 261–268.
[76] Crowe J. H., Hoekstra F. A., and Crowe L. M., 1992,“Anhydrobiosis,” Annual review of physiology, **54**, pp. 579–599.
[77] Singer M. A., and Lindquist S., 1998,“Thermotolerance in Saccharomyces cerevisiae: the Yin and Yang of trehalose,” Trends in biotechnology, **16**(11), pp. 460–468.
[78] Simola M., Hanninen A. L., Stranius S. M., and Makarow M., 2000,“Trehalose is required for conformational repair of heat-denatured proteins in the yeast endoplasmic reticulum but not for maintenance of membrane traffic functions after severe heat stress,” Molecular microbiology, **37**(1), pp. 42–53.
[79] Wiemken A., 1990,“Trehalose in yeast, stress protectant rather than reserve carbohydrate,” Antonie van Leeuwenhoek, **58**(3), pp. 209–217.
[80] Attfield P. V., 1997,“Stress tolerance: the key to effective strains of industrial baker's yeast,” Nature biotechnology, **15**(13), pp. 1351–1357.
[81] Neves M. J., and Francois J., 1992,“On the mechanism by which a heat shock induces trehalose accumulation in Saccharomyces cerevisiae,” The Biochemical journal, **288 (Pt 3)**, pp. 859–864.
[82] Parrou J. L., Teste M. A., and Francois J., 1997,“Effects of various types of stress on the metabolism of reserve carbohydrates in Saccharomyces cerevisiae: genetic evidence for a stress-induced recycling of glycogen and trehalose,” Microbiology (Reading, England), **143 (Pt 6)**, pp. 1891–1900.
[83] Grba S., Oura E., and Suomalainen H., 1975,“On the formation of glycogen and trehalose in baker's yeast,” European J. Appl Microbiol., **2**(1), pp. 29-37.
[84] Hottiger T., Schmutz P., and Wiemken A., 1987,“Heat-induced accumulation and futile cycling of trehalose in Saccharomyces cerevisiae,” Journal of Bacteriology, **169**(12), pp. 5518–5522.
[85] Hottiger T., Boller T., and Wiemken A., 1989,“Correlation of trehalose content and heat resistance in yeast mutants altered in the RAS/adenylate cyclase pathway: is trehalose a thermoprotectant?,” FEBS letters, **255**(2), pp. 431–434.
[86] Attfield P. V., 1987,“Trehalose accumulates in Saccharomyces cerevisiae during exposure to agents that induce heat shock response,” FEBS letters, **225**(1-2), pp. 259–263.
[87] Panek A. C., Vania J. J., Paschoalin M. F., and Panek D., 1990,“Regulation of trehalose metabolism in Saccharomyces cerevisiae mutants during temperature shifts,” Biochimie, **72**(1), pp. 77–79.
[88] Winkler K., Kienle I., Burgert M., Wagner J. C., and Holzer H., 1991,“Metabolic regulation of the trehalose content of vegetative yeast,” FEBS letters, **291**(2), pp. 269–272.
[89] Ribeiro M. J., Silva J. T., and Panek A. D., 1994,“Trehalose metabolism in Saccharomyces cerevisiae during heat-shock,” Biochimica et biophysica acta, **1200**(2), pp. 139–147.
[90] Alexandre H., Plourde L., Charpentier C., and Francois J., 1998,“Lack of correlation between trehalose accumulation, cell viability and intracellular acidification as induced by various stresses in Saccharomyces cerevisiae,” Microbiology (Reading, England), **144 (Pt 4)**, pp. 1103–1111.
[91] Panadero J., Pallotti C., Rodriguez-Vargas S., Randez-Gil F., and Prieto J. A., 2006,“A downshift in temperature activates the high osmolarity glycerol (HOG) pathway, which determines freeze tolerance in Saccharomyces cerevisiae,” The Journal of biological chemistry, **281**(8), pp. 4638–4645.

[92] Martinez-Pastor M. T., Marchler G., Schuller C., Marchler-Bauer A., Ruis H., and Estruch F., 1996,"The Saccharomyces cerevisiae zinc finger proteins Msn2p and Msn4p are required for transcriptional induction through the stress response element (STRE)," The EMBO journal, **15**(9), pp. 2227–2235.
[93] Gorner W., Durchschlag E., Martinez-Pastor M. T., Estruch F., Ammerer G., Hamilton B., Ruis H., and Schuller C., 1998,"Nuclear localization of the C2H2 zinc finger protein Msn2p is regulated by stress and protein kinase A activity," Genes & development, **12**(4), pp. 586–597.
[94] Gorner W., Durchschlag E., Wolf J., Brown E. L., Ammerer G., Ruis H., and Schuller C., 2002,"Acute glucose starvation activates the nuclear localization signal of a stress-specific yeast transcription factor," The EMBO journal, **21**(1-2), pp. 135–144.
[95] Wever V. de, Reiter W., Ballarini A., Ammerer G., and Brocard C., 2005,"A dual role for PP1 in shaping the Msn2-dependent transcriptional response to glucose starvation," The EMBO journal, **24**(23), pp. 4115–4123.
[96] Estruch F., 2000,"Stress-controlled transcription factors, stress-induced genes and stress tolerance in budding yeast," FEMS Microbiology Reviews, **24**(4), pp. 469–486.
[97] Causton H. C., Ren B., Koh S. S., Harbison C. T., Kanin E., Jennings E. G., Lee T. I., True H. L., Lander E. S., and Young R. A., 2001,"Remodeling of yeast genome expression in response to environmental changes," Molecular biology of the cell, **12**(2), pp. 323–337.
[98] Ward M. P., Gimeno C. J., Fink G. R., and Garrett S., 1995,"SOK2 may regulate cyclic AMP-dependent protein kinase-stimulated growth and pseudohyphal development by repressing transcription," Molecular and cellular biology, **15**(12), pp. 6854–6863.
[99] Pedruzzi I., Burckert N., Egger P., and Virgilio C. de, 2000,"Saccharomyces cerevisiae Ras/cAMP pathway controls post-diauxic shift element-dependent transcription through the zinc finger protein Gis1," The EMBO journal, **19**(11), pp. 2569–2579.
[100] Pedruzzi I., Dubouloz F., Cameroni E., Wanke V., Roosen J., Winderickx J., and Virgilio C. de, 2003,"TOR and PKA signaling pathways converge on the protein kinase Rim15 to control entry into G0," Molecular cell, **12**(6), pp. 1607–1613.
[101] Zaman S., Im Lippman S., Zhao X., and Broach J. R., 2008,"How Saccharomyces responds to nutrients," Annual review of genetics, **42**, pp. 27–81.
[102] Virgilio C. de, and Loewith R., 2006,"The TOR signalling network from yeast to man," The international journal of biochemistry & cell biology, **38**(9), pp. 1476–1481.
[103] Enjalbert B., Parrou J. L., Teste M. A., and Francois J., 2004,"Combinatorial control by the protein kinases PKA, PHO85 and SNF1 of transcriptional induction of the Saccharomyces cerevisiae GSY2 gene at the diauxic shift," Molecular genetics and genomics MGG, **271**(6), pp. 697–708.
[104] Huang D., Farkas I., and Roach P. J., 1996,"Pho85p, a cyclin-dependent protein kinase, and the Snf1p protein kinase act antagonistically to control glycogen accumulation in Saccharomyces cerevisiae," Molecular and cellular biology, **16**(8), pp. 4357–4365.
[105] Wilson W. A., Mahrenholz A. M., and Roach P. J., 1999,"Substrate targeting of the yeast cyclin-dependent kinase Pho85p by the cyclin Pcl10p," Molecular and cellular biology, **19**(10), pp. 7020–7030.
[106] Jones, E. W., and G. R. Fink, 1982. *Regulation of amino acid and nucleotide biosynthesis in yeast*, pp. 181-299 in The Molecular Biology of the Yeast Saccharomyces: Metabolism and Gene Expression, edited by J. N. Strathern, E. W. Jones, and J. R. Broach, Cold Spring Harbor Laboratory Press, Cold Spring Harbor, NY.
[107] Ljungdahl P. O., and Daignan-Fornier B., 2012,"Regulation of amino acid, nucleotide, and phosphate metabolism in Saccharomyces cerevisiae," Genetics, **190**(3), pp. 885–929.
[108] Alifano P., Fani R., Lio P., Lazcano A., Bazzicalupo M., Carlomagno M. S., and Bruni C. B., 1996,"Histidine biosynthetic pathway and genes: structure, regulation, and evolution," Microbiological reviews, **60**(1), pp. 44–69.
[109] Terrance G. Cooper, 1982,"Nitrogen Metabolism in Saccharomyces cerevisiae," Cold Spring Harbor Monograph Archive; Volume 11B (1982): The Molecular Biology of the Yeast Saccharomyces: Metabolism and Gene Expression.
[110] Boris Magasanik, 1992,"6 Regulation of Nitrogen Utilization," Cold Spring Harbor Monograph Archive; Volume 21B (1992): Volume II: The Molecular and Cellular Biology of the Yeast Saccharomyces: Gene Expression.
[111] Magasanik B., and Kaiser C. A., 2002,"Nitrogen regulation in Saccharomyces cerevisiae," Gene, **290**(1-2), pp. 1–18.
[112] Godard P., Urrestarazu A., Vissers S., Kontos K., Bontempi G., van Helden J., and Andre B., 2007,"Effect of 21 different nitrogen sources on global gene expression in the yeast Saccharomyces cerevisiae," Molecular and cellular biology, **27**(8), pp. 3065–3086.
[113] Hazelwood L. A., Daran J.-M., van Maris, Antonius J A, Pronk J. T., and Dickinson J. R., 2008,"The Ehrlich pathway for fusel alcohol production: a century of research on Saccharomyces cerevisiae metabolism," Applied and environmental microbiology, **74**(8), pp. 2259–2266.
[114] Hetherington A. M., and Raven J. A., 2005,"The biology of carbon dioxide," Current biology CB, **15**(11), pp. R406-10.
[115] Pro Oxygen, 2015,"CO_2now," http://co2now.org/.
[116] Jones R. P., and Greenfield P. F., 1982,"Effect of carbon dioxide on yeast growth and fermentation," Enzyme and Microbial Technology, **4**(4), pp. 210–223.
[117] Dixon N. M., and Kell D. B., 1989,"The inhibition by CO_2 of the growth and metabolism of micro-organisms," The Journal of applied bacteriology, **67**(2), pp. 109–136.
[118] Shimoda M., Cocunubo-Castellanos J., Kago H., Miyake M., Osajima Y., and Hayakawa I., 2001,"The influence of dissolved CO(2) concentration on the death kinetics of Saccharomyces cerevisiae," Journal of applied microbiology, **91**(2), pp. 306–311.
[119] Amoroso G., Morell-Avrahov L., Muller D., Klug K., and Sultemeyer D., 2005,"The gene NCE103 (YNL036w) from Saccharomyces cerevisiae encodes a functional carbonic anhydrase and its transcription is regulated by the concentration of inorganic carbon in the medium," Molecular microbiology, **56**(2), pp. 549–558.
[120] Orij R., Brul S., and Smits G. J., 2011,"Intracellular pH is a tightly controlled signal in yeast," Biochimica et biophysica acta, **1810**(10), pp. 933–944.
[121] Yagi H., and Yoshida F., 1977,"Desorption of carbon dioxide from fermentation broth," Biotechnol. Bioeng., **19**(6), pp. 801–819.
[122] Garcia-Gonzalez L., Geeraerd A. H., Spilimbergo S., Elst K., van Ginneken L., Debevere J., Van Impe, J F, and Devlieghere F., 2007,"High pressure carbon dioxide inactivation of microorganisms in foods: the past, the present and the future," International journal of food microbiology, **117**(1), pp. 1–28.
[123] Pasteur, L. and Joubert, 1877,"Etude sur la maladie charbonneuse," C. R. Acad. Sc., (84), pp. 900–905.

[124] Chen S. L., and Gutmains F., 1976,“Carbon dioxide inhibition of yeast growth in biomass production,” Biotechnology and bioengineering, **18**(10), pp. 1455–1462.
[125] Norton J. S., and Krauss R. W., 1972,“The inhibition of cell division in Saccharomyces cerevisiae (Meyen) by carbon dioxide,” Plant and Cell Physiology, **13**(1), pp. 139–149.
[126] Akashi K., and Shirai, H. and Hirose, Y., 1979,“Inhibitory effects of carbon dioxide and oxygen in amino acid fermentation,” J. Ferment. Technol.(57), pp. 317–320.
[127] Kuriyama H., Mahakarnchanakul W., Matsui S., and Kobayashi H., 1993,“The effects of pCO_2 on yeast growth and metabolism under continuous fermentation,” Biotechnol Lett, **15**(2), pp. 189-194.
[128] Zelle R. M., Hulster E. de, Kloezen W., Pronk J. T., and van Maris, Antonius JA, 2010,“Key Process Conditions for Production of C_4 Dicarboxylic Acids in Bioreactor Batch Cultures of an Engineered Saccharomyces cerevisiae Strain,” Applied and environmental microbiology AEM.
[129] Mashego M., 2005. *Robust experimental methods to study in-vivo pre-steady statekinetics of primary metabolism in Saccharomyces cerevisiae*, TU Delft.
[130] Aboka F. O., van Winden, Wouter A., Reginald M. M., van Gulik, Walter M., van de Berg, Marco, Oudshoorn A., and Heijnen J. J., 2012,“Identification of informative metabolic responses using a minibioreactor: a small step change in the glucose supply rate creates a large metabolic response in Saccharomyces cerevisiae,” Yeast, **29**(3-4), pp. 95–110.
[131] Cherry J. M., Hong E. L., Amundsen C., Balakrishnan R., Binkley G., Chan E. T., Christie K. R., Costanzo M. C., Dwight S. S., Engel S. R., Fisk D. G., Hirschman J. E., Hitz B. C., Karra K., Krieger C. J., Miyasato S. R., Nash R. S., Park J., Skrzypek M. S., Simison M., Weng S., and Wong E. D., 2011,“Saccharomyces Genome Database: the genomics resource of budding yeast,” Nucleic Acids Research, **40**(09.01.2015), pp. D700.
[132] Ringger S., 2014. *Metabolische Flussanalyse ausgewählter Flieÿgleichgewichte zur Vorbereitung von Stimulus Response Experimenten in Saccharomyces cerevisiae: Metabolic ux analysis of pre-elected steady states in preparation for stimulus response experiments in Saccharomyces cerevisiae*, Bachelorarbeit, Institut der Bioverfahrenstechnik, Universität Stuttgart.
[133] Verduyn C., Postma E., Scheffers W. A., and Van Dijken, J P, 1992,“Effect of benzoic acid on metabolic fluxes in yeasts: a continuous-culture study on the regulation of respiration and alcoholic fermentation,” Yeast (Chichester, England), **8**(7), pp. 501–517.
[134] Buchholz J., Graf M., Blombach B., and Takors R., 2014,“Improving the carbon balance of fermentations by total carbon analyses,” Biochemical Engineering Journal, **90**, pp. 162–169.
[135] Henderson JW, Ricker RD, Bidlingmeyer BA, Woodward C, 2000,“Rapid, Accurate, Sensitive and Reproducible Analysis of Amino Acids: .,” Agilent Publication Number 5980-1193EN. Agilent Technologies, Palo Alto, CA.
[136] Parrou J. L., and Francois J., 1997,“A simplified procedure for a rapid and reliable assay of both glycogen and trehalose in whole yeast cells,” Analytical biochemistry, **248**(1), pp. 186–188.
[137] Ochs Jelena, 2013. *Einuss von stickstomitierung auf metabolische aktivität und resveratrolsynthese in saccharomyces cerevisiae.*, University of Stuttgart.
[138] Sander R.,“Compilation of Henry's law constants (version 4.0) for water as solvent,”(15), pp. 4399–4981.
[139] Patnaik P. R., 2003,“Oscillatory metabolism of Saccharomyces cerevisiae: an overview of mechanisms and models,” Biotechnology advances, **21**(3), pp. 183–192.
[140] Lodeyro A. F., Calcaterra N. B., and Roveri O. A., 2001,“Inhibition of steady-state mitochondrial ATP synthesis by bicarbonate, an activating anion of ATP hydrolysis,” Biochimica et Biophysica Acta (BBA) - Bioenergetics, **1506**(3), pp. 236–243.
[141] Kresnowati M., Suarez-Mendez C. M., van Winden W. A., van Gulik W. M., and Heijnen J. J., 2008,“Quantitative physiological study of the fast dynamics in the intracellular pH of Saccharomyces cerevisiae in response to glucose and ethanol pulses,” Metabolic engineering, **10**(1), pp. 39–54.
[142] Perlin D. S., San Francisco, Michael J. D., Slayman C. W., and Rosen B. P., 1986,“H+ATP stoichiometry of proton pumps from Neurospora crassa and Escherichia coli,” Archives of biochemistry and biophysics, **248**(1), pp. 53–61.
[143] Zhao R., and Reithmeier, R. A. F., 2001,“Expression and characterization of the anion transporter homologue YNL275w in Saccharomyces cerevisiae,” American Journal of Physiology - Cell Physiology, **281**(1 50-1), pp. C33.
[144] López R., Enríquez E., and Peña A., 1999,“Effects of weak acids on cation accumulation, ΔpH and ΔΨ in yeast,” Yeast, **15**(7), pp. 553–562.
[145] Zippin J. H., Levin L. R., and Buck J., 2001,“CO_2/HCO3−-responsive soluble adenylyl cyclase as a putative metabolic sensor,” Trends in Endocrinology & Metabolism, **12**(8), pp. 366–370.
[146] Thevelein J. M., and De Winde, Johannes H., 1999,“Novel sensing mechanisms and targets for the cAMP–protein kinase A pathway in the yeast Saccharomyces cerevisiae,” Molecular Microbiology, **33**(5), pp. 904–918.
[147] Ulaszewski S., Hilger F., and Goffeau A., 1989,“Cyclic AMP controls the plasma membrane H+-ATPase activity from Saccharomyces cerevisiae,” FEBS letters, **245**(1-2), pp. 131–136.
[148] Muller G., and Bandlow W., 1987,“Protein phosphorylation in yeast mitochondria: cAMP-dependence, submitochondrial localization and substrates of mitochondrial protein kinases,” Yeast (Chichester, England), **3**(3), pp. 161–174.
[149] Lange H. C., and Heijnen J. J., 2001,“Statistical reconciliation of the elemental and molecular biomass composition of Saccharomyces cerevisiae,” Biotechnology and bioengineering, **75**(3), pp. 334–344.
[150] MESSENGUY F., COLIN D., and HAVE J. T., 1980,“Regulation of compartmentation of amino acid pools in Saccharomyces cerevisiae and its effects on metabolic control,” European Journal of Biochemistry, **108**(2), pp. 439–447.
[151] Kitamoto K., Yoshizawa K., Ohsumi Y., and Anraku Y., 1988,“Dynamic aspects of vacuolar and cytosolic amino acid pools of Saccharomyces cerevisiae,” Journal of Bacteriology, **170**(6), pp. 2683–2686.